UNIVERSITY OF CALIFORNIA

Los Angeles

Immunomodulation of Cardiovascular Pathology in Chronic Kidney Disease

A dissertation submitted in partial satisfaction of the requirements for the degree Doctor of Philosophy in Molecular, Cell, and Developmental Biology

by

Jessica Layman Sea

2016

ABSTRACT OF THE DISSERTATION

Immunomodulation of Cardiovascular Pathology

in Chronic Kidney Disease

by

Jessica Layman Sea

Doctor of Philosophy in Molecular, Cell, and Developmental Biology

University of California, Los Angeles, 2016

Professor Martin Hewison, Co-Chair

Professor John S. Adams, Co-Chair

Cardiovascular disease (CVD) is the most common cause of the death among patients with chronic kidney disease (CKD). Fibroblast growth factor (FGF) 23, a potent regulator of the vitamin D system, is markedly upregulated early in CKD, with levels increasing as kidney function declines. Clinical studies suggest connections between FGF23 and cardiovascular complications associated with CKD, as both are strongly correlated to decreased renal output. Vitamin D deficiency is another serious co-morbidity associated with CKD. A key regulator of innate immune function, vitamin D plays an important role in CVD propagated by chronic inflammation. However, the contributions FGF23 and vitamin D to CKD-related

cardiovascular pathologies remain uncharacterized. This dissertation explores the various roles of FGF23 and vitamin D in monocytes and endothelial cells with a focus on CKD-induced cardiovascular co-morbidities.

CVD, particularly atherosclerosis, is initiated by systemic inflammation, endothelial dysfunction, and aberrant lipid profiles, with key players being monocyte/macrophage populations and the endothelium. The vitamin D system is well characterized in monocytes, acting in both antimicrobial and anti-inflammatory capacities. CKD is marked by chronic inflammation, which is also a key contributor to atherosclerosis. FGF23 is traditionally known for down regulating renal vitamin D synthesis. Given the connections between vitamin D and monocytes with CVD, we first sought to determine whether FGF23 had any effect on the vitamin D system in these cells. Here we demonstrate the ability for FGF23 to limit the immune properties of vitamin D in monocytes, and thus potentially contribute to the abnormal inflammatory patterns known to initiate CVD.

We next investigated the interactions between monocytes and endothelial cells in the context of CKD. Incubating co-cultures of human aortic endothelial cells and monocytes with FGF23 caused both phenotypic and functional changes in both cell types related to CVD. In the final two chapters, we focus on characterizing alternative functions of vitamin D in monocytes and endothelial cells. First, we demonstrate vitamin D indirectly facilitates monocyte iron sequestration related to anemia of CKD. Then, we also show that vitamin D exhibits antioxidative

properties in endothelial cells that may play a beneficial in atherosclerotic plaque regression.

Taken together, we hope the work presented in this dissertation will provide new insights into the immune interactions that contribute to CKD pathogenesis or host protection. Understanding the interplay between the immune system and the endothelial microenvironment is a critical step to the eventual development of immunotherapies for CVD.

The dissertation of Jessica Layman Sea is approved.

Utpal Banerjee

Karen Marie Lyons

Luisa M Iruela-Arispe

Martin Hewison, Committee Co-Chair

John S. Adams, Committee Co-Chair

University of California, Los Angeles

2016

DEDICATION

To Uncle Jim

TABLE OF CONTENTS

LIST OF TABLES AND FIGURES viii
ACKNOWLEDGEMENTS xi
VITA xv
PUBLICATIONS xvi

Chapter 1: Introduction 1
References 15

Chapter 2: Fibroblast growth factor 23 inhibits extrarenal synthesis of 1,25-dihydroxyvitamin D in human monocytes 19
References 28

Chapter 3: Fibroblast growth factor 23 alters endothelial-driven monocyte lipid accumulation 33
References 66

Chapter 4: Suppression of iron-regulatory hepcidin by vitamin D 71
References 80

Chapter 5: 1,25-dihydroxyvitamin D mitigates hypoxic responses in human aortic endothelial cells 84
References 106

Chapter 6: Conclusion 110
References 114

LIST OF TABLES AND FIGURES

Chapter 1: Introduction

Figure 1.1 Prognosis of CKD by glomerular filtration rate and albuminuria 13

Figure 1.2 Figure 1.2 FGF23 and 1,25D regulation feedback loop 14

Chapter 2: Fibroblast growth factor 23 inhibits extrarenal synthesis of 1,25-dihydroxyvitamin D in human monocytes

Table 1. Expression of mRNA for FGFRs and Klotho in PBMCm 24

Table 2. Relative Expression of Vitamin D- and FGF23-Related Genes in PDm Versus PBMCm 27

Fig. 1. Expression and regulation of fibroblast growth factor receptors (FGFR) and Klotho in PBMCm 24

Fig. 2. FGF23 modulates FGFR signaling in PBMCm 25

Fig. 3. FGF23 suppresses expression and activity of CYP27B1 in PBMCm 26

Fig. 4. FGF23 suppresses expression CYP27B1 in monocytes from peritoneal dialysates 27

Supplemental Figure 1. Relationship between FGFR1 and Klotho mRNA expression and expression of genes associated with vitamin D metabolism and function in PBMCm 31

Supplemental Figure 2. Effect of toll-like receptor 2 activation on vitamin D- and FGF23-related gene expression in PBMCm 32

Chapter 3: Fibroblast growth factor 23 alters endothelial-driven monocyte lipid accumulation

Table 3.1 Expression of mRNA for FGFRs and Klotho in HAEC 54

Figure 3.1 Responses to FGF23 in HAEC 55

Figure 3.2 FGF23 alters lipid accumulation in co-cultures of HAEC and monocytes 57

Figure 3.3 CM_{FGF23} driven monocyte lipid accumulation is time-dependent 59

Figure 3.4 CM_{FGF23} specifically alters modified LDL uptake by monocytes 60

Figure 3.5 CM from HAEC treated with FGF23 alters monocyte lipid accumulation 62

Figure 3.6 HAEC secreted factor is above 10kDa 63

Figure 3.7 EDN1 mRNA expression in HAEC treated with FGF23 64

Supplemental Figure 3.1 FGF23 does not increase adhesion markers in HAEC 65

Chapter 4: Suppression of Iron-Regulatory Hepcidin by Vitamin D

Figure 1 Vitamin D suppresses expression of hepcidin (HAMP) in human monocytes and hepatocytes 74

Figure 2 VDR-mediated suppression of hepcidin (HAMP) gene expression by 1,25D 75

Figure 3 Effect of vitamin D metabolites on ferroportin and ferritin expression in human monocytes and hepatocytes 76

Figure 4 Effects of supplementation with vitamin D_2 on circulating hepcidin levels in healthy humans 77
Figure 5 Vitamin D and the hepcidin-ferroportin iron-regulatory axis 77
Supplemental Table 1 In silico nuclear receptor site prediction for vitamin D response elements in the *HAMP* gene promoter (-1071 bp) 82
Supplemental Figure 1 Effect of vitamin D on expression of hepcidin in mice 83

Chapter 5: 1,25-dihydroxyvitamin D mitigates hypoxic responses in human aortic endothelial cells

Figure 5.1 CYP27B1 expression in HAEC treated with TNFα 98
Figure 5.2 HAEC do not convert 25D to 1,25D at baseline or when stimulated with TNFα 99
Figure 5.3 Expression of the VDR in HAEC 101
Figure 5.4 HAEC and HUVEC responses to inflammatory-stimulation in vitamin D supplemented conditions 102
Figure 5.5 Effects of 1,25D on VEGF and DDIT4 expression in HAEC 104
Supplemental Figure 5.1 Expression of CYP27B1 in HAEC and HUVEC 105

ACKNOWLEDGEMENTS

First, I would like to acknowledge my joint laboratory mentors: Dr. Martin Hewison and Dr. John S. Adams. I would like to thank Dr. Martin Hewison for the guidance and support he provided during my graduate career. Your enduring optimism and support kept me going through even the most difficult projects. I would also like to thank Dr. John S. Adams for his support, and for giving me the independence to grow into a confident, self-sufficient scientist. With your help, I know I am fully prepared to continue my journey pursuing an academic career.

I would also like to thank the members of my doctoral committee: Dr. Utpal Banerjee, Dr. Karen Lyons, and Dr. Luisa Iruela-Arispe. Thank you for your many critiques and insights that have helped move my project forward and pushed me to think critically and independently. I would especially like to thank Dr. Banerjee, your confidence in me made a world of difference.

Additionally, I would like to thank Dr. Isidro Salusky and his team, whom have been instrumental in my success in graduate school. Isidro, Kate Wesseling-Perry, Justine Bacchetta, Renata Pereira, Barbara Gales, and Mark Hanudel, thank you for welcoming me into your team. To Isidro, thank you for your unwavering support and confidence in me as both a scientist and future physician. To Kate, who was the first to show excitement in this project, I am forever grateful for your encouragement to pursue it. You have been an inspiration. I'd also like to thank Justine for her friendship and guidance. Her contagious interest in FGF23 led me to study its effects in a cardiovascular setting.

I would also like to thank Phil Liu. His expertise and mentorship have been invaluable to my PhD training, and his humor and funny YouTube videos were the perfect dose of comedic relief.

To my lab mates, thank you for your friendship and support. In no particular order, I'd like to thank: Rene Chun, Avi De Leon, Alex Garcia, Nancy Liu, Kathryn Zavala, and Wareeratn "Joyce" Chengprapakorn. I would especially like to thank my undergraduate students, Michelle Khrom and Michelle Reynoso for their hard work and significant contributions to this project.

To all my friends and family who have supported me throughout this journey- thank you from the bottom of my heart.

My good friends, Karthika Balasubramanian and Miriam Guemes, I know you'll both hate that you're mentioned in this, but to borrow from Miriam- "that's why we're friends!" Thank you for your support, advice, and friendship. Especially all those times you stayed late with me when my experiments ran longer than expected- you'd think I'd be better at estimating these things by now.

To my parents and brother Russ, thank you for your unfaltering love and support through this process, and for reminding me of the world that exists outside of lab.

Most of all I'd like to thank my husband Matt, for your endless support through the most challenging times, and for always believing in me. I couldn't have done it without you.

Chapter 2 is a reprint of the full citation: Bacchetta J, Sea JL, Chun RF, Lisse TS, Wesseling-Perry K, Gales B, Adams JS, Salusky IB, Hewison M. Fibroblast growth factor 23 inhibits extrarenal synthesis of 1,25-dihydroxyvitamin D in human monocytes. J Bone Miner Res. 2013 Jan;28(1):46-55. doi: 10.1002/jbmr.1740. PubMed PMID: 22886720; PubMed Central PMCID: PMC3511915.

Chapter 3 is a version of the manuscript: Jessica L. Sea[1], Michelle Khrom[1], Avelino De Leon[2], Michelle Reynoso[1], Martin Hewison[3], Katherine Wesseling-Perry[4], Isidro Salusky[4], Philip T. Liu[2]. Fibroblast growth factor 23 alters endothelial-driven monocyte lipid accumulation. This manuscript is currently in preparation to submit to Arteriosclerosis, Thrombosis, and Vascular Biology. For specific contributions: JLS conceived the study, designed and performed experiments, and jointly prepared the manuscript with PTL; MK performed experiments, extracted RNA, and performed RT-PCR; AD performed flow cytometry assays; MR performed experiments; PIs: MH, KWP, IBS, PTL.

Chapter 4 is a reprint of the full citation: Bacchetta J, Zaritsky JJ, Sea JL, Chun RF, Lisse TS, Zavala K, Nayak A, Wesseling-Perry K, Westerman M, Hollis BW, Salusky IB, Hewison M. Suppression of iron-regulatory hepcidin by vitamin D. J Am Soc Nephrol. 2014 Mar;25(3):564-72. doi: 10.1681/ASN.2013040355. Epub 2013 Nov 7. PubMed PMID: 24204002; PubMed Central PMCID: PMC3935584.

Chapter 5 is a version of the manuscript: Jessica L. Sea[1], Michelle Khrom[1], Bing Li[4], Michelle Maritza Reynoso[1], Daniel Cohn[4], Martin Hewison[3], Philip T.

Liu[4]. 1,25-dihydroxyvitamin D mitigates hypoxic responses in human aortic endothelial cells. This manuscript is currently in preparation to submit to Journal of Bone and Mineral Research. For specific contributions: JLS jointly conceived the study with MH and PTL, designed and performed experiments, and jointly prepared the manuscript with PTL and KWP; MK performed experiments, conducted RNA extraction, and performed RT-PCR analysis, MR performed experiments, BL contributed to bioinformatics analysis. PIs: DC, IB, MH, KWP, and PTL.

This dissertation was supported by the following funding sources: Ruth L. Kirschstein National Research Service Award T32HL69766 (2012-2015); NIH/NIDDK R21 DK091672-01A1; NIH/NIDDK R01AR037399-01.

VITA

2010	B.S. Biology California State University Channel Islands Camarillo, California
2010	CSUCI Honors in Biology California State University Channel Islands Camarillo, California
2012-2015	Award Recipient UCLA Vascular Biology Training Grant University of California, Los Angeles
2011-2016	Graduate Student Researcher Department of Molecular, Cell, and Developmental Biology University of California, Los Angeles

PUBLICATIONS

Jessica L. Sea, Michelle Khrom, Avelino De Leon, Martin Hewison, Katherine Wesseling-Perry, Isidro Salusky, and Philip T. Liu. Fibroblast growth factor alters endothelial-driven macrophage lipid accumulation. *Manuscript in preparation for submission.*

Jessica L. Sea, Michelle Khrom, Bing Li, Michelle Maritza Reynoso, Katherine Wesseling-Perry, Isidro Salusky, Martin Hewison, Philip T. Liu. 1,25-dihydroxyvitamin D mitigates hypoxic responses in human aortic endothelial cells. *Manuscript in preparation for submission.*

Zhou, R., Park, J. W., Chun, R., Lisse, T., Garcia, A., Zavala, K., **Sea, J**., Lu, Z., Xu, J., Xing, Y., Adams, J., Hewison, M. Heterogeneous nuclear ribonucleoprotein C1/C2 links transcriptional and splicing actions of 1,25-dihydroxyvitamin D. *Submitted to Nucleic Acids Research.*

Bacchetta, J., Zaritsky, J. J., **Sea, J. L.**, Chun, R. F., Lisse, T. S., Zavala, K. Wesseling-Perry, K., Westerman M., Hollis B.W., Salusky I.B., Hewison, M. (2014). Suppression of Iron-Regulatory Hepcidin by Vitamin D. *Journal of the American Society of Nephrology: JASN*, *25*(3), 564–572. doi:10.1681/ASN.2013040355.

Bacchetta, J., **Sea, J. L.**, Chun, R. F., Lisse, T. S., Wesseling-Perry, K., Gales, B., Adams, J.S., Saluksky, I.B., Hewison, M. (2013). FGF23 inhibits extra-renal synthesis of 1,25-dihydroxyvitamin D in human monocytes. *Journal of Bone and Mineral Research: The Official Journal of the American Society for Bone and Mineral Research*, *28*(1), 46–55. doi:10.1002/jbmr.1740.

Chapter 1

Introduction

Chronic kidney disease: a brief overview

Chronic kidney disease (CKD) is a debilitating disease affecting over 26 million Americans, roughly 10% of Americans and up to 16% of the population worldwide [1-3]. CKD is defined by any structural and/or functional change in the kidney regardless of the cause that persists for at least 3 months [4]. The most common causes of renal disease are diabetes (44%) and high blood pressure (28%) [2, 3]. Renal dysfunction often goes undetected early in disease, and when left untreated CKD can lead to serious complications including cardiovascular diseases, inflammation, anemia, bone disease, nerve damage, and infections [5-10]. Despite similar incidence rates of CKD across sex and ethnicity, women and minorities are at a significantly higher risk for developing End Stage Renal Disease (ESRD) requiring dialysis and organ transplantation [3]. Causes for these differences are not clear; however, the increased prevalence of diabetes and hypertension in minority populations as well as limited access to healthcare may be contributing factors [11].

The severity of CKD is classified into 5 stages that are determined by glomerular filtration rate (GFR) and albuminuria as outlined in Figure 1 [4]. Stage 1 of CKD is characterized by normal renal function with a GFR above 90 mL/min; but with signs of kidney damage such as proteinuria or hematuria. In stage 2 of CKD, kidneys are performing at a less than optimal efficiency with a GFR between 60-89mL/min. However, due to the silent nature of CKD symptoms during stages 1 and 2, patients often go undiagnosed unless tests are being run to diagnosis other

conditions such as diabetes or high blood pressure, both of which are the leading causes of CKD. Depending on the cause of renal dysfunction, it can take months to years before patients notice changes that would lead them to seek medical care. Uncontrolled CKD grossly increases the risk of developing co-morbidities, most often hypertension, dyslipidemia, cardiovascular disease (CVD), and systemic inflammation [11].

Patients begin to experience symptoms of CKD during stage 3, which is split into two groups: 3a (GFR 45-59mL/min) and 3b (GFR 30-44mL/min). However, in this stage, the symptoms of CKD are relatively mild and rather non-specific: mild fatigue, loss of appetite, and difficulty concentrating. Secondary hyperparathyroidism and anemia start developing during stage 3, and become progressively worse as the disease moves into stage 4 CKD.

Stage 4, classified as severe CKD, is the point at which more serious uremic symptoms begin with patients experiencing nausea, vomiting, loss of appetite, cognitive disruptions, and nervous system issues resulting from the increase of uremia. Signs and symptoms of anemia, which is associated with CKD, include shortness of breath, fatigue, pallor, and tachycardia [12]. Signs and symptoms of renal osteodystrophy include bone pain, fractures, deformities, and, in children, growth failure. Often times, complications of renal dysfunction such as hypertension, anemia, and bone disease also arise during stage 3 CKD. With a GFR between 15-29mL/min, patients usually begin dialysis to manage waste product expulsion from the blood. Although all patients with CKD are at an increased risk

of CVD, stage 4 severe CKD is the most common stage at which patients develop cardiovascular diseases with congestive heart disease, atherosclerosis, and vascular calcifications being the most common. As kidney function declines to a GFR less than 15mL/min, patients enter end stage renal disease (ESRD) whereby the kidneys function at less than 5% efficacy. At this stage, urine production ceases, the physical and cognitive symptoms worsen, and patients require dialysis and/or kidney transplant for survival.

CKD precipitates several co-morbidities including systemic inflammation, dyslipidema, and cardiovascular disease (CVD) [5, 11]. Chronic inflammation and aberrant lipid profiles observed in CKD patients likely contribute to the accelerated rate at which patients develop CVD. There are no cures for CKD, therefore treatments focus on managing the systemic effects resulting from declining renal function. Co-morbid conditions of CKD add to the complexity of managing the patient's health and wellness, particularly when drugs are required to treat autoimmune diseases and/or hypertension would be cleared by in an otherwise healthy patient's kidneys.

Clinical components of renal disease

CKD is an endocrine disease impacting several organ systems and a multitude of autocrine, paracrine, and endocrine signaling networks. Molecules that are most significant and clinically relevant to CKD include: fibroblast growth factor (FGF) 23, vitamin D, phosphate, and parathyroid hormone (PTH). Elevated serum

FGF23 is the earliest detectable sign of renal dysfunction and is often observed with systemic inflammation [13, 14]. The etiology of increased FGF23 is not clear and its relation to chronic inflammation is widely unknown. Whether inflammation precedes the increase in serum FGF23 or vice-versa remains controversial [15, 16]. Also occurring early in CKD is a rise in serum phosphate that correlates with decreased renal output [17].

Although increased serum FGF23 levels are observed prior to elevations in serum phosphate, hyperphosphatemia associated with CKD contributes to increased FGF23 levels, hypocalcaemia, and vitamin D deficiency. Phosphate-induced decreases in serum calcium and 1,25-dihydroxyvitamin D3 (1,25D) is thought to be the leading cause of secondary hyperparathyroidism observed in CKD as phosphate binders taken by patients in renal failure have been shown to partially reduce elevated PTH levels. These mineral imbalances can lead to renal osteodystrophy associated with CKD resulting in brittle bones and growth impairment. In the early stages of CKD, circulating PTH levels remain steady; however as the disease progresses, despite using phosphate binders, PTH levels increase with decreasing GFR. Collectively, high PTH, high FGF23, and low vitamin D bioavailability, if left untreated, lead to severe bone disease and increase the risk of cardiovascular complications.

Several methods of treatment are employed to address the systemic metabolic changes caused by CKD. Dietary restrictions to reduce phosphate ingestion, as well as supplementation of phosphate binders, vitamin D, and calcium

are the primary modalities used to mitigate secondary hyperparathyroidism. However, some dietary restrictions can be difficult for patients to adhere to consistently; and even complete compliance only partially alleviates increasing PTH levels, which are inversely proportional to renal function. Currently, therapeutics to offset increasing FGF23 levels are not available; however, animal studies using neutralizing antibodies have demonstrated promise by lowering FGF23 levels and reducing secondary hyperparathyroidism in rats. This demonstrates the future possibility of lowering FGF23 levels early in CKD pathogenesis to potentially alleviate severe systemic metabolic imbalances in these patients. Furthermore, most cases of CKD are complicated by co-morbidities such as anemia, bone disease, high blood pressure, diabetes, and cardiovascular disease that also require close monitoring, as well as additional dietary guidelines, supplements, and mediations.

Regulation of vitamin D and FGF23

Vitamin D3, an inactive metabolite, undergoes a multi-step metabolism, carried out in several different tissues. It is converted by hepatic 25-hydroxylase to 25-hydroxyvitamin D3 (25D), a pre-hormone. The majority of circulating 25D is then converted in the kidney into the active metabolite 1,25-dihydroxyvitamin D3 (1,25D) by Cytochrome P450, Family 27, Subfamily B, Polypeptide 1 (CYP27B1) (Figure 1.2). However, extra-renal expression of CYP27B1 as well as 1,25D synthesis is well established in innate immune cells, including monocytes. Vitamin D functions classically to maintain skeletal integrity by regulating calcium and

phosphate balance. Deficiency in vitamin D results in disrupted in bone turnover and mineralization patterns leading to several bone diseases including rickets and osteomalacia. In the past few decades, extra-renal functions of vitamin D have elucidated key roles in immunomodulation via eliciting bacterial killing and regulating anti-inflammatory actions. However, the effects of vitamin D deficiency in chronic inflammatory diseases such as CKD and CVD remain to be fully characterized.

Under normal physiological conditions, 1,25D binds to intracellular vitamin D receptor (VDR), a transcription factor that subsequently heterodimerizes with retinoic acid receptor (RXR) to induce expression of several target genes. Excess serum 1,25D up-regulates expression of FGF23 in osteoblasts. In turn, FGF23 regulates phosphate reabsorption in the kidney and suppresses renal expression of CYP27B1. Together, FGF23 and vitamin D participate in a tightly regulated feedback system to maintain homeostatic balance within the bone-kidney axis.

Atherosclerosis: Pathogenesis and propagation of disease

Atherosclerosis is a disease in which fatty plaques build up on the luminal surface of arterial walls leading to CVD including coronary heart disease, peripheral heart disease, and stroke. Increased blood pressure, a sign of endothelial dysfunction, is the earliest clinically detectable sign of CVD, and is usually the result of inflammatory insults. Elevated lipid concentrations in the blood, particularly low-density lipoprotein (LDL) and its variants are thought to be key

players in the initiation of CVD by activating monocytes and triggering endothelial responses. Endothelial activation in response to inflammatory cytokines, chemokines, and activated monocytes consists of increased expression of cell surface adherence markers: vascular cell adhesion marker (VCAM1), intracellular cell adhesion marker (ICAM1), and endothelial selectin (E-sel). These endothelial cell surface proteins interact with receptors on the surface of monocytes, functioning to slow their pace and eventually facilitate monocyte extravasation into the sub-endothelial space. As activated monocytes traverse the endothelial barrier, becoming macrophages, phenotypic and functional changes occur to allow them to resolve the issues that triggered the initial activation. Build-up of oxidized LDL (ox-LDL) in the sub-endothelial space initiates monocyte recruitment and cascading activation events. Monocytes recruited by ox-LDL mature into phagocytic macrophages to engulf and clear excess ox-LDL. As the disease progresses, lipid-engulfing macrophages become out-numbered by the increasing concentration of lipids, and become unable to effectively clear ox-LDL, leading to the formation of an atherosclerotic plaque. This pattern continues through the early stages of the disease, with increasing numbers of phagocytic macrophages engulfing excessive amounts of lipids to eventually form lipid-laden foam cells. These apoptotic foam cells, unable to escape the sub-endothelial space burst, expelling their intracellular contents. Pro-inflammatory macrophages respond to the cell debris by flooding the sub-endothelial space and secreting chemokines to attract additional immune cells, thus perpetuating the vicious and futile cycle.

Collectively over time, excess ox-LDL, foam cells, inflammatory macrophages, and cell debris form a necrotic lipid core. As the necrotic core grows larger from accumulating particles, stress builds on the thin layer of dysfunctional endothelial cells maintaining the lipid core. As the lesion grows, this necrotic cap becomes brittle, increasing the risk of plaque rupture. Anti-inflammatory macrophages in the lipid core that classically function in wound repair secrete matrix metalloproteinases (MMP) that act to stabilize the necrotic cap.

Atherosclerotic lesions are littered with a wide range of polarized macrophage subtypes; however, those functioning in a pro-inflammatory or anti-inflammatory capacity are the most prevalent and most influential in the lipid core. The balance of resident macrophage subtypes in the lipid core largely determines the composition of the lesion and the surrounding extracellular matrix proteins. Certain macrophage subtypes are beneficial early in the disease, but over time become counterproductive to plaque resolution. During early pathogenesis, macrophages polarized toward either pro-inflammatory or lipid-engulfing phenotypes are necessary for lipid clearance. However, over time they become part of the problem as pro-inflammatory macrophages disburse cytokines and chemokines that recruit additional immune cells into the plaque, thereby increasing the size of lipid core. Later in the disease, apoptotic foam cells also contribute to plaque growth and destabilization. Anti-inflammatory macrophages that are not necessarily beneficial or harmful at the start of the disease are invaluable later on as they function to stabilize the plaque, and in some cases can induce plaque

regression. Mature atherosclerotic plaques containing a higher percentage of anti-inflammatory macrophages are associated with better disease prognosis whereas lesions with higher proportions of pro-inflammatory macrophages are associated with poor prognosis. Atherosclerosis is a complex disease, and ultimately, understanding the contributions of the cell types involved in the pathogenesis and progression of the disease will facilitate the development of increasingly targeted therapeutics to treat it.

Atherosclerosis in CKD

Cardiovascular emergencies stemming from CVD are the leading cause of death in patients with CKD, followed by infection resulting from a compromised immune system. Renal dysfunction is a huge risk factor for developing CVD, and as the incidence of CKD increases, so does the incidence of CVD. Over 10% of the US population suffers from CKD, and this number is projected to increase, adding to the public health burden in the coming years. Current treatment limitations for renal failure aimed at managing the secondary effects of CKD until transplantation, highlights the urgency for new therapeutics targeting molecular aberrancies contributing to cardiovascular dysfunction. Of the many potential factors that are dysregulated in CKD, elevation of FGF23 occurs at the onset of renal decline with serum concentrations dramatically increasing over the lifetime of the disease. Previous studies have demonstrated correlations between elevated FGF23 and left ventricular hypertrophy suggesting FGF23 may play a role in other cardiovascular

pathologies associated with CKD. Calcium, phosphorus, and vitamin D dysregulation are also huge risk factors for CVD.

One of the most prevalent cardiovascular events associated with CKD is atherosclerosis leading to CVD [18-20]. The multifaceted nature of both CVD and CKD compounds the co-morbid etiology; and the chronological order of events leading to the diseases, both independently and together, remains largely unclear. However, there is a consensus among the scientific and medical communities regarding the main players contributing to increased risk of CVD in CKD. Several traditional risk factors for developing CVD in the absence of renal dysfunction include hypertension, aberrant lipid profiles, and chronic inflammation [18]. Each of these risk factors can also be caused by CKD and therefore likely play important roles in the pathogenesis of CKD-induced CVD.

In addition to filtration and excretion of waste products from the blood, the kidneys are also responsible for regulating vasoconstriction and vasodilation thereby controlling blood pressure. Patients with CKD not caused by hypertension are at an increased risk of developing high blood pressure as renal function declines. Rising blood pressure leads to an increase in turbulent blood flow causing endothelial dysfunction, a key step in initiating CVD. Aberrant lipid profiles, including high concentrations of cholesterol and ox-LDL, are commonly observed in CKD. Increasing levels of ox-LDL in circulation accumulate in the sub-endothelial space, triggering activation and extravasation of monocytes to aid in lipid clearance. In the short-term, this is a vital part of maintaining tissue homeostasis; however,

chronically elevated levels of ox-LDL and monocyte activation can lead to eventual systemic inflammation and atherosclerotic plaque formation.

Particularly troubling is the correlation between childhood renal disease and cardiovascular disease [21]. Children lacking the traditional risk factors for CVD seen in the majority of adults with CKD- smoking, hypertension, diabetes, etc- are still highly susceptible to CVD [22-24]. Just like adults, children with CKD die from cardiovascular pathologies resulting from renal dysfunction [25]. FGF23, which is abnormally high very early in CKD, is a likely contributor to the cardiovascular events associated with CKD. However, little is known about the effects of FGF23 on the cardiovascular system and the mechanism by which it contributes to CVD. This dissertation aims to elucidate the functions of FGF23 in the cardiovascular system and clarify its role in CKD/CVD pathology.

FIGURE 1.1

Prognosis of CKD by glomerular filtration rate (GFR) and albuminuria

Green= low risk

Yellow= moderate risk

Orange= high risk

Red= very high risk

GFR categories (ml/min/ 1.73 m^2) Description and range				Persistent albuminuria categories Description and range		
				A1	A2	A3
				Normal to mildly increased	Moderately increased	Severely increased
				<30 mg/g <3 mg/mmol	30-300 mg/g 3-30 mg/mmol	>300 mg/g >30 mg/mmol
	G1	Normal or high	≥90			
	G2	Mildly decreased	60-89			
	G3a	Mildly to moderately decreased	45-59			
	G3b	Moderately to severely decreased	30-44			
	G4	Severely decreased	15-29			
	G5	Kidney failure	<15			

Figure 1.1 Prognosis of CKD by glomerular filtration rate and albuminuria

Figure adapted from KDIGO Clinical Practice Guideline for the Evaluation and Management of Chronic Kidney Disease 2012; pg19.

FIGURE 1.2

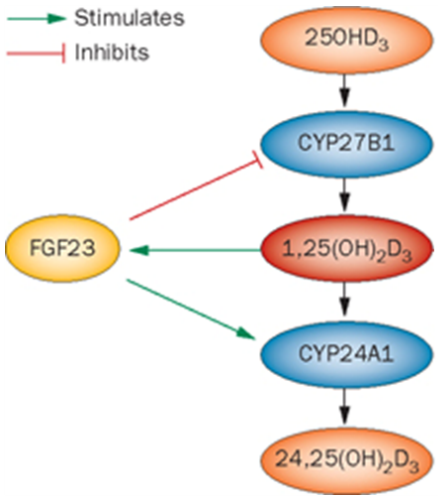

Figure 1.2 FGF23 and 1,25D regulation feedback loop

Pre-hormone $25OHD_3$ (25D) is converted to active $1,25(OH)_2D_3$ (1,25D) by CYP27B1. CYP24A1 metabolizes 1,25D to inactive $24,25(OH)_2D_3$. 1,25D induces FGF23 secretion from the bone. In turn, FGF23 down regulates 1,25D in two ways: by inhibiting CYP27B1 and by inducing CYP24A1. Figure adapted from Sterling, K.A., et al., *The immunoregulatory function of vitamin D: implications in chronic kidney disease.* Nat Rev Nephrol, 2012. 8(7): p. 403-12.

REFERENCES

1. Jha, V., et al., *Chronic kidney disease: global dimension and perspectives.* Lancet, 2013. **382**(9888): p. 260-72.
2. *Chronic Kidney Disease (CKD) Surveillance Project*. [cited 2016; Available from: https://nccd.cdc.gov/ckd/.
3. (CDC), C.f.D.C.a.P. *National Chronic Kidney Disease Fact Sheet: General Information and National Estimates on Chronic Kidney Disease in the United States*. 2014; Available from: http://www.cdc.gov/diabetes/pubs/pdf/kidney_factsheet.pdf.
4. KDIGO, *Clinical Practice Guideline for the Evaluation and Management of Chronic Kidney Disease*, in *Kidney Disease: Improving Global Outcomes (KDIGO) CKD Work Group*2012, Kidney International Supplements. p. 1-150.
5. Foley, R.N., P.S. Parfrey, and M.J. Sarnak, *Clinical epidemiology of cardiovascular disease in chronic renal disease.* Am J Kidney Dis, 1998. **32**(5 Suppl 3): p. S112-9.
6. Shulman, N.B., et al., *Prognostic value of serum creatinine and effect of treatment of hypertension on renal function. Results from the hypertension detection and follow-up program. The Hypertension Detection and Follow-up Program Cooperative Group.* Hypertension, 1989. **13**(5 Suppl): p. I80-93.

7. Stenvinkel, P., et al., *Inflammation and outcome in end-stage renal failure: does female gender constitute a survival advantage?* Kidney Int, 2002. **62**(5): p. 1791-8.

8. Impellizzeri, D., et al., *Targeting inflammation: new therapeutic approaches in chronic kidney disease (CKD).* Pharmacol Res, 2014. **81**: p. 91-102.

9. Toyoda, K. and T. Ninomiya, *Stroke and cerebrovascular diseases in patients with chronic kidney disease.* Lancet Neurol, 2014. **13**(8): p. 823-33.

10. Vellanki, K. and V.K. Bansal, *Neurologic Complications of Chronic Kidney Disease.* Curr Neurol Neurosci Rep, 2015. **15**(8): p. 50.

11. Ene-Iordache, B., et al., *Chronic kidney disease and cardiovascular risk in six regions of the world (ISN-KDDC): a cross-sectional study.* Lancet Glob Health, 2016. **4**(5): p. e307-19.

12. Tsagalis, G., *Renal anemia: a nephrologist's view.* Hippokratia, 2011. **15**(Suppl 1): p. 39-43.

13. Isakova, T., et al., *Fibroblast growth factor 23 is elevated before parathyroid hormone and phosphate in chronic kidney disease.* Kidney Int, 2011. **79**(12): p. 1370-8.

14. Portale, A.A., et al., *Disordered FGF23 and mineral metabolism in children with CKD.* Clin J Am Soc Nephrol, 2014. **9**(2): p. 344-53.

15. Dai, B., et al., *A comparative transcriptome analysis identifying FGF23 regulated genes in the kidney of a mouse CKD model.* PLoS One, 2012. **7**(9): p. e44161.

16. Munoz Mendoza, J., et al., *Fibroblast growth factor 23 and Inflammation in CKD.* Clin J Am Soc Nephrol, 2012. **7**(7): p. 1155-62.

17. Penne, E.L., et al., *Role of residual renal function in phosphate control and anemia management in chronic hemodialysis patients.* Clin J Am Soc Nephrol, 2011. **6**(2): p. 281-9.

18. Kotur-Stevuljevic, J., et al., *Hyperlipidemia, oxidative stress, and intima media thickness in children with chronic kidney disease.* Pediatr Nephrol, 2013. **28**(2): p. 295-303.

19. Turkmen, K., et al., *The relationship between oxidative stress, inflammation, and atherosclerosis in renal transplant and end-stage renal disease patients.* Ren Fail, 2012. **34**(10): p. 1229-37.

20. Fyfe-Johnson, A.L., et al., *Serum fibroblast growth factor-23 and incident hypertension: the atherosclerosis risk in communities study.* J Hypertens, 2016.

21. Flynn, J.T., *Cardiovascular disease in children with chronic renal failure.* Growth Horm IGF Res, 2006. **16 Suppl A**: p. S84-90.

22. Chavers, B.M., et al., *Cardiovascular disease in pediatric chronic dialysis patients.* Kidney Int, 2002. **62**(2): p. 648-53.

23. Lin, I.C., et al., *Low urinary citrulline/arginine ratio associated with blood pressure abnormalities and arterial stiffness in childhood chronic kidney disease.* J Am Soc Hypertens, 2016. **10**(2): p. 115-23.

24. Shroff, R.C., et al., *Circulating angiopoietin-2 is a marker for early cardiovascular disease in children on chronic dialysis.* PLoS One, 2013. **8**(2): p. e56273.

25. Parekh, R.S., et al., *Cardiovascular mortality in children and young adults with end-stage kidney disease.* J Pediatr, 2002. **141**(2): p. 191-7.

Chapter 2

Fibroblast growth factor 23 inhibits extrarenal synthesis of 1,25-dihydroxyvitamin D in human monocytes

PREFACE

Serum levels of FGF23 are significantly elevated even in the earliest stages of CKD, and continue to rise throughout disease progression. Playing a role in endocrine mineral homeostasis, FGF23 down regulates renal metabolism of vitamin D. The pre-active form of vitamin D, 25-hydroxyvitamin D (25D), is converted by Cytochrome P450, Family 27, Subfamily B, Polypeptide 1 (CYP27B1) to the active metabolite 1,25-dihydroxyvitamin D3 (1,25D). By suppressing expression of CYP27B1, FGF23 reduces 1,25D synthesis and secretion.

Several extra-renal functions of vitamin D have been characterized, particularly in monocytes, which express CYP27B1 and convert 25D to 1,25D. Active vitamin D plays several roles in mediating immune responses to bacterial infection, functioning both as an autocrine and paracrine effector. The aim of this paper was to characterize extra-renal vitamin D functions in a pathological setting mimicking CKD. Several *in vitro* models were employed including monocyte cultures obtained from health donors as well as monocytes from patients in renal failure.

The data presented in this publication illustrates the regulatory effects of FGF23 on vitamin D metabolism and subsequent bioavailability in monocytes. Our results suggest a mechanism by which FGF23 may quench vitamin D-driven immune responses necessary for CKD patients to combat infections.

ORIGINAL ARTICLE

JBMR

Fibroblast Growth Factor 23 Inhibits Extrarenal Synthesis of 1,25-Dihydroxyvitamin D in Human Monocytes

Justine Bacchetta,[1,2] Jessica L Sea,[1] Rene F Chun,[1] Thomas S Lisse,[1] Katherine Wesseling-Perry,[2] Barbara Gales,[2] John S Adams,[1] Isidro B Salusky,[2] and Martin Hewison[1]

[1]UCLA Orthopaedic Hospital, Department of Orthopaedic Surgery, Orthopedic Hospital Research Center, David Geffen School of Medicine, University of California at Los Angeles, Los Angeles, CA, USA

[2]Department of Pediatrics, David Geffen School of Medicine, University of California at Los Angeles, Los Angeles, CA, USA

ABSTRACT

Vitamin D is a potent stimulator of monocyte innate immunity, and this effect is mediated via intracrine conversion of 25-hydroxyvitamin D (25OHD) to 1,25-dihydroxyvitamin D ($1,25(OH)_2D$). In the kidney, synthesis of $1,25(OH)_2D$ is suppressed by fibroblast growth factor 23 (FGF23), via transcriptional suppression of the vitamin D-activating enzyme 1α-hydroxylase (CYP27B1). We hypothesized that FGF23 also suppresses CYP27B1 in monocytes, with concomitant effects on intracrine responses to $1,25(OH)_2D$. Healthy donor peripheral blood mononuclear cell monocytes (PBMCm) and peritoneal dialysate monocyte (PDm) effluent from kidney disease patients were assessed at baseline to confirm the presence of mRNA for FGF23 receptors (FGFRs), with Klotho and FGFR1 being more strongly expressed than FGFR2/3/4 in both cell types. Immunohistochemistry showed coexpression of Klotho and FGFR1 in PBMCm and PDm, with this effect being enhanced following treatment with FGF23 in PBMCm but not PDm. Treatment with FGF23 activated mitogen-activated protein kinase (MAPK) and protein kinase B (Akt) pathways in PBMCm, demonstrating functional FGFR signaling in these cells. FGF23 treatment of PBMCm and PDm decreased expression of mRNA for CYP27B1. In PBMCm this was associated with downregulation of 25OHD to $1,25(OH)_2D$ metabolism, and concomitant suppression of intracrine induced 24-hydroxylase (CYP24A1) and antibacterial cathelicidin (LL37). FGF23 suppression of CYP27B1 was particularly pronounced in PBMCm treated with interleukin-15 to stimulate synthesis of $1,25(OH)_2D$. These data indicate that FGF23 can inhibit extra-renal expression of CYP27B1 and subsequent intracrine responses to $1,25(OH)_2D$ in two different human monocyte models. Elevated expression of FGF23 may therefore play a crucial role in defining immune responses to vitamin D and this, in turn, may be a key determinant of infection in patients with chronic kidney disease (CKD).

KEY WORDS: MONOCYTES; VITAMIN D; INNATE IMMUNITY; FGF23; PERITONEAL DIALYSIS

Introduction

Fibroblast growth factor 23 (FGF23) is a protein synthesized by osteocytes and osteoblasts that plays a key role in the "bone-parathyroid-kidney" axis and the regulation of phosphate/calcium/vitamin D metabolism.[1–3] FGF23 acts mainly as a phosphaturic factor, inhibiting the expression of type IIa sodium-phosphate co-transporters on the apical membrane of proximal tubular cells, thus leading to inhibition of phosphate reabsorption.[4] However, FGF23 also suppresses renal synthesis of the active form of vitamin D, 1,25-dihydroxyvitamin D ($1,25(OH)_2D$) by inhibiting expression of the enzyme 25-hydroxyvitamin D-1α-hydroxylase (CYP27B1) while stimulating the catabolic enzyme vitamin D-24-hydroxylase (CYP24A1).[4] FGF23 null mice present with a premature aging phenotype as well as severe growth retardation, abnormal skeletogenesis, vascular and soft tissue calcification, hyperphosphatemia, and increased renal expression of CYP27B1.[5] The importance of CYP27B1 as a target for FGF23 is further illustrated by the abrogation of FGF23-knockout skeletal and biochemical abnormalities in FGF23/CYP27B1 double-knockout mice.[6,7]

In addition to its effects on mineral and skeletal homeostasis, vitamin D can also act as a potent modulator of immune function.[8,9] In particular, active $1,25(OH)_2D$ can enhance innate immune handling of bacteria via the induction of antibacterial proteins such as cathelicidin (LL37) and β-defensin 2.[10,11] Cells such as monocytes expressing both CYP27B1 and the nuclear vitamin D receptor (VDR) are able to achieve this by localized

Received in original form October 27, 2011; revised form July 10, 2012; accepted August 2, 2012; accepted manuscript online August 9, 2012.
Address correspondence to: Martin Hewison, PhD, UCLA Orthopaedic Hospital Department of Orthopaedic Surgery, 615 Charles E. Young Drive South, Room 410D, Los Angeles, CA 90095-7358, USA. E-mail: mhewison@mednet.ucla.edu
Additional Supporting Information may be found in the online version of this article.

Journal of Bone and Mineral Research, Vol. 28, No. 1, January 2013, pp 46–55
DOI: 10.1002/jbmr.1740

conversion of 25OHD to $1,25(OH)_2D$ and subsequent VDR-mediated transactivation of antibacterial proteins.[12,13] This intracrine mode of action is enhanced by a variety of immunomodulatory factors, notably following the recognition of pathogen-associated molecular patterns by pattern-recognition receptors.[12,13] Monocyte synthesis of $1,25(OH)_2D$ and associated induction of antibacterial activity can also be enhanced by cytokines such as interleukin-15 (IL-15),[14] and interferon γ (IFNγ).[15] Conversely, other cytokines such as IL-4 suppress monocyte accumulation of $1,25(OH)_2D$ by enhancing its catabolism via the enzyme 24-hydroxylase (CYP24A1), and thereby inhibit intracrine induction of antibacterial activity in these cells.[15] These observations highlight the pivotal importance of vitamin D metabolism in mediating innate immune responses to infection, and underline the potential immune impact of factors that are able to regulate this metabolism. In the current study, we sought to determine whether FGF23 can contribute to this immune regulation of vitamin D metabolism.

In humans, aberrant expression of FGF23 was initially linked to hypophosphatemic rickets,[16] but current data suggest that this is far more complex, and includes a role for FGF23 in oncogenic osteomalacia.[17] In chronic kidney disease (CKD), elevated serum levels of FGF23 are detectable at early stages of the disease, prior to dysregulation of serum phosphate and parathyroid hormone (PTH).[18,19] In this setting, FGF23 levels have a prognostic value, with higher levels of serum FGF23 being associated with poorer health outcomes.[20–23] Although this appears to be a result, at least in part, of vascular and atherogenic effects of FGF23,[24,25] infection is also a key cause of mortality in CKD patients. Aside from the increased risk of infection due to immunosuppressive therapies in CKD patients undergoing kidney transplantation,[26] CKD itself is a state of acquired immune deficiency.[27] The incidence of bacterial infections in CKD dialysis patients is higher than in the general population[28,29] and infections are the second leading cause of death in such patients. The immune dysfunction observed in CKD patients, such as impaired polymorphonuclear cell apoptosis,[30] has been attributed to many different factors, including iron overload, uremic toxins, and dialysis.[27] To date, there have been no published studies of FGF23 and immune function, although some reports of FGF23-null mice have described atrophy of the thymus, spleen, and lymph nodes, and decreased capacity for T cell proliferation.[6] In the current study we explored a possible role for FGF23 as a mediator of immune dysfunction via its effects on vitamin D metabolism in monocytes.

Materials and Methods

Isolation and initial treatment of peripheral blood mononuclear cells from healthy donors

Ficoll-isolated peripheral blood mononuclear cells (PBMCs) derived from anonymous healthy donors (screened in accordance with standard transfusion medicine protocols) were obtained from the Center for AIDS Research Virology Core/BSL3 Facility (supported by NIH award AI-28697 and by the UCLA AIDS Institute and the UCLA Council of Bioscience Resources, Los Angeles, CA, USA). PBMC monocytes (PBMCm) were enriched by adherence by incubating 5×10^6 PBMCs per well in 12-well plates for 2 hours in Roswell Park Memorial Institute medium (RPMI) (Invitrogen, Carlsbad, CA, USA) with 1% human serum (HS) (Human AB serum; Omega Scientific, Tarzana, CA, USA).

Isolation of monocytes from peritoneal dialysate effluents by iterative centrifugation

Samples of overnight dwell dialysates were collected from patients undergoing peritoneal dialysis as approved by the UCLA Human Subject Protection Committee, with consent forms being obtained from all parents/patients. Dialysate samples were decanted into 500-mL sterile centrifuge tubes, and then centrifuged at 1200*g* for 10 minutes at room temperature. Supernatants were discarded and cell pellets were combined and re-centrifuged using the same parameters. After again discarding supernatants, viable cells were counted by hemocytometer following staining with Trypan blue. After a third centrifugation the remaining cells were used in vitro for isolation of peritoneal dialysate monocytes (PDm). PDm were selected by adherence by incubating 5×10^6 PD cells per well in 12-well plates for 12 hours in RPMI with 1% HS. All samples were obtained from patients with no evidence of peritonitis.

Culture and treatment of PBMCm and PDm

PBMCm and PDm were cultured at 37°C in 5% CO_2 in 12-well plastic cell culture plates using medium containing RPMI 1640, 10% HS, and granulocyte-macrophage colony stimulating factor (GM-CSF) 10 IU/mL (PeproTechInc, Rocky Hood, NJ, USA) for various time periods (6 or 24 hours). Treatments were carried out using recombinant human FGF23 (100 ng/mL, 2604-FG; R&D Systems, Minneapolis, MN, USA), recombinant human IL-15 (200 ng/mL) (247-IL; R&D Systems) or both in comparison to vehicle-treated cells (PBS 1×). The pan fibroblast growth factor receptor (FGFR) inhibitor PD173074 (250 nM) (Sigma Aldrich, St Louis, MO, USA) was used 1 hour before treating cells with FGF23, with control cells receiving DMSO as vehicle. At the end of incubation periods cells were either lysed with RNAzol and frozen at –80°C or processed for Western blot analyses. All culture conditions were carried out in duplicate for RT-PCR analyses.

Extraction of RNA and reverse transcription

After lysing cells PBMCm or PDm with RNAzol, RNA was extracted using chloroform, isopropanol, ethanol, and glycogen, as described.[13] After resuspending the resulting RNA in RNase-free water, aliquots (300 ng) were reverse-transcribed as recommended by the manufacturer (SuperScript III Reverse Transcriptase; Invitrogen) as described.[13]

Quantitative real-time RT-PCR amplification of cDNAs

Expression of mRNAs for VDR, CYP27B1, CYP24A1, LL37, fibroblast growth factor receptor (FGFR)1, FGFR2, FGFR3, FGFR4, Klotho, and tumor necrosis factor α (TNF-α) was quantified using a Stratagene MX3005P device using PBMCm or PDm, as recommended by the manufacturer and as described.[13]

Approximately 7.5 ng of cDNA was used per reaction. All reactions were normalized by multiplex analysis with the housekeeping 18S rRNA gene (Applied Biosystems, Foster City, CA, USA). Data were obtained as threshold cycle (Ct) values, corresponding to the cycle number at which logarithmic PCR plots cross a calculated threshold line, and were further used to determine the change in Ct values (ΔCt), corresponding to the difference between the Ct of the target gene and the Ct of the housekeeping 18S rRNA gene. PCR amplification of target gene cDNA was conducted using TaqMan human gene expression assays, as described.[13] The probes and primer kits used for each gene were as follows: Hs00172113-m1 for VDR, Hs00168017-m1 for CYP27B1, Hs00167999-m1 for CYP24A1, Hs00189038-m1 for LL37, Hs00915134-g1 for FGFR1, Hs01552926-m1 for FGFR2, Hs00179829-m1 for FGFR3, Hs01106908-m1 for FGFR4, Hs00183100-m1 for Klotho, and Hs00174128-m1 for TNFα (Applied Biosystems). All reactions were amplified under the following conditions: 95°C for 10 minutes followed by 40 cycles of 95°C for 30 seconds, 55°C for 1 minute, and 72°C for 1 minute. Reactions were initially expressed as mean ± SD ΔCt values and values for fold-change relative to vehicle-treated cells were determined using the equation $2^{-\Delta Ct}$.

Western blot analyses

For Western blot analysis of FGFR-mediated MAPK and Akt phosphorylation pathways in PBMCm, preliminary experiments showed that optimal expression of phosphorylated MAPK (pMAPK) and Akt (pAkt) was achieved after serum-starvation (0.1% HS) of these cells for 1 and 2 hours, respectively. During this serum starvation period, cells were treated with vehicle or an FGFR inhibitor (FGFRi, 250 nM), and then treated for a further 1 hour with either vehicle, FGF23 (100 ng/mL), FGFRi (250 nM), or FGF23 in combination with FGFRi. At the end of this treatment period, cells were treated with protein lysis buffer (NP40 Cell Lysis Buffer; Invitrogen, Camarillo, CA, USA), the proteinase inhibitor phenylmethylsulfonyl fluoride (PMSF), a proteinase inhibitor cocktail (P8340, 10 μL per mL of NP40; Sigma Aldrich, St. Louis, MO, USA) and phosphatase inhibitor cocktail (P5726, 10 μL per mL of NP40; Sigma Aldrich), and centrifuged at 4°C at 5000*g* for 20 minutes. Supernatants were then collected and stored at −20°C. Equal amounts of lysate protein were separated by electrophoresis using 10% SDS-PAGE gels with a biotinylated protein ladder (7727; Cell Signaling Technology, Danvers, MA, USA). Resulting blots were incubated for 24 hours with primary antibodies directed against total MAPK (p44/42 Erk1/2) (dilution 1/1000), phosphoMAPK (p44/42 Erk1/2) (dilution 1/800), total Akt (1/1000) and phospho-Akt (1/400) (all Cell Signaling Technology, Danvers, MA, USA; catalog numbers 9102, 9101, 4691, and 4060, respectively). A horseradish peroxidase (HRP) system with an enhanced chemiluminescence (ECL) system was then used for the incubation of secondary antibodies (1 hour, dilution 1/2000) and image development (Phototype-HRP Western blot detection system anti-rabbit 7074, anti-mouse 7076, anti-biotin 7075, and 20× LumiGlo Reagent/20× Peroxide 7003; Cell Signaling Technology). Western blot analyses were quantified using ImageJ software (NIH, Bethesda, MD, USA).

Immunofluorescence analyses

PBMCm or PDm were seeded at 2×10^6 per well in a four-well glass slide (Lab Tek II Chamber Slide System; NalgeNuncInc, Naperville, IL, USA), and cultured in the same medium and with the same reagents described above. After an initial fixation in 500 μL per well of paraformaldehyde (4%) for 10 minutes, slides were subject to the following: three washes with PBS 1×; incubation with 500 μL of a mixture of PBS 1× and Tween 0.2% for 10 minutes; three washes with PBS 1×; incubation with 500 μL of a mixture of PBS 1× and dry milk 5% for 30 minutes; three washes with PBS 1×; incubation for 1 hour in 300 μL of a mixture of PBS 1×, bovine serum albumin, and the following primary antibodies: FGFR1 (Flg-C-15-sc-121, 1/100; Santa Cruz Biotechnologies, Inc., Santa Cruz, CA, USA) and Klotho (246, 1/100, a kind gift from Dr. Jeffrey Lavigne; Immutopics, Inc., San Clemente, CA, USA). After three washes with PBS 1×, slides were then incubated with secondary antibodies labeled with Alexa 488 and 594 (anti-goat and anti-rabbit; Invitrogen, Camarillo, CA, USA) for 1 hour, washed three times with PBS 1×. Nuclear staining was carried out using 100 μL of 4′,6-diamidino-2-phenylindole dihydrochloride (DAPI; Sigma-Aldrich) (1/10 000 for 5 minutes). Slides were then fixed with mounting media (Prolong Gold Antifade Reagent, P36930; Invitrogen) and stored at 4°C in the dark. Imaging was then carried out using a 60× lens, with the Nikon NIS Elements software.

Analysis of 25OHD metabolism by PBMCm

The effects of FGF23 on synthesis of $1,25(OH)_2D$ and 24,25-dihydroxyvitamin D ($24,25(OH)_2D$) by PBMCm were assessed by quantifying the metabolism of radiolabeled 25OHD as described.[31] Briefly, aliquots of cells were incubated with radiolabeled ^{3}H-25OHD substrate (300,000 cpm, 155Ci/mmol; Perkin Elmer, Waltham, MA, USA) for 6 hours in serum-free culture medium. The resulting mix of ^{3}H-vitamin D metabolites was then extracted from the total cell lipids using initial C18 Sep-pak purification (Waters, Milford, MA, USA) and subsequent HPLC (ZorbaxSil column; Agilent, Santa Clara, CA, USA) separation of 1α-hydroxylated and 24-hydroxylated vitamin D metabolites. ^{3}H-25OHD, ^{3}H-$24,25(OH)_2D$ and ^{3}H-$1,25(OH)_2D$ was quantified by Beta-Ram in-line scintillation counting (Lablogic, Brandon, FL, USA). Data were reported as femtomoles of vitamin D metabolites produced/hour/10^6 cells from $n = 5$ separate cell preparations.

Statistics

Data are presented as mean ± SEM for fold-changes in mRNA expression and HPLC metabolism data, and as mean ± SD for raw RT-PCR data and Western blot analyses. Experimental means were compared statistically using an unpaired Student's *t* test. Where indicated, multifactorial data involving FGF23 and co-treatments were compared using one way analysis of variance (ANOVA) with the Holm-Sidak method used as a post hoc multiple comparison procedure. Statistical analyses were carried out using raw ΔCt values and fold-changes. Spearman correlation test was used for bivariate analyses.

Table 1. Expression of mRNA for FGFRs and Klotho in PBMCm

	ΔCt (mean ± SD)	Fold change to relative to FGFR1
FGFR1	11.32 ± 1.56	1
FGFR2	22.15 ± 2.07	0.00055
FGFR3	Undetectable	0
FGFR4	24.34 ± 1.90	0.00012
Klotho	21.12 ± 2.04	0.00112

Expression of mRNA for FGFR1, -2, -3, -4, and Klotho in baseline (untreated) PBMCm. Data are shown as mean ΔCt PCR amplification values ± SD, normalized to expression of the housekeeping gene 18S rRNA (central column), and fold-change in mRNA expression relative to the most highly expressed mRNA (FGFR1) (right column), both $n = 35$ donor batches of PBMCm.

FGFR = fibroblast growth factor receptor; PBMCm = peripheral blood mononuclear cell–derived monocytes; ΔCt = threshold cycle change.

Results

Expression and regulation of FGFRs in PBMCm

To assess the ability of monocytes to respond to FGF23, PBMCm were analyzed for expression of different FGFRs and the FGFR co-receptor Klotho. As shown in Table 1, basal, untreated cultures of PBMCm expressed mRNA for FGFR1, -2 and -4 as well as Klotho but did not express FGFR3. Although expression of FGFR1 was much higher than other FGFRs or Klotho, analysis of PBMCm from multiple donors showed a strong positive correlation between mRNA for FGFR1 and Klotho (Fig. 1*A*), CYP27B1 (Supplemental Fig. 1A), and the antibacterial factor LL37 (Supplemental Fig. 1B), but not CYP24A1 (Supplemental Fig. 1C). Treatment of PBMCm with FGF23 (100 ng/mL) suppressed expression of mRNA for Klotho at 6 hours, and FGFR1 at 24 hours (Fig. 1*B*). Immunofluorescence confirmed that PBMCm express protein for Klotho and FGFR1, with coincident expression of the two proteins in some but not all untreated PBMCm cells (Fig. 1*C*). Treatment with FGF23 (24 hours) enhanced expression of protein for Klotho and FGFR1 in some but not all cells (Fig. 1*C*).

Effects of FGF23 on FGFR signaling in PBMCm

Having demonstrated expression of FGFR1 and Klotho in PBMCm, we next sought to characterize the signaling response of these receptors following exposure to FGF23. Initial analyses showed that optimal expression of phosphorylated MAPK (pMAPK) and Akt (pAkt) was achieved after serum-starvation (1% HS) pretreatment for 1 and 2 hours respectively (Fig. 2*A*). Expression of pMAPK and pAkt was induced after treatment with FGF23 (100 ng/mL) for 30 minutes (Fig. 2*A*, *B*), with no further induction of pMAPK or pAkt after 60 or 120 minutes (data not shown). Pretreatment of PBMCm with the FGFR inhibitor PD173074 (FGFRi, 250 nM) for 1 hour suppressed the activation

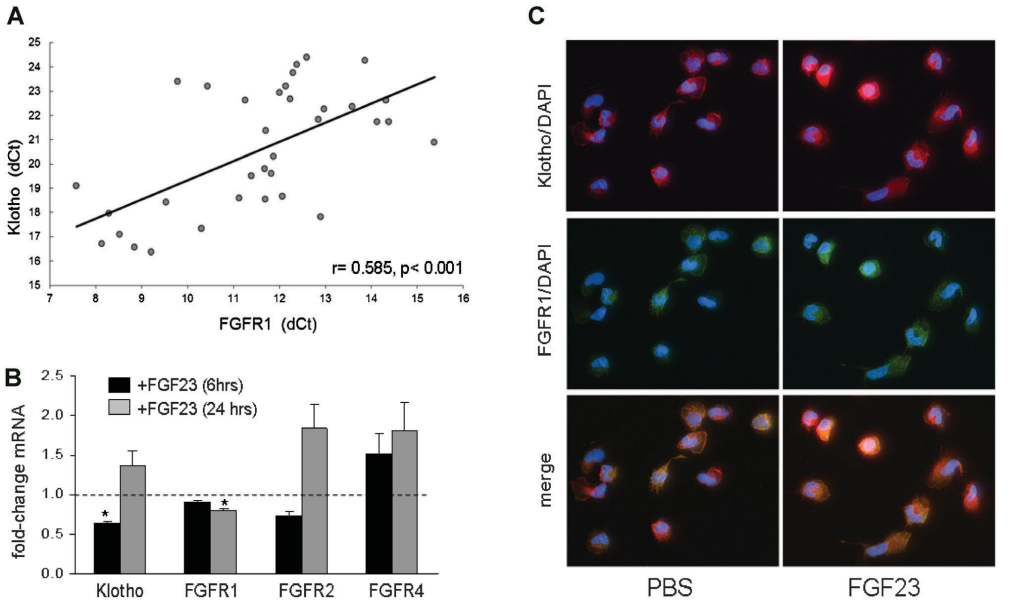

Fig. 1. Expression and regulation of fibroblast growth factor receptors (FGFR) and Klotho in PBMCm. (*A*) Baseline expression of FGFR1 mRNA in PBMCm correlates with Klotho mRNA (Spearman correlation coefficient of 0.585, $p < 0.001$, 35 different batches of PBMCs). (*B*) Effect of FGF23 (100 ng/mL) on expression of mRNA Klotho, FGFR1, FGFR2, and FGFR4 in PBMCm in vitro was assessed after 6 hours (black bars) and 24 hours (gray bars) treatments. Data show combined results using PBMCm from healthy donors at 6 hours (eight donors) and 24 hours (five donors). (*C*) Effect of FGF23 (100 ng/mL, 24 hours) on expression of Klotho (red), FGFR-1 (green), and nuclear DAPI (blue) protein in PBMCm, as determined by immunofluorescence microscopy. Merged immunofluorescence shows coexpression of FGFR1 and Klotho in PBMCm.

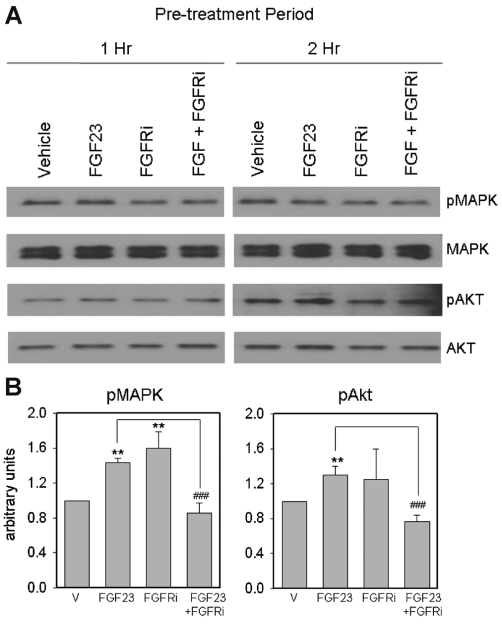

Fig. 2. FGF23 modulates FGFR signaling in PBMCm. (*A*) Effect of FGF23 (100 ng/mL) on MAPK and Akt signaling in PBMCm. Data are shown as representative Western blots showing expression of protein for: total MAPK; phosphoMAPK (pMAPK); total Akt; phosphoAkt (pAkt). PBMC were pretreated under conditions of serum deprivation (0.1% human serum) for either 1 hour or 2 hours with or without an FGFR inhibitor (FGFRi, 250 nM), and then treated with or without vehicle or FGF23 (100 ng/mL) for a further 1 hour. (*B*) Quantification of changes in expression of pMAPK (1 hour pretreatment, left panel) and pAkt (2 hour pretreatment, right panel) expression normalized to total MAPK and Akt, respectively. Data were determined using ImageJ software and represent mean ± SD values for $n = 3$ separate donor PBMCm cultures. **statistically different from vehicle-treated PBMCm, $p < 0.01$; $^{\#\#}$statistically different from FGF23-treated PBMCm, $p < 0.01$.

of these two phosphorylation pathways following treatment with FGF23 (Fig. 2*A*, *B*).

FGF23 decreases expression of CYP27B1 and intracrine synthesis of 1,25(OH)$_2$D in PBMCm

Treatment with FGF23 (100 ng/mL) decreased expression of mRNA for CYP27B1 in PBMCm after 6 and 24 hours (Fig. 3*A*). This effect was paralleled by decreased expression of the 1,25(OH)$_2$D-target genes CYP24A1 (6 and 24 hours) and LL37 (24 hours) (Fig. 3*A*). PBMCm pretreated with IL-15 (48 hours) showed a twofold increase in CYP27B1 mRNA relative to vehicle-treated cells, but this effect was inhibited by subsequent exposure to FGF23 (100 ng/mL, 24 hours) (Fig. 3*B*). HPLC analysis of vitamin D metabolism in five different batches of PBMCm showed that treatment with FGF23 inhibited monocyte synthesis of active 1,25(OH)$_2$D (Fig. 3*C*, *D*). Vehicle-treated cells (9.9 ± 2.9 fmol/hour/10^6 cells), and cells treated with FGF23 alone (10.9 ± 4.2 fmol/hour/10^6 cells) showed similar levels of 1,25(OH)$_2$D production. However, cells treated with IL-15 showed a significant increase in synthesis of 1,25(OH)$_2$D (76.3 ± 12.1 fmol/hour/10^6 cells), with this effect being significantly inhibited by co-treatment with FGF23 (42.5 ± 9.5 fmol/hour/10^6 cells). Synthesis of 24,25(OH)$_2$D was undetectable under each culture condition (Fig. 3*D*).

FGF23-mediated suppression of intracrine vitamin D activity in monocytes isolated from peritoneal dialysate effluent

Monocytes isolated from peritoneal effluents of patients undergoing maintenance continuous peritoneal dialysis (PDm), showed a fivefold higher basal expression of FGFR1 and eightfold higher levels of CYP24A1 (Table 2). Treatment of PDm in vitro with FGF23 (100 ng/mL) resulted in similar responses to those observed with PBMCm: expression of mRNA for CYP27B1, CYP24A1, and Klotho was decreased after 6 hours of treatment with FGF23 (Fig. 4*A*); by contrast, expression of LL37 was unaffected by treatment with FGF23, although baseline expression of LL37 in PDm cells was 0.12 relative to that observed in PBMCm (Table 2). At the protein level, coexpression of Klotho and FGFR1 was observed in basal and FGF23-treated cultures of PDm (Fig. 4*B*).

Discussion

Vitamin D is a potent regulator of innate[32] and adaptive immunity,[8] with these effects being highly dependent on local conversion of 25OHD to 1,25(OH)$_2$D by monocytes[12,13] and/or dendritic cells (DCs).[33,34] This intracrine activation of vitamin D within the immune system is sensitively induced by immunogenic stimuli,[12,13] or exposure to cytokines such as IL-15[14] or IFNγ.[15] Although induction of CYP27B1 appears to be important for normal immune function, overactivity of the enzyme has been linked to pathological conditions such as granulomatous disease and associated hypercalcemia.[35] Specific mechanisms that may help to prevent CYP27B1 overactivity following a pathogenic challenge include induction of the vitamin D catabolic enzyme CYP24A1.[36] In monocytes, as classically observed in the kidney, 1,25(OH)$_2$D itself potently induces expression of CYP24A1 with this effect being enhanced following Toll-like receptor (TLR) activation.[12] However, induction of monocyte vitamin D catabolism is not restricted to 1,25(OH)$_2$D-mediated self-regulation. Recent studies have shown that the cytokine IL-4 suppresses intracrine-induced antibacterial responses to 25OHD through enhanced monocyte 24-hydroxylase activity.[15] This mechanism suggests that T cells from the adaptive immune system are able to attenuate synthesis of 1,25(OH)$_2$D by monocytes and/or DCs indirectly via induction of 24-hydroxylase vitamin D catabolism. What is less clear is whether CYP27B1 itself is a target for suppression of monocyte 1,25(OH)$_2$D production. In classical vitamin D endocrinology, renal expression of CYP27B1 is inhibited by FGF23 as a counterpoint to the stimulatory actions of PTH.[5] The aim of

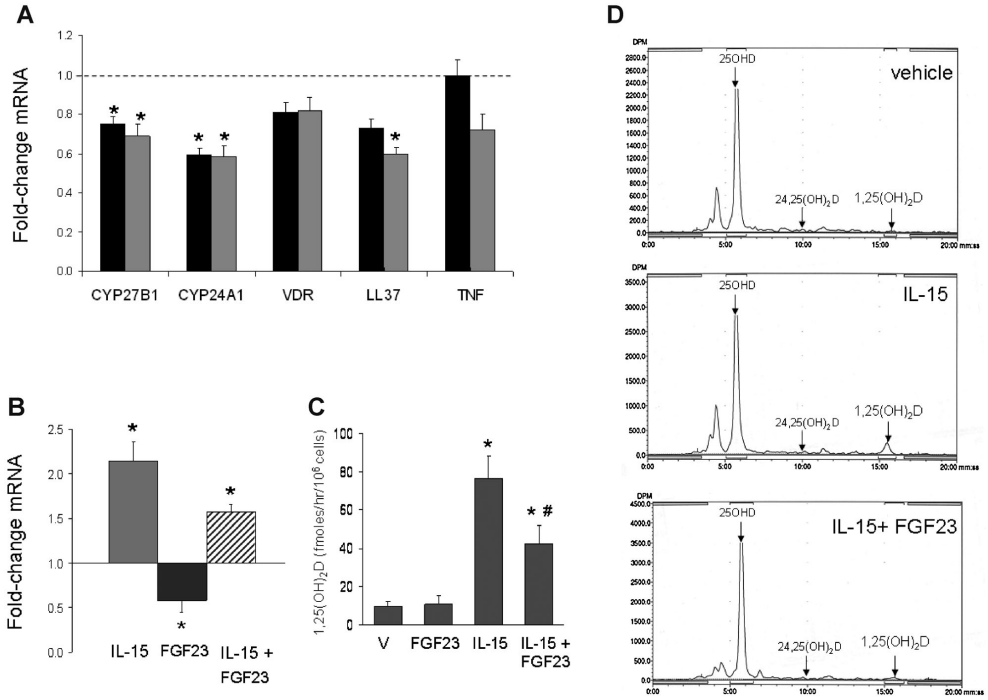

Fig. 3. FGF23 suppresses expression and activity of CYP27B1 in PBMCm. (*A*) Effect of FGF23 (100 ng/mL) at 6 hours (black bars) and 24 hours (gray bars) on expression of mRNA for CYP27B1, CYP24A1, VDR, LL37, and tumor necrosis factor α (TNFα) in PBMCm. Data shown are mean $\pm$ SEM fold changes in mRNA expression relative to vehicle-treated cells for PBMCm from eight different healthy donors. (*B*) Effect of FGF23 (100 ng/mL, 24 hours) alone or following preactivation of cells with interleukin-15 (IL-15, 200 ng/mL, 48 hours) on CYP27B1 mRNA expression in PBMCm. Data are shown as fold change in CYP27B1 mRNA relative to vehicle-treated cells for PBMCm from three different healthy donors. (*C*) Effect of vehicle (V) or FGF23 (100 ng/mL, 24 hours) alone or following preactivation of cells with IL-15 (200 ng/mL, 48 hours) on conversion of 25OHD to $1,25(OH)_2D$ in PBMCm. Data are shown as femtomoles $1,25(OH)_2D$ synthesized/hour/10^6 cells for PBMCm from $n = 5$ different healthy donors. (*D*) Effect of FGF23 (100 ng/mL, 24 hours) alone or after preactivation of cells with IL-15 (200 ng/mL, 48 hours) on conversion of 25OHD to $1,25(OH)_2D$ in PBMCm. Data are shown as representative HLPC analyses for each treatment. *statistically different compared to vehicle, $p < 0.05$; #statistically different from IL-15–treated cells, $p < 0.05$.

the current study was to determine whether similar FGF23-mediated regulation of CYP27B1 occurs in an extrarenal setting.

The significant decrease of CYP27B1 expression and activity in FGF23-treated monocytes is consistent with the classical actions of FGF23 on renal synthesis of $1,25(OH)_2D$. However, our data contrast previous studies describing FGF23-mediated upregulation of CYP27B1 in another extrarenal tissue, namely parathyroid cells.[37] The precise physiological basis for these different extrarenal activities of FGF23 is unclear, and effects on parathyroid cells may simply represent an alternative mechanism to enhance vitamin D-mediated control of PTH secretion. In classical vitamin D endocrinology, FGF23-mediated suppression of CYP27B1 is accompanied by increased expression of the catabolic enzyme CYP24A1, with the latter acting to further attenuate renal production of $1,25(OH)_2D$.[4,38,39] It was therefore interesting to note that monocyte expression of CYP24A1 is suppressed by FGF23 in parallel with its effects on CYP27B1. The most likely explanation is that, in the absence of cytokines such as IL-4, monocyte expression of CYP24A1 is primarily dependent on local synthesis of $1,25(OH)_2D$. Because synthesis of $1,25(OH)_2D$ is decreased in the presence of FGF23, expression of CYP24A1 will also decline. Renal expression of CYP24A1 is also stimulated by $1,25(OH)_2D$ but it is known to be sensitive to other endocrine factors such as PTH, which has been reported to regulate both transcription of CYP24A1[40] and stability of the resulting mRNA.[41] Thus, FGF23-mediated regulation of CYP24A1 in the kidney may be entirely different to its effects in monocytes.

Previous studies have reported expression of FGFR1 in interstitial inflammatory renal monocytes,[42] but, to the best of our knowledge, our data provide the first evidence for combined expression of FGFR1 and Klotho in monocytes outside the kidney. In other cell types FGF23 has been shown to bind to multiple FGFRs.[38,43–45] For example, recent studies have shown that FGFR3 and FGFR4 are the most likely receptors for FGF23-mediated regulation of serum $1,25(OH)_2D$ levels.[44] Neverthe-

Table 2. Relative Expression of Vitamin D- and FGF23-Related Genes in PDm Versus PBMCm

	ΔCtPDm (mean ± SD)	ΔCtPBMCm (mean ± SD)	Fold-change relative to PBMCm
CYP27B1	12.09 ± 2.21	11.90 ± 2.94	0.88
CYP24A1	17.59 ± 2.90	20.58 ± 3.11	7.96*
VDR	12.47 ± 3.60	14.14 ± 4.04	3.17
LL37	22.38 ± 3.58	19.38 ± 3.05	0.12*
Klotho	19.23 ± 2.03	20.57 ± 2.42	2.53
FGFR1	9.57 ± 3.06	11.78 ± 2.05	4.63*

Baseline expression of mRNAs for CYP27B1, CYP24A1, VDR, cathelicidin (LL37), Klotho, and FGFR1 in PDm was compared to the expression of these genes in PBMCm. Data in left-hand and central columns are shown as raw mRNA expression (ΔCt) data (mean ± SD) for the gene of interest normalized to expression of the housekeeping 18S rRNA gene. Data in the right-hand column are shown as fold-change mRNA expression for PDm relative to the equivalent gene in PBMCm. Combined results from 14 batches of PD cells and 45 batches of PBMCm.

PDm = peritoneal dialysate monocytes; PBMCm = peripheral blood mononuclear cell–derived monocytes; ΔCt = threshold cycle change; VDR = vitamin D receptor; LL37 = cathelicidin; FGFR1 = fibroblast growth factor receptor 1.

*Statistically different from PBMCm, $p < 0.05$.

less, the relatively high levels of FGFR1 in PBMCm and PDm suggest that this is the likely principal target for FGF23 in these cells, with Klotho acting as a co-receptor. Irrespective of the precise receptor isoform involved in mediating inhibition of monocyte CYP27B1, the MAPK and Akt phosphorylation pathways that appear to be activated by FGF23 in monocytes have also been linked to FGF23 responses in other cell types.[38,43,46,47] This contrasts with recent studies of FGF23 responses in cardiomyocytes, which were Klotho-and MAPK/Akt-independent.[45] Functional interplay between FGF23 and vitamin D in monocytes is supported by other observations from our study. First, both PBMC and PD monocytes show decreased expression of Klotho and FGFR1 after treatment with FGF23. Second, at baseline, there is a strong positive relationship between mRNA expression for Klotho and FGFR1, but also between FGFR1 and CYP27B1 and between FGFR1 and LL37. Finally, the PD cells, from patients chronically exposed to high circulating levels of FGF23,[48] have a lower baseline expression of LL37 relative to PBMCm. This provides a potential explanation for the lack of significant suppression of LL37 expression in PDm treated with FGF23 in vitro.

Decreased monocyte function following exposure to FGF23 may influence several disease scenarios. The key role of FGF23 in phosphate physiology was first highlighted in pediatric autosomal dominant hypophosphatemic rickets (ADHR).[16] Unlike CKD and end-stage renal disease,[48,49] ADHR involves only moderately increased circulating levels of FGF23, and is not known to present with the same infections observed in CKD, except for a tendency to dental abscesses,[50] and some reported pulmonary infections.[51] The latter may be due to effects of increased FGF23, but may also involve thoracic deformations induced by rickets or direct effects of vitamin D deficiency.[52,53] However, elevated FGF23 may influence other aspects of vitamin D physiology. Increased levels of vitamin D have been associated

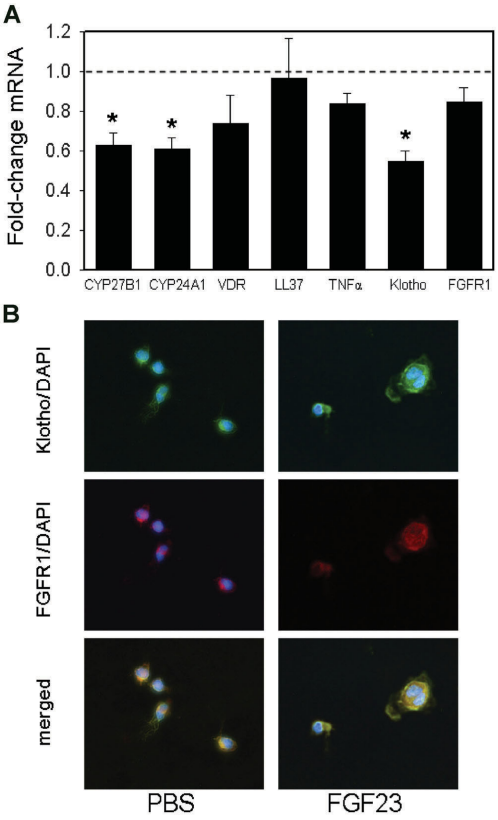

Fig. 4. FGF23 suppresses expression of CYP27B1 in monocytes from peritoneal dialysates. (*A*) Effect of FGF23 (100 ng/mL, 6 hours) on expression of mRNA for CYP27B1, CYP24A1, Klotho, and FGFR1 in peritoneal dialysate monocytes (PDm). Data are shown as mean ± SEM fold change in mRNA expression relative to vehicle-treated cells for PDm from $n = 7$ different donors. (*B*) Immunofluorescence analysis of protein for Klotho (green), FGFR-1 (red), and nuclear DAPI (blue) in PDm. Merged immunofluorescence shows coexpression of FGFR1 and Klotho in PDm. *statistically different from vehicle-treated PDm, $p < 0.05$.

with improved survival and cardiovascular status in CKD patients,[54] whereas vitamin D treatments have also been linked to decreased risk of cardiovascular deaths among dialysis patients.[55,56] Conversely, high circulating levels of FGF23 are strongly associated with risk of mortality and cardiovascular disease in patients with CKD,[23] and we propose that this may be due, at least in part, to FGF23-mediated dysregulation of extrarenal vitamin D function. The precise mechanisms linking FGF23, vitamin D, and cardiovascular disease are as yet unclear but could involve suppression of the intracrine immunomodulatory actions of 25OHD in disease-affected cells. This may include monocytes and DCs, but endothelial cells are also known to express CYP27B1, with the latter being induced by inflammatory stimuli.[57]

The most immediate clinical implication of the data presented in this study is the potential link between elevated FGF23 and impaired innate immunity in CKD. As detailed above, CKD is a state of acquired immune deficiency involving both cellular and humoral immunity,[27] and circulating levels LL37 in this population appear to be an independent risk factor of mortality by infections.[58] In a similar fashion, higher quartiles of serum FGF23 are associated with an increased risk of mortality across the spectrum of CKD,[23,59] and non-CKD populations,[60] mainly in terms of cardiovascular mortality; therapy with vitamin D sterols is associated with reduced mortality in dialysis patients.[55,56] Prospective randomized trials will be required to define the role of FGF23 on overall patient survival as well as the impact of therapy with vitamin D. Although therapeutic targeting of FGF23 may be a strategy to delay the onset of secondary hyperparathyroidism and bone and mineral disorders associated with CKD, the effects of such an approach on global and cardiovascular morbimortality have yet to be studied. However, based on data presented here, we propose that therapies aimed at lowering circulating levels of FGF23 may have immediate benefits for the morbimortality induced by infections in the CKD population.

To date, studies of vitamin D-induced innate immunity have focused exclusively on monocytes derived from PBMCs.[12,13] Stubbs and colleagues[61] demonstrated modulation of vitamin D-dependent biomarkers in PBMC following native oral vitamin D supplementation in hemodialysis patients, but without any evaluation of a potential interplay between vitamin D and FGF23 pathways. However, in CKD it seems more likely that antibacterial activity will arise from tissue-localized monocytes and macrophages rather than from the circulating populations of these cells. With this in mind, a key objective of the current study was to characterize the vitamin D system and vitamin D-induced immunity in a population of cells more closely associated with infection in CKD patients, namely PDm. Previous studies have shown that peritoneal macrophages from dialysis patients are able to synthesize $1,25(OH)_2D$,[62] but the relevance of this finding to innate immunity remains unclear. PDm and PBMCm express similar levels of CYP27B1, but the relatively high levels of FGFR1/Klotho in PDm may facilitate FGF23 suppression of CYP27B1 in these cells. Despite this, FGF23 treatment did not significantly suppress LL37 expression in PDm. One explanation for this is that baseline levels of LL37 are lower in PDm relative to PBMC, and may thus be resistant to further suppression. Conversely, baseline expression of CYP24A1 is significantly higher in PDm relative to PBMCm and this is also likely to influence intracrine responses to 25D in these cells.

In future studies, it will be interesting to characterize further the difference between PDm and PBMCm with respect to vitamin D-mediate immune function. For the current study it was not possible to obtain sufficient blood from the pediatric CKD donors of the PD cells to enable parallel isolation of PBMCm. However, direct comparison between these two populations of monocytes may provide important new insights on the immunomodulatory effects of vitamin D in vivo. Future studies will also need to further clarify the wider impact of FGF23 on immune function. The current study focuses on the intracrine effects of vitamin D on monocyte function but it is also possible that FGF23 will act to suppress CYP27B1 in other immune cells that express this enzyme, such as DCs.[33,34] In this way, FGF23 may not only influence innate antibacterial responses to infection but it may also affect antigen presentation by DCs and concomitant adaptive T cell/B cell immune activity. This may be particularly important in CKD patients in whom inflammation is a key feature of disease pathophysiology, with reported links to patient vitamin D status.[63] Effects of FGF23 on DC vitamin D metabolism and antigen presentation may also impact on adaptive immune response to kidney transplantation. Recent studies from our group have highlighted association between FGF23 levels, deteriorating kidney function and host-graft rejection in pediatric CKD transplantation patients.[64] The role of immune vitamin D metabolism in this setting has yet to be studied but may provide an important mechanism for future therapeutic intervention to improve transplantation success.

Disclosures

All authors state that they have no conflicts of interest.

Acknowledgments

This work was supported in part by educational grants (AcadémieFrançaise/Jean Walter Zellidja, RéunionPédiatrique de la Région Rhône Alpes, SociétéFrançaise de Pédiatrie/Evian, Fondation pour la RechercheMédicale, Philippe Foundation, to JB), by a grant from the Center for D-receptor Activation Research (CeDAR, to MH), by NIH grant DK0911672 (to MH), by USPHS grants DK 67563, DK 35423, DK 80984, and funds from the Casey Lee Ball Foundation (to lBS and KWP).We thank Deborah Krakow, MD, Anna Sarukhanov, and Margarita Ivanova (UCLA) for their help with the Western blot analyses.

Authors' roles: JB performed the experiments as well as the statistical analyses, and wrote the manuscript; JLS, RFC, and TSL did some of the experimental work; KWP and IBS helped to design the study and to analyze the results; JSA helped to analyze data; BG was involved in patient recruitment; MH initially designed the study, helped to analyze the results, and edited the manuscript.

References

1. Liu S, Quarles LD. How fibroblast growth factor 23 works. J Am Soc Nephrol. 2007;18(6):1637–47.
2. Yamazaki Y, Tamada T, Kasai N, Urakawa I, Aono Y, Hasegawa H, Fujita T, Kuroki R, Yamashita T, Fukumoto S, Shimada T. Anti-FGF23 neutralizing antibodies show the physiological role and structural features of FGF23. J Bone Miner Res. 2008;23(9):1509–18.
3. Yoshiko Y, Wang H, Minamizaki T, Ijuin C, Yamamoto R, Suemune S, Kozai K, Tanne K, Aubin JE, Maeda N. Mineralized tissue cells are a principal source of FGF23. Bone. 2007;40(6):1565–73.
4. Shimada T, Hasegawa H, Yamazaki Y, Muto T, Hino R, Takeuchi Y, Fujita T, Nakahara K, Fukumoto S, Yamashita T. FGF-23 is a potent regulator of vitamin D metabolism and phosphate homeostasis. J Bone Miner Res. 2004;19(3):429–35.
5. Shimada T, Kakitani M, Yamazaki Y, Hasegawa H, Takeuchi Y, Fujita T, Fukumoto S, Tomizuka K, Yamashita T. Targeted ablation of Fgf23

demonstrates an essential physiological role of FGF23 in phosphate and vitamin D metabolism. J Clin Invest. 2004;113(4):561–8.

6. Razzaque MS, Sitara D, Taguchi T, St-Arnaud R, Lanske B. Premature aging-like phenotype in fibroblast growth factor 23 null mice is a vitamin D-mediated process. The FASEB J. 2006;20(6):720–2.
7. Sitara D, Razzaque MS, St-Arnaud R, Huang W, Taguchi T, Erben RG, Lanske B. Genetic ablation of vitamin D activation pathway reverses biochemical and skeletal anomalies in Fgf-23-null animals. Am J Pathol. 2006;169(6):2161–70.
8. Hewison M, Vitamin D. Vitamin D and innate and adaptive immunity. Vitam Horm. 2011;86:23–62.
9. Adams JS, Hewison M. Unexpected actions of vitamin D: new perspectives on the regulation of innate and adaptive immunity. Nat Clin Pract Endocrinol Metab. 2008;4(2):80–90.
10. Gombart AF, Borregaard N, Koeffler HP. Human cathelicidin antimicrobial peptide (CAMP) gene is a direct target of the vitamin D receptor and is strongly up-regulated in myeloid cells by 1,25-dihydroxyvitamin D3. FASEB J. 2005;19(9):1067–77.
11. Wang TT, Nestel FP, Bourdeau V, Nagai Y, Wang Q, Liao J, Tavera-Mendoza L, Lin R, Hanrahan JW, Mader S, White JH. Cutting edge: 1,25-dihydroxyvitamin D3 is a direct inducer of antimicrobial peptide gene expression. J Immunol. 2004;173(5): 2909–12.
12. Liu PT, Stenger S, Li H, Wenzel L, Tan BH, Krutzik SR, Ochoa MT, Schauber J, Wu K, Meinken C, Kamen DL, Wagner M, Bals R, Steinmeyer A, Zugel U, Gallo RL, Eisenberg D, Hewison M, Hollis BW, Adams JS, Bloom BR, Modlin RL. Toll-like receptor triggering of a vitamin D-mediated human antimicrobial response. Science. 2006; 311(5768):1770–3.
13. Adams JS, Ren S, Liu PT, Chun RF, Lagishetty V, Gombart AF, Borregaard N, Modlin RL, Hewison M. Vitamin d-directed rheostatic regulation of monocyte antibacterial responses. J Immunol. 2009; 182(7):4289–95.
14. Krutzik SR, Hewison M, Liu PT, Robles JA, Stenger S, Adams JS, Modlin RL. IL-15 links TLR2/1-induced macrophage differentiation to the vitamin D-dependent antimicrobial pathway. J Immunol. 2008; 181(10):7115–20.
15. Edfeldt K, Liu PT, Chun R, Fabri M, Schenk M, Wheelwright M, Keegan C, Krutzik SR, Adams JS, Hewison M, Modlin RL. T-cell cytokines differentially control human monocyte antimicrobial responses by regulating vitamin D metabolism. Proc Natl Acad Sci U S A. 2010; 107(52):22593–8.
16. Consortium A. Autosomal dominant hypophosphataemic rickets is associated with mutations in FGF23. Nat Genet. 2000;26(3): 345–8.
17. Jonsson KB, Zahradnik R, Larsson T, White KE, Sugimoto T, Imanishi Y, Yamamoto T, Hampson G, Koshiyama H, Ljunggren O, Oba K, Yang IM, Miyauchi A, Econs MJ, Lavigne J, Juppner H. Fibroblast growth factor 23 in oncogenic osteomalacia and X-linked hypophosphatemia. N Engl J Med. 2003;348(17):1656–63.
18. Danziger J. The bone-renal axis in early chronic kidney disease: an emerging paradigm. Nephrol Dial Transplant. 2008;23(9): 2733–7.
19. Isakova T, Wahl P, Vargas GS, Gutierrez OM, Scialla J, Xie H, Appleby D, Nessel L, Bellovich K, Chen J, Hamm L, Gadegbeku C, Horwitz E, Townsend RR, Anderson CA, Lash JP, Hsu CY, Leonard MB, Wolf M. Fibroblast growth factor 23 is elevated before parathyroid hormone and phosphate in chronic kidney disease. Kidney Int. 2011;79(12): 1370–8.
20. Fliser D, Kollerits B, Neyer U, Ankerst DP, Lhotta K, Lingenhel A, Ritz E, Kronenberg F, Kuen E, Konig P, Kraatz G, Mann JF, Muller GA, Kohler H, Riegler P. Fibroblast growth factor 23 (FGF23) predicts progression of chronic kidney disease: the Mild to Moderate Kidney Disease (MMKD) Study. J Am Soc Nephrol. 2007;18(9):2600–8.
21. Kazama JJ, Gejyo F, Shigematsu T, Fukagawa M. Role of circulating fibroblast growth factor 23 in the development of secondary hyperparathyroidism. Ther Apher Dial. 2005;9(4):328–30.
22. Nakanishi S, Kazama JJ, Nii-Kono T, Omori K, Yamashita T, Fukumoto S, Gejyo F, Shigematsu T, Fukagawa M. Serum fibroblast growth factor-23 levels predict the future refractory hyperparathyroidism in dialysis patients. Kidney Int. 2005;67(3):1171–8.
23. Gutierrez OM, Mannstadt M, Isakova T, Rauh-Hain JA, Tamez H, Shah A, Smith K, Lee H, Thadhani R, Juppner H, Wolf M. Fibroblast growth factor 23 and mortality among patients undergoing hemodialysis. N Engl J Med. 2008;359(6):584–92.
24. Mirza MA, Hansen T, Johansson L, Ahlstrom H, Larsson A, Lind L, Larsson TE. Relationship between circulating FGF23 and total body atherosclerosis in the community. Nephrol Dial Transplant. 2009; 24(10):3125–31.
25. Mirza MA, Larsson A, Lind L, Larsson TE. Circulating fibroblast growth factor-23 is associated with vascular dysfunction in the community. Atherosclerosis. 2009;205(2):385–90.
26. Parasuraman R, Samarapungavan D, Venkat KK. Updated principles and clinical caveats in the management of infection in renal transplant recipients. Transplant Rev (Orlando). 2010;24(2):43–51.
27. Cohen G, Haag-Weber M, Horl WH. Immune dysfunction in uremia. Kidney Int Suppl. 1997;62:S79–82.
28. Sarnak MJ, Jaber BL. Mortality caused by sepsis in patients with end-stage renal disease compared with the general population. Kidney Int. 2000;58(4):1758–64.
29. Collins AJ, Foley RN, Gilbertson DT, Chen SC. The state of chronic kidney disease, ESRD, and morbidity and mortality in the first year of dialysis. Clin J Am Soc Nephrol. 2009;4(Suppl 1):S5–11.
30. Sardenberg C, Suassuna P, Andreoli MC, Watanabe R, Dalboni MA, Manfredi SR, dos Santos OP, Kallas EG, Draibe SA, Cendoroglo M. Effects of uraemia and dialysis modality on polymorphonuclear cell apoptosis and function. Nephrol Dial Transplant. 2006;21(1): 160–5.
31. Wu S, Ren S, Nguyen L, Adams JS, Hewison M. Splice variants of the CYP27b1 gene and the regulation of 1,25-dihydroxyvitamin D3 production. Endocrinology. 2007;148(7):3410–8.
32. Hewison M. Antibacterial effects of vitamin D. Nat Rev Endocrinol. 2011;7(6):337–45.
33. Hewison M, Freeman L, Hughes SV, Evans KN, Bland R, Eliopoulos AG, Kilby MD, Moss PA, Chakraverty R. Differential regulation of vitamin D receptor and its ligand in human monocyte-derived dendritic cells. J Immunol. 2003;170(11):5382–90.
34. Fritsche J, Mondal K, Ehrnsperger A, Andreesen R, Kreutz M. Regulation of 25-hydroxyvitamin D3-1 alpha-hydroxylase and production of 1 alpha,25-dihydroxyvitamin D3 by human dendritic cells. Blood. 2003;102(9):3314–6.
35. Kallas M, Green F, Hewison M, White C, Kline G. Rare causes of calcitriol-mediated hypercalcemia: a case report and literature review. J Clin Endocrinol Metab. 2010;95(7):3111–7.
36. Sakaki T, Kagawa N, Yamamoto K, Inouye K. Metabolism of vitamin D3 by cytochromes P450. Front Biosci. 2005;10:119–34.
37. Krajisnik T, Bjorklund P, Marsell R, Ljunggren O, Akerstrom G, Jonsson KB, Westin G, Larsson TE. Fibroblast growth factor-23 regulates parathyroid hormone and 1alpha-hydroxylase expression in cultured bovine parathyroid cells. J Endocrinol. 2007;195(1):125–31.
38. Razzaque MS. FGF23-mediated regulation of systemic phosphate homeostasis: is Klotho an essential player? Am J Physiol Renal Physiol. 2009;296(3):F470–6.
39. Juppner H, Wolf M, Salusky IB. FGF-23: More than a regulator of renal phosphate handling? J Bone Miner Res. 2010;25(10):2091–7.
40. Yang W, Friedman PA, Kumar R, Omdahl JL, May BK, Siu-Caldera ML, Reddy GS, Christakos S. Expression of 25(OH)D3 24-hydroxylase in

distal nephron: coordinate regulation by 1,25(OH)2D3 and cAMP or PTH. Am J Physiol. 1999;276(4 Pt 1):E793–805.

41. Zierold C, Mings JA, DeLuca HF. Regulation of 25-hydroxyvitamin D3-24-hydroxylase mRNA by 1,25-dihydroxyvitamin D3 and parathyroid hormone. J Cell Biochem. 2003;88(2):234–7.
42. Rossini M, Cheunsuchon B, Donnert E, Ma LJ, Thomas JW, Neilson EG, Fogo AB. Immunolocalization of fibroblast growth factor-1 (FGF-1), its receptor (FGFR-1), and fibroblast-specific protein-1 (FSP-1) in inflammatory renal disease. Kidney Int. 2005;68(6):2621–8.
43. Shimada T, Urakawa I, Isakova T, Yamazaki Y, Epstein M, Wesseling-Perry K, Wolf M, Salusky IB, Juppner H. Circulating fibroblast growth factor 23 in patients with end-stage renal disease treated by peritoneal dialysis is intact and biologically active. J Clin Endocrinol Metab. 2010;95(2):578–85.
44. Gattineni J, Twombley K, Goetz R, Mohammadi M, Baum M. Regulation of serum 1,25(OH)2 vitamin D3 levels by fibroblast growth factor 23 is mediated by FGF receptors 3 and 4. Am J Physiol Renal Physiol. 2011;301(2):F371–7.
45. Faul C, Amaral AP, Oskouei B, Hu MC, Sloan A, Isakova T, Gutierrez OM, Aguillon-Prada R, Lincoln J, Hare JM, Mundel P, Morales A, Scialla J, Fischer M, Soliman EZ, Chen J, Go AS, Rosas SE, Nessel L, Townsend RR, Feldman HI, St John Sutton M, Ojo A, Gadegbeku C, Di Marco GS, Reuter S, Kentrup D, Tiemann K, Brand M, Hill JA, Moe OW, Kuro OM, Kusek JW, Keane MG, Wolf M. FGF23 induces left ventricular hypertrophy. J Clin Invest. 2011;121(11):4393–408.
46. Goetz R, Beenken A, Ibrahimi OA, Kalinina J, Olsen SK, Eliseenkova AV, Xu C, Neubert TA, Zhang F, Linhardt RJ, Yu X, White KE, Inagaki T, Kliewer SA, Yamamoto M, Kurosu H, Ogawa Y, Kuro-o M, Lanske B, Razzaque MS, Mohammadi M. Molecular insights into the klotho-dependent, endocrine mode of action of fibroblast growth factor 19 subfamily members. Mol Cell Biol. 2007;27(9):3417–28.
47. Ranch D, Zhang MY, Portale AA, Perwad F. Fibroblast growth factor 23 regulates renal 1,25-dihydroxyvitamin D and phosphate metabolism via the MAP kinase signaling pathway in Hyp mice. J Bone Miner Res. 2011;26(8):1883–90.
48. Wesseling-Perry K, Pereira RC, Wang H, Elashoff RM, Sahney S, Gales B, Juppner H, Salusky IB. Relationship between plasma fibroblast growth factor-23 concentration and bone mineralization in children with renal failure on peritoneal dialysis. J Clin Endocrinol Metab. 2009;94(2):511–7.
49. Bacchetta J, Dubourg L, Harambat J, Ranchin B, Abou-Jaoude P, Arnaud S, Carlier MC, Richard M, Cochat P. The influence of glomerular filtration rate and age on fibroblast growth factor 23 serum levels in pediatric chronic kidney disease. J Clin Endocrinol Metab. 2010;95(4):1741–8.
50. Bacchetta J, Salusky IB. Evaluation of hypophosphatemia: lessons from patients with genetic disorders. Am J Kidney Dis. 2012; 59(1):152–9.
51. Kitajima I, Maruyama I, Matsubara H, Osame M, Igata A. Immune dysfunction in hypophosphatemic vitamin D-resistant rickets: immunoregulatory reaction of 1 alpha(OH) vitamin D3. Clin Immunol Immunopathol. 1989;53(1):24–31.
52. Koeffler HP, Bishop JE, Reichel H, Singer F, Nagler A, Tobler A, Walka M, Norman AW. Lymphocyte cell lines from vitamin D-dependent rickets type II show functional defects in the 1 alpha,25-dihydroxyvitamin D3 receptor. Mol Cell Endocrinol. 1990;70(1):1–11.
53. Muhe L, Lulseged S, Mason KE, Simoes EA. Case-control study of the role of nutritional rickets in the risk of developing pneumonia in Ethiopian children. Lancet. 1997;349(9068):1801–4.
54. Souberbielle JC, Body JJ, Lappe JM, Plebani M, Shoenfeld Y, Wang TJ, Bischoff-Ferrari HA, Cavalier E, Ebeling PR, Fardellone P, Gandini S, Gruson D, Guerin AP, Heickendorff L, Hollis BW, Ish-Shalom S, Jean G, von Landenberg P, Largura A, Olsson T, Pierrot-Deseilligny C, Pilz S, Tincani A, Valcour A, Zittermann A. Vitamin D and musculoskeletal health, cardiovascular disease, autoimmunity and cancer: Recommendations for clinical practice. Autoimmun Rev. 2010;9(11):709–15.
55. Shoji T, Shinohara K, Kimoto E, Emoto M, Tahara H, Koyama H, Inaba M, Fukumoto S, Ishimura E, Miki T, Tabata T, Nishizawa Y. Lower risk for cardiovascular mortality in oral 1alpha-hydroxy vitamin D3 users in a haemodialysis population. Nephrol Dial Transplant. 2004;19(1): 179–84.
56. Negri AL. Association of oral calcitriol with improved survival in non-dialysed and dialysed patients with CKD. Nephrol Dial Transplant. 2009;24(2):341–4.
57. Zehnder D, Bland R, Chana RS, Wheeler DC, Howie AJ, Williams MC, Stewart PM, Hewison M. Synthesis of 1,25-dihydroxyvitamin D(3) by human endothelial cells is regulated by inflammatory cytokines: a novel autocrine determinant of vascular cell adhesion. J Am Soc Nephrol. 2002;13(3):621–9.
58. Gombart AF, Bhan I, Borregaard N, Tamez H, Camargo CA Jr, Koeffler HP, Thadhani R. Low plasma level of cathelicidin antimicrobial peptide (hCAP18) predicts increased infectious disease mortality in patients undergoing hemodialysis. Clin Infect Dis. 2009;48(4): 418–24.
59. Jean G, Terrat JC, Vanel T, Hurot JM, Lorriaux C, Mayor B, Chazot C. High levels of serum fibroblast growth factor (FGF)-23 are associated with increased mortality in long haemodialysis patients. Nephrol Dial Transplant. 2009;24(9):2792–6.
60. Parker BD, Schurgers LJ, Brandenburg VM, Christenson RH, Vermeer C, Ketteler M, Shlipak MG, Whooley MA, Ix JH. The associations of fibroblast growth factor 23 and uncarboxylated matrix Gla protein with mortality in coronary artery disease: the Heart and Soul Study. Ann Intern Med. 2010;152(10):640–8.
61. Stubbs JR, Idiculla A, Slusser J, Menard R, Quarles LD. Cholecalciferol supplementation alters calcitriol-responsive monocyte proteins and decreases inflammatory cytokines in ESRD. J Am Soc Nephrol. 2010;21(2):353–61.
62. Hayes ME, O'Donoghue DJ, Ballardie FW, Mawer EB. Peritonitis induces the synthesis of 1 alpha,25-dihydroxyvitamin D3 in macrophages from CAPD patients. FEBS Lett. 1987;220(2):307–10.
63. Zehnder D, Quinkler M, Eardley KS, Bland R, Lepenies J, Hughes SV, Raymond NT, Howie AJ, Cockwell P, Stewart PM, Hewison M. Reduction of the vitamin D hormonal system in kidney disease is associated with increased renal inflammation. Kidney Int. 2008;74(10):1343–53.
64. Wesseling-Perry K, Tsai EW, Ettenger RB, Juppner H, Salusky IB. Mineral abnormalities and long-term graft function in pediatric renal transplant recipients: a role for FGF-23? Nephrol Dial Transplant. 2011;26(11):3779–84.

Supplemental Figure 1

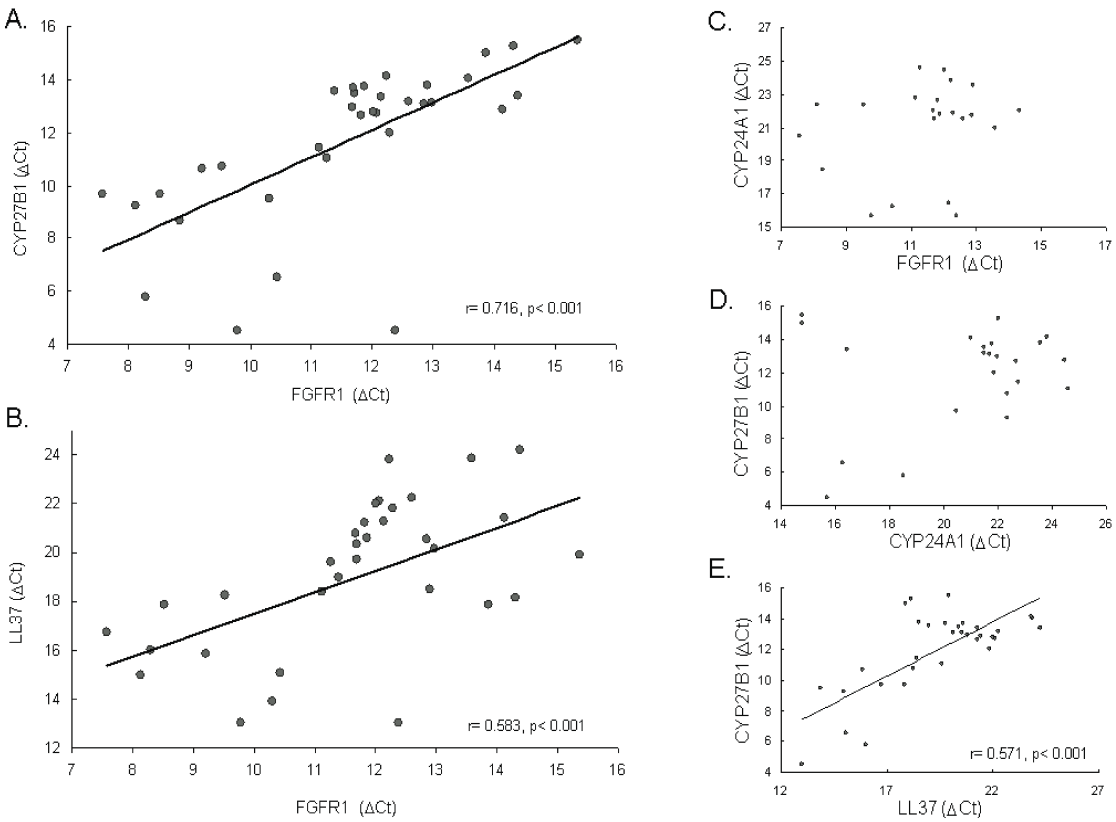

Supplemental Figure 1. Relationship between FGFR1 and Klotho mRNA expression and expression of genes associated with vitamin D metabolism and function in PBMCm

As well as correlating with Klotho expression, in 35 different batches of PBMCs at baseline, FGFR-1 levels also correlated with the expression of vitamin D dependent genes in PBMCm: CYP27B1 (Spearman correlation, r= 0.716, p< 0.001, 1S-A) and LL37(Spearman correlation, r= 0.583, p< 0.001, 1S-B). Of note, there was no relationship between baseline FGFR-1 expression and CYP24A1 (1S-C), nor between CYP27B1 and CYP24A1 (1S-D); Klotho expression was associated with no other genes apart from FGFR-1 (Figure 1A).By contrast, the baseline expression of CYP27B1 and LL37 correlated (r= 0.571, p<0.001, 1S-E).

Supplemental Figure 2

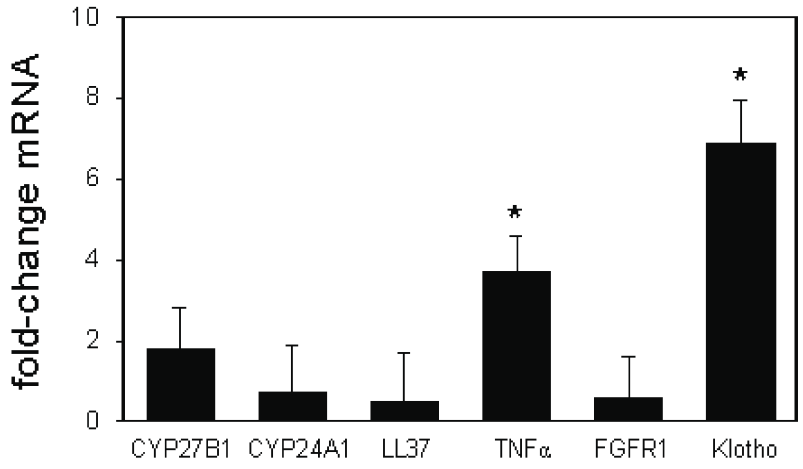

Supplemental Figure 2. Effect of toll-like receptor 2 activation on vitamin D- and FGF23-related gene expression in PBMCm

Effect of the toll-like receptor (TLR)2 ligand 19 kDa lipoprotein (100 ng/ml, 6hrs) on expression of mRNA for CYP27B1, CYP24A1, VDR, LL37 and tumor necrosis factor α (TNFα), FGFR1 and Klotho in PBMCm. Data shown are mean ± SEM fold-changes in mRNA expression relative to vehicle-treated cells for PBMCm from 5 different healthy donors. * = statistically different from vehicle-treated PBMCm, $p < 0.05$.

Chapter 3

Fibroblast growth factor 23 alters endothelial-driven monocyte lipid accumulation

Fibroblast growth factor 23 alters endothelial-driven monocyte lipid accumulation

Jessica L. Sea[1], Michelle Khrom[1], Avelino De Leon[2], Martin Hewison[3], Katherine Wesseling-Perry[4], Isidro Salusky[4], and Philip T. Liu[2]

[1]Department of Molecular, Cell and Developmental Biology, University of California at Los Angeles, Los Angeles, CA

[2]Department of Orthopaedic Surgery, Orthopaedic Hospital Research Center, University of California at Los Angeles, Los Angeles, CA

[3]Centre for Endocrinology, Diabetes and Metabolism, The University of Birmingham, Birmingham, UK

[4]Department of Pediatrics, David Geffen School of Medicine, University of California at Los Angeles, Los Angeles, CA

ABSTRACT

Chronic kidney disease (CKD) precipitates several co-morbidities, the most prevalent being cardiovascular disease (CVD), which is also the highest cause of mortality in these patients. Renal dysfunction perpetuates the systemic inflammation, aberrant lipid metabolism, and endothelial dysfunction that initiates macrophage extravasation and lipid accumulation contributing to CVD pathogenesis. Although high levels of circulating fibroblast growth factor (FGF) 23 have been linked to CKD/CVD progression, the effects of FGF23 on endothelial cell and macrophage dysfunction is unknown. We hypothesized that FGF23 alters endothelial-macrophage interactions contributing to disease progression. To investigate this, we established a co-culture system using primary human aortic endothelial cells (HAEC) and monocytes isolated from human peripheral blood mononuclear cells (PBMC) to mimic the endothelial-monocyte niche. FGF23 stimulation of co-cultures resulted in a decreased lipid accumulation in HAEC and an increase lipid uptake by monocyte/macrophages, in which physical interactions between the two cell types was not required. When conditioned media (CM) from FGF23-stimulated HAEC was added directly to monocytes, there was a significant, time-dependent increase in macrophage lipid accumulation compared to CM from vehicle-treated HAEC. Interestingly, there was no significant change in the cell surface expression of CD209 and CD163, markers that have been previously used to assess human macrophage subset polarization. Collectively, these results suggest that FGF23 stimulates endothelial cells, leading to increased lipid phagocytosis by

surrounding macrophages. The major finding of this study proposes a mechanism by which FGF23 promotes CVD pathogenesis in patients with CKD, by driving an influx of lipid-accumulating macrophages, a major step in the progression toward lipid-laden foam cells that are characteristic of CVD.

INTRODUCTION

Chronic kidney disease (CKD) effects approximately 1 in 10 people in the US, and among those afflicted with the disease, Hispanic and Black populations are disproportionately affected [1, 2]. The leading cause of death of patients with CKD is cardiovascular disease (CVD), which is the result of systemic inflammation, endothelial dysfunction, and aberrant lipid metabolism perpetuated by declining renal function [3-6]. One of the first clinically detectable signs of renal dysfunction is an elevation in serum fibroblast growth factor (FGF) 23 [7, 8]. Although this correlation is well supported by clinical evidence, the relationship between elevated FGF23 and CVD remains unclear.

CVD is initiated by inflammation, endothelial activation, and high levels of oxidized low-density lipoproteins (ox-LDL) accumulating in the sub-endothelial space that contribute to the generation of reactive oxygen species. The combination of these events results in endothelial dysfunction and the recruitment of circulating monocytes to the sub-endothelial space [9-11]. As monocytes extravasate through the endothelial barrier, they differentiate into phagocytic macrophages to engulf and clear excess ox-LDL [10-13]. As macrophages increase ox-LDL uptake, they transform into foam cells, which are characterized as large, lipid-containing macrophages. As the disease progresses, the rate of lipid accumulation increases, surpassing the rate at which macrophages can clear the ox-LDL [10, 13]. The foam-cells, fragile due to the increased size, often burst, spilling their intracellular contents into the sub-endothelial space, causing recruitment of inflammatory

macrophages thus perpetuating the cycle of CVD pathology. Accumulation of lipids, cells, and cell debris, that first appear as a fatty plaque, forms a hypoxic, necrotic lipid core [14]. Decreased stability of the necrotic core resulting from exponential cell accumulation eventually leads to either vessel occlusion or rupture resulting in a cardiovascular emergency.

The stability and growth of the necrotic core is greatly influenced by the macrophage subtypes present in the developing lesion [9-11, 14-19]. Cardiovascular lesions with a higher proportion of inflammatory macrophages are associated with more aggressive plaque growth and poor disease prognosis; whereas, necrotic cores with a higher number of phagocytic macrophages are associated with better disease prognosis, and may in some cases, contribute to plaque regression [9, 16-21]. The ability of the endothelium to drive monocyte differentiation into macrophages is documented; however, the mechanism(s) inducing and driving macrophage polarization are not well understood. There is evidence suggesting that as a default in a healthy vessel, this niche triggers polarization of macrophages of an anti-inflammatory phenotype [20]. Understanding the factors that regulate or perturb this endothelium-driven macrophage differentiation and polarization will be a key step to development of immunotherapies for CKD/CVD.

Given the correlation between elevated FGF23 in CKD and the increased risk of CVD, we sought to elucidate the role of FGF23 in the development of CVD pathology. In this paper, we explored the effects of FGF23 on the endothelial-monocyte microenvironment that is crucial for initiation and progression of

atherosclerosis. Here we demonstrate that FGF23 alters monocyte lipid accumulation in this microenvironment, and therefore may be a target for future therapeutics aimed at mitigating CVD in patients with diminished renal function.

MATERIALS AND METHODS

Endothelial cell culture

Primary human aortic endothelial cells, HAEC (cat no. 2535), cultured in EGM-2 BulletKit (cat. no. 3162) were purchased from Lonza (Walkersville, MD). Cells used were between passages four to eight for all experiments. Endothelial cells were grown to 75-100% confluence prior to experimentation.

Isolation of monocytes from healthy donor peripheral blood mononuclear cells

Ficoll-isolated peripheral blood mononuclear cells (PBMC) were obtained from anonymous healthy donors by the Center for AIDS Research Virology Core/BSL3 Facility (supported by NIH award Al-28697 and by the UCLA AIDS Institute and the UCLA Council of Bioscience Resources, Los Angeles, CA, USA). PBMC were enriched for monocytes via plastic adherence by incubating PBMC in Roswell Park Memorial Institute (RPMI 1640) medium (cat. no. 11875-093) purchased from Invitrogen (Carlsbad, CA, USA) containing 1% fetal bovine serum (FBS) purchased from Corning (cat. no. 35016CV) for 2 hours. Cells are washed twice with serum-free RPMI no remove non-adherent cells.

Treatment with FGF23

Experiments with monocultures and co-cultures of HAEC and/or PBMC were done using RPMI 1640 containing 2% FBS at 37°C in 5% CO_2. Recombinant human FGF23 (cat. no. 2604-FG) obtained from R&D Systems (Minneapolis, MN) was

reconstituted in PBS contain 0.1% BSA in accordance with manufacture's instructions. Cell cultures were treated with either FGF23 (100ng/ml) or 0.2% PBS containing 0.1% BSA. Following incubation with FGF23, cells were further processed dependent upon experimental objectives.

RNA extraction and cDNA synthesis by reverse transcription

RNeasy Mini Kits (cat. no. 74104) purchased from Qiagen (Valencia, CA) were used to extract RNA from cells in accordance with the manufacture's instructions. Aliquots of 1μg RNA were then reverse-transcribed using SuperScript III Reverse Transcriptase as recommended by the manufacturer (cat. no. 18080093, Invitrogen, Carlsbad, CA).

Quantitative real-time RT-PCR amplification of cDNA

Taqman human gene expression assays were used for PCR amplification of target gene cDNA per the manufacture's instructions and as previously described (Applied Biosystems, Foster City CA) [22]. Stratagene MX3005P machine was used to quantify mRNA expression of target genes. Reactions were amplified using the following conditions: 10 minutes at 95°C, 40 cycles of 95°C for 30 seconds, followed by 1 minute at 55°C and 1 minute at 72°C. Data were expressed as mean ± SD ΔCt values. Individual reactions were normalized by multiplex analysis with 18S rRNA housekeeping gene (Applied Biosystems, Foster City, CA). Fold-change values were calculated using the equation $2^{-\Delta Ct}$ as previously described [22]. The probes and

primer kits purchased from Applied Biosystems include: FGFR1 (Hs00915134-g1), FGFR2 (Hs01552926-m1), FGFR3 (Hs00179829-m1), FGFR4 (Hs01106908-m1), and Klotho (Hs00183100-m1).

Protein isolation and western blots

For experiments assessing phosphorylation activity, cells were serum-starved overnight prior to the addition of FGF23 (100ng/ml). For time-course experiments, cells were treated for 1, 2, 5, 10, 30, and 60 minute periods before protein extraction. Following the experiment, cells were lysed with RIPA buffer (cat. no. R0278, Sigma Aldrich, St. Louis, MO) containing 1% protease inhibitor cocktail (cat. no. P8340, Sigma Aldrich, St. Louis, MO) and 1% phosphatase inhibitor cocktail (cat. no. P5726, Sigma Aldrich, St. Louis, MO). Protein lysates were centrifuged at 4°C at 5000*g* for 20 minutes and supernatants were collected and stored at -20°C. Protein lysates were separated by molecular weight using 10% SDS-PAGE followed by western blot transfer and immunoblotting. Biotinylated protein ladder (cat. no. 7727, Cell Signaling Technology, Danvers, MA, USA) was used to validate molecular weights. After blocking with 5% BSA, blots were incubated overnight at 4°C with primary antibody against human Phospho-ERK1/2 (cat. no.), ERK1/2 (cat. no.), Phospho-AKT (cat. no.), and AKT (cat. no.). Horse-radish peroxidase (HRP)-conjugated secondary antibodies: anti-rabbit (cat. no. 7074) and anti-biotin (cat. no. 7075) were incubated for 1 hour at room temperature. Enhanced Chemiluminescence Western Blotting Substrate (cat. no. 32106) purchased from

Pierce Thermo Fisher (Carlsbad, CA) was used to detect HRP. Densitometery of band intensities was quantified using ImageJ software (National Institutes of Health, Bethesda, MD).

Co-cultures and fluorescence microscopy with DiI-Ac-LDL

Primary cultures of HAEC were plated into 4- or 8-well chamber slides and pre-treated with FGF23 for 1 hour prior to the addition of PBMC isolated from healthy donors. Co-cultures were incubated for 72 hours in 37°C with 5% CO_2. Following the incubation period, co-cultures were incubated with acetylated low density Lipoprotein labeled with 1,1'-dioctadecyl-3,3,3',3'- tetramethylindo-carbocyanine perchlorate (DiI-Ac-LDL; cat. no. L3484) purchased from Thermo Scientific for an additional 4 hours. Media was then removed and cells were washed twice before fixing with 1% PFA for 10 minutes at 4°C. Slides were mounted with Vectashield Antifade mounting media with DAPI (cat. no. H-1200) purchased from Vector Laboratories (Birmingame, CA) and analyzed with fluorescence light microscope. Multiple planes of view were captured for each treatment and images were quantified using ImageJ software to measure mean fluorescence intensity (MFI) and percentage of cells with fluorescence.

Collection and separation of HAEC conditioned media

Primary cultures of HAEC were plated into 6-well plates and treated with either FGF23 (100ng/ml) or vehicle control. For all time course experiments, cultures were

allowed to incubate between 1-24hrs. A 3-hour incubation was used for all other experiments. Following the treatment period, conditioned media was collected and centrifuged at 5,000*g* for 20 minutes in 4°C. Supernatant was transferred to fresh tubes and stored at -80°C. For experiments requiring filtration, 2ml of the supernatant from each sample was additionally separated by centrifugal filtration using Ultra-4 Centrifugal Filter Concentrator (cat. no. UFC801008) purchased from Millipore (Billirica, MA). Proteins too large to pass through the filter were suspended in 2ml of RPMI media. All conditioned media samples were immediately added to monocyte cultures or stored in -80°C for later use.

RESULTS

FGFR expression and stimulation in response to FGF23 in HAEC

To determine if endothelial cells are a potential target cell population for FGF23 driven responses, HAEC were assessed for expression of FGF receptors (FGFR) and FGF co-receptor Klotho. Data in Table 1 show that HAEC express mRNA for all FGF receptors and Klotho. Our previous research in monocytes indicated a role for FGF23 in regulating FGFR1 and Klotho [22]. To test whether this occurred in endothelial cells, HAEC were treated with FGF23 (100ng/ml) for 24 hours and analyzed for changes in mRNA levels of FGFR1-4 and Klotho (Figure 3.1A). Treatment with FGF23 suppressed FGFR2 expression, but did not affect mRNA expression of FGFR1, 3, 4.

After demonstrating HAEC express the machinery required to respond to FGF23, we explored whether FGF23 would elicit changes in signaling pathways. Time-course experiments were conducted by stimulating HAEC with FGF23 (100ng/ml) and assessing activation of ERK1/2 and AKT after 1, 2, 5, 10, 30, and 60 minutes of FGF23 exposure (Fig. 3.1B, C). Western blot analysis demonstrated a time-dependent increase in ERK1/2 phosphorylation, with peak activation at 10 minutes post-stimulation. A subsequent time-dependent decrease in phosphorylated-ERK1/2 was observed following the 10-minute time point. Western blot analysis indicated a lack of phosphorylation activity of AKT in response to FGF23 at any of the time points assessed suggesting FGF23 selectively stimulates the ERK1/2 pathway in the endothelium (Data not shown).

To assess whether FGF23 can induce endothelial activation, the expression of cell surface adhesion proteins that are characteristic of activated endothelium were measured. RT-PCR results demonstrated FGF23 did not alter expression of vascular cell adhesion molecule (VCAM) 1, intracellular adhesion molecule (ICAM) 1, or endothelial selectin (E-selectin) (Supplemental Figure 3.1), all of which are considered classical markers for endothelial cell activation.

Effects of FGF23 on lipid accumulation in HAEC and monocytes

Given the importance of the endothelial/monocyte macrophage interface in CVD and the evidence showing FGF23 has the ability to trigger responses in both cell types, we examined whether FGF23 had any effect on the interactions between endothelial and monocyte populations. To explore the effects of FGF23 on the endothelial-monocyte microenvironment, we employed a co-culture system to determine whether FGF23 could affect cellular responses to modified LDL molecules since increased production of oxidized low-density lipoprotein (ox-LDL) in circulation is a key contributor to CVD.

Uptake of DiI-Ac-LDL, a well-established mimic of ox-LDL, was unaffected in HAEC monocultures treated with FGF23, and the minor change seen in lipid uptake in monocultures of PBMC-derived monocytes was not statistically significant (Figure 3.2A-C). However, HAEC from the co-cultures demonstrated a robust uptake of DiI-Ac-LDL that was significantly reduced upon FGF23 exposure. Because this result was not observed in monocultures of HAEC, this suggests that

changes in lipid localization were dependent upon the interaction between the endothelial cells and monocytes in co-culture.

FGF23-driven lipid uptake in monocytes is independent of physical contact with HAEC

Since FGF23 only effects monocyte lipid accumulation in the presence of HAEC, we sought to determine whether this effect was dependent upon physical interactions between the two cell types. We collected conditioned media from HAEC that had been treated with either vehicle or FGF23 for various lengths of time (1, 2, 4, 8, 18, and 24 hours). PBMC-derived monocytes were then incubated in each sample of conditioned media for 72 hours, followed by 4 hour incubation with DiI-Ac-LDL. Monocytes treated with CM_{FGF23} exhibited incremental time-dependent increases in lipid uptake that were absent in monocytes treated with CM_{Veh} (Figure 3.3). FGF23 alone did not affect monocyte lipid accumulation (Figure 3.2, column 1). Monocytes treated with CM_{FGF23} from the 4 hour time point took up the most amount of DiI-Ac-LDL. This result led us to use HAEC treatment periods between 3-4 hours for subsequent experiments.

To confirm this finding, monocytes were treated with either CM_{Veh} or CM_{FGF23} for 72hrs, followed by DiI-Ac-LDL incubation, and then analyzed by flow cytometry. Cultures treated with CM_{FGF23} showed a significantly higher percentage of monocytes taking up DiI-Ac-LDL as compared to monocytes incubated in CM_{Veh} (Figure 3.4A). To ascertain whether the increase in DiI-Ac-LDL uptake by

monocytes was the result of increased generalized phagocytosis, 10kDa MW FITC-dextran conjugated beads were added to monocytes treated with either CM_{Veh} or CM_{FGF23}. Internalized particles were quantified by flow cytometry (n=4). There were no changes in the percentage of cells taking up FITC-dextran beads observed between monocytes treated with CM_{Veh} or CM_{FGF23} indicating that FGF23-driven lipid uptake by monocytes is specific for modified LDL particles (Figure 3.4B). Results also show no change in mean fluorescence intensity per cell taking up either DiI-Ac-LDL or FITC-dextran between CM_{Veh}- and CM_{FGF23}- treated monocytes.

HAEC stimulation by FGF23 drives expression of differentiation marker CD209

Given the changes in macrophage function, we investigated if FGF23 induced alterations in macrophage polarization during the endothelial/monocyte interaction. To do this, we measured expression of CD209, a marker for macrophage differentiation, in the co-cultures of monocytes and endothelial cells treated with FGF23 using flow cytometry. Results of these experiments showed a significant increase in CD209+ macrophages (Figure 3.5).

To confirm CD209 expression was increasing as a result of FGF23 in the co-cultures, we then tested for an increase in CD209+ macrophages in experiments using monocytes treated with CM_{Veh} or CM_{FGF23}. Similar to co-culture experiments, there was a significant increase in CD209+ macrophages in cultures treated with CM_{FGF23} compared with CM_{Veh} (Figure 3.5). This supports the hypothesis that in

addition to function changes, monocytes were also undergoing phenotypic changes to facilitate increased lipid accumulation.

Identification of HAEC-derived protein causing monocyte differentiation

Since conditioned media from HAEC treated with FGF23 was sufficient to cause monocyte lipid accumulation, we hypothesized that FGF23 stimulates HAEC to secrete a factor driving monocyte differentiation. To explore this, we used a 10kDa MW filter to separate both CM_{Veh} and CM_{FGF23} into two groups each: media containing molecules smaller than 10kDa and greater than 10kDa, before incubating with monocytes. Cultures of monocytes treated with CM_{FGF23}(<10kDa) were unable to produce differentiated, lipid engulfing monocytes. However, monocytes treated with CM_{FGF23}(>10kDa) showed comparable uptake of DiI-Ac-LDL as unfiltered CM_{FGF23}. (Figure 3.6). Given that conditioned media containing only particles above 10kDa was able to induce a response, it is likely that the HAEC secreted factor is a protein or protein complex. Further investigation is required to confirm this and to identify the factor. Preliminary data of mRNA for the 24kDa protein, Endothelin 1 shows a trending increase in HAEC after 6 hours of FGF23 treatment.

DISCUSSION

Our data show that HAEC express mRNA of all FGF receptors, with FGFR1 being the predominant isoform. Klotho, the co-receptor required in most cell types for FGF23 binding, is also expressed at the mRNA level albeit at low levels. Work done by Myles Wolfe and Christian Faul's groups demonstrated FGF23 is capable of stimulating cardiomyocytes in vitro in the absence of Klotho leading to left ventricular hypertrophy [23, 24]. Thus, Klotho may not be necessary for FGF23 stimulation of certain cell types in a cardiovascular setting, possibly including endothelial cells. Previous research conducted by our group in monocytes showed FGF23 stimulated both ERK1/2 and AKT activation [22]. However, only ERK1/2 activation was observed in HAEC in response to FGF23 alluding to a specific and selective function for FGF23 in the cardiovascular system.

Monocyte lipid accumulation is a key component to the initiation and propagation of CVD. Patients with CKD are at a much larger risk of developing CVD, particularly if they are experiencing dyslipidemia resulting from renal failure [25, 26]. Therefore, mitigating the effects of lipid accumulation in these patients is crucial to averting CVD development. Elevation in serum FGF23 are inevitable in CKD and is typically among the first molecular abnormalities observed [7, 8, 27]. However, until now, it has been largely unknown whether or how FGF23 contributes to cardiovascular disease. Here, we provide evidence for a pathological role of FGF23 in an endothelial-dependent initiation of monocyte differentiation classically associated with CVD.

Monocytes in co-culture with endothelial cells and FGF23 display increased expression of CD209 as well as increased uptake of the ox-LDL mimic, DiI-Ac-LDL, as compared to co-cultures without FGF23. This result is dependent upon endothelial stimulation by FGF23 as monocytes cultured alone were unaffected by FGF23. Interestingly though, this dependency on the endothelium does not require direct physical interaction. The monocyte-endothelial niche is a dynamic microenvironment, consisting of transient interactions between the two cell types that drive several biological processes. Given that conditioned media from endothelial cells treated with FGF23 elicited a change in CD209 expression and lipid uptake in monocytes, it is very likely that FGF23 is stimulating the secretion of a molecule from the endothelium that acts to regulate monocyte polarization. Additional support of the changes in lipid localization were apparent from data showing a decrease in HAEC DiI-Ac-LDL uptake in co-cultures. Alone, HAEC were unaffected by FGF23. However, HAEC analyzed after co-culture containing FGF23 and subsequent DiI-Ac-LDL exposure showed a dramatic decrease in lipid uptake compared to co-cultures treated with vehicle. This result directly complements our data demonstrating an increase in monocyte lipid uptake in co-cultures with FGF23. Collectively, the data presented here demonstrates FGF23 has an indirect effect on monocyte lipid accumulation, specifically modified LDL that is evoked by time-dependent FGF23 stimulation of HAEC. Furthermore we confirmed that this effect was independent of any physical contact between monocytes and the endothelium indicating that FGF23 is likely causing HAEC to secrete a factor that

is initiating monocyte differentiation. To our knowledge, this is the first and only study to show that FGF23 causes monocyte polarization through stimulation of endothelial cells. This finding is crucial for the advancement of therapeutics targeting cardiovascular complications associated with chronic kidney disease.

Future directions to include exploring the a potential role for Endothelin 1

Endothelin-1 (ET-1) has been characterized for its role in monocyte polarization, induction of lipid accumulation and quick release in hypoxia-stimulated endothelial cells [28, 29]. We therefore hypothesized it may also be secreted in response to FGF23. Current studies are investigating Et-1 as a possible factor in FGF23/endothelial-induced monocyte differentiation. Et-1 is both transcriptionally and post-translationally regulated and is stored in endothelial vesicles exocytose upon certain types of endothelial stimulation [30-34]. This mechanism is in line with our data showing an effect after only a few hours of HAEC FGF23 exposure. Preliminary results measuring endothelin-1 mRNA in HAEC after FGF23 stimulation for various periods of time showed a trending increase after 6 hours suggesting FGF23 may additionally transcriptionally regulate endothelin-1. This result is consistent with previous results demonstrating an effect on monocyte differentiation using HAEC CM treated for only 3 hours with FGF23 and the time course experiments showing peak lipid accumulation in monocytes treated with 4hr CM_{FGF23}. Taken together, this data indicate that FGF23 may trigger the expulsion of intracellular vesicles containing endothelin-1 from

HAEC into the media where it binds its receptor on monocytes, initiating differentiation. Future studies will aim to clarify the relationship between FGF23 stimulation and endothelin-1 secretion in endothelial cells.

TABLE 3.1

Table 3.1 Expression of mRNA for FGFRs and Klotho in HAEC

Genes	ΔCt (mean ± SEM)	Log_2 of fold change relative to Klotho
FGFR1	7.88 ± 0.32	14.69
FGFR2	19.10 ± 0.62	2.91
FGFR3	17.33 ± 0.24	5.49
FGFR4	16.54 ± 0.56	6.14
Klotho	23.15 ± 1.05	0.00

Table 3.1 Expression of mRNA for FGFRs and Klotho in HAEC

Untreated HAEC express mRNA for FGFR1, 2, 3, and 4, and Klotho. Data are shown as mean ΔCt PCR amplification values ± SEM, after normalization to expression of housingkeeping gene 18S rRNA (column 2). Log transformed fold change of mRNA expression relative to Klotho expression shows the predominantly expressed receptor in HAEC is FGFR1 (column 3). Results represent average of n=3. FGFR= fibroblast growth factor receptor; ΔCt=threshold cycle change.

FIGURE 3.1

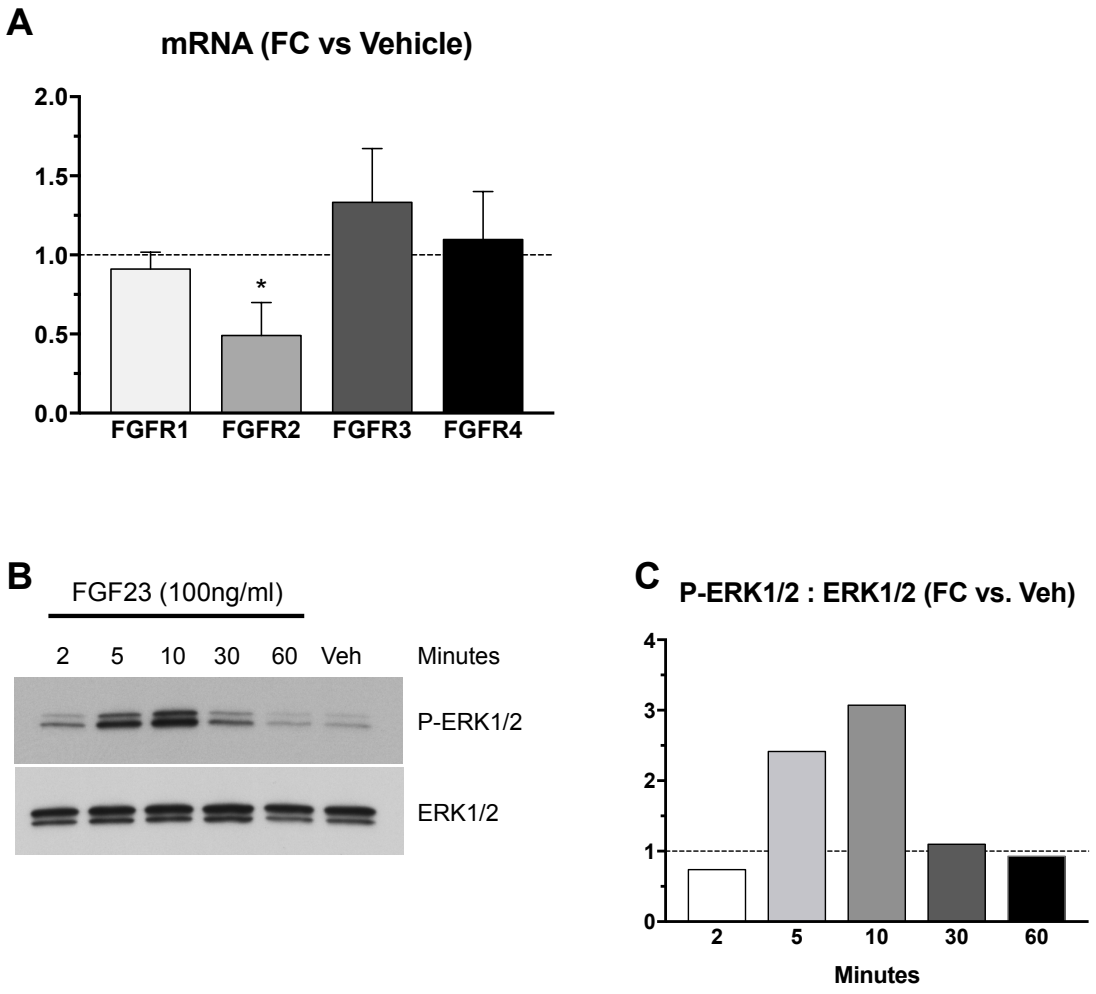

Figure 3.1 Responses to FGF23 in HAEC

FGFRs mRNA as measured by RT-PCR and ERK1/2 activity as measure by Western blot analysis. **(A)** FGF23 (100ng/ml) suppressed mRNA expression of FGFR2 (*$p<0.05$), but did not significantly effect FGFR1, 3, or 4 in HAEC after 24hrs. **(B)** Representative Western blot showing protein expression of ERK1/2 and phosphorylated ERK1/2 (P-ERK1/2). HAEC were treated with FGF23 (100ng/ml) for 2, 5, 10, 30, and 60 in serum-free medium. FGF23 stimulation resulted in time-

dependent increases in ERK1/2 phosphorylation, reaching peak activation (3.07 fold change) at 10 minutes. (C) Densitometery of band intensities was quantified using ImageJ software. Data shows fold change of phosphor-ERK1/2 relative to total ERK1/2 protein. FGF23 did not result in changes in phosphorylated AKT in HAEC (data not shown).

FIGURE 3.2

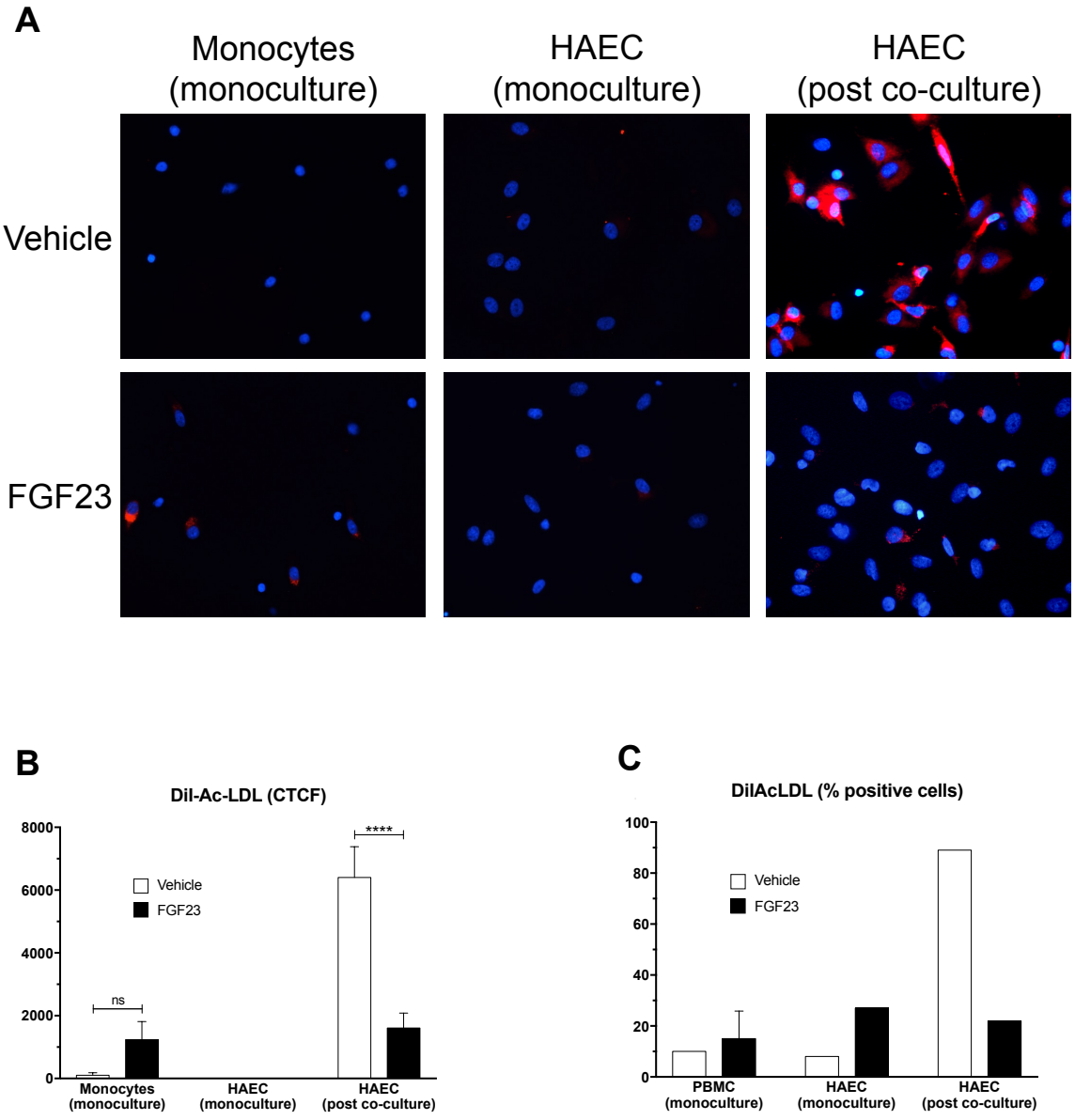

Figure 3.2 FGF23 alters lipid accumulation in co-cultures of HAEC and monocytes

Analysis of images captured by fluorescence microscopy. **(A)** PBMC-derived monocytes incubated with either FGF23 (100ng/ml) or vehicle exhibited no

significant differences in the amount of DiI-Ac-LDL uptake or in the number of cells taking up DiI-Ac-LDL (column 1). HAEC did not uptake a significant amount of DI-Ac-LDL in either FGF23 or vehicle treated cultures (column 2). HAEC cultured and treated with FGF23 in the presence of monocytes showed a significant reduction (****$p<0.0001$) of DiI-Ac-LDL uptake as well as the number of cells taking up DiI-Ac-LDL as compared to vehicle control (column 3). **(B)** DiI-Ac-LDL intensity was quantified by ImageJ software. CTCF= corrected total cell fluorescence. **(C)** Percent DiI-Ac-LDL positive cells was calculated with the equation % positive= number cells with DiI-Ac-LDL/ total number of cells in plane of view. Measurements represent the average of four planes of view per image and four biological replicates.

FIGURE 3.3

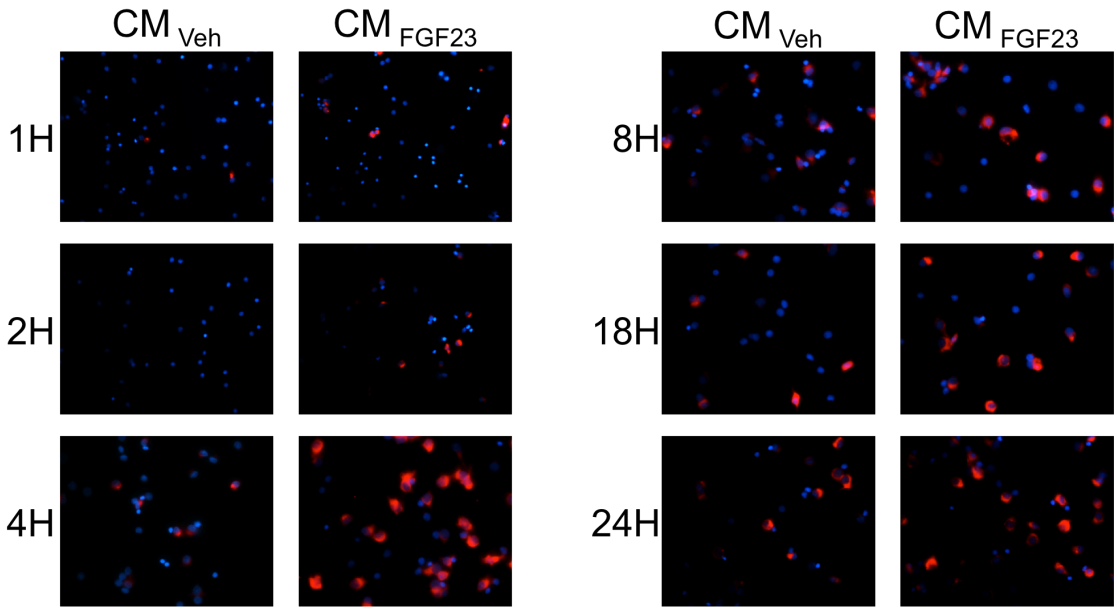

Figure 3.3 CM_{FGF23} driven monocyte lipid accumulation is time-dependent

Analysis of images captured by fluorescence microscopy. PBMC-derived monocytes incubated with HAEC conditioned media treated with FGF23 (100ng/ml) exhibited a time-dependent increase in uptake of DiI-Ac-LDL. HAEC conditioned media was collected after 1, 2, 4, 8, 18, and 24 hour exposure to FGF23 (100ng/ml) prior to incubation with monocytes.

FIGURE 3.4

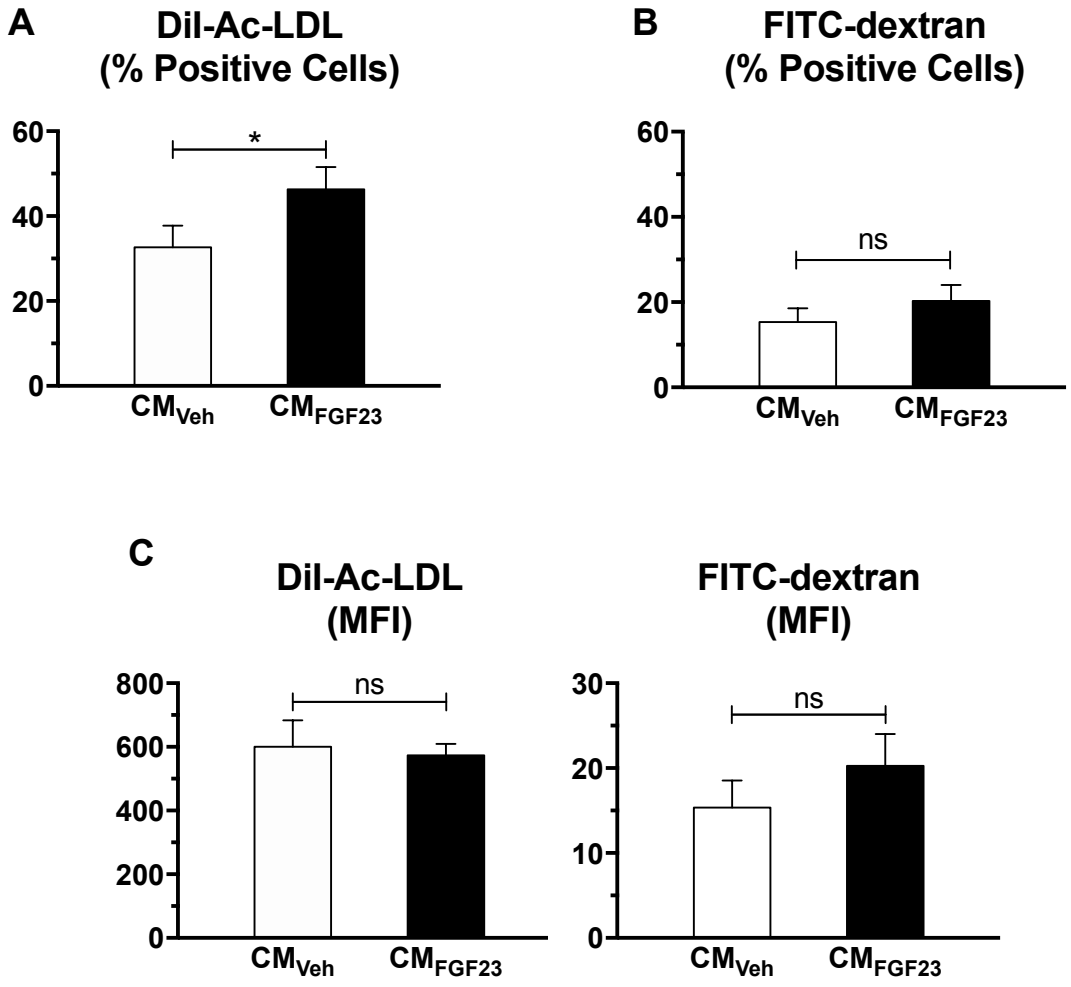

Figure 3.4 CM_{FGF23} specifically alters modified LDL uptake by monocytes

Flow cytometry analysis of monocytes incubated with conditioned media from HAEC treated with either FGF23 (CM_{FGF23}) or vehicle (CM_{Veh}). **(A)** Monocytes treated with CM_{FGF23} exhibited an increase in the number of cells taking up DiI-Ac-LDL as compared to monocytes treated with CM_{Veh} (*$p < 0.05$). **(B)** There was no

significant difference in the number of cells taking up FITC-dextran between CM_{FGF23} and CM_{Veh}. (C) MFI was unchanged for both DiI-Ac-LDL and FITC-dextran.

FIGURE 3.5

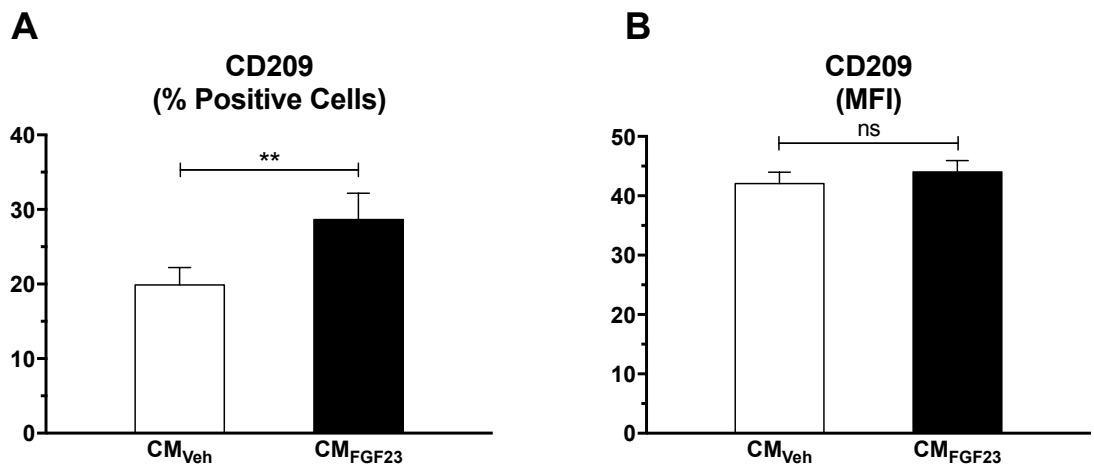

Figure 3.5 CM from HAEC treated with FGF23 alters monocyte lipid accumulation

Flow cytometry analysis of monocytes incubated with conditioned media from HAEC treated with either FGF23 CM_{FGF23} or vehicle CM_{Veh}. **(A)** The number of CD209+ monocytes was significantly (**$p < 0.001$) increased in monocyte cultures incubated with CM_{FGF23} as compared to CM_{Veh}. **(B)** MFI was unchanged between treatment groups.

FIGURE 3.6

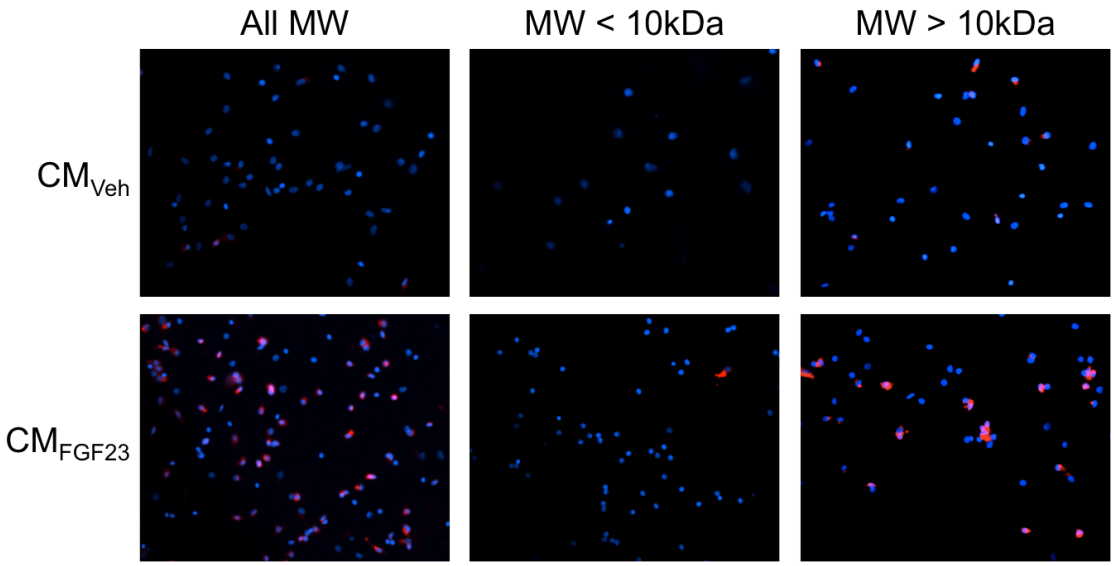

Figure 3.6 HAEC secreted factor is above 10kDa

CM_{Veh} and CM_{FGF23} were each separated by a 10kDa molecular weight cut off prior to incubation with monocytes. CM_{FGF23} containing molecules above 10 kDa elicited the same monocyte DiI-Ac-LDL uptake as the unfiltered CM_{FGF23}, whereas CM_{FGF23} containing only molecules below 10kDa had no effect on DiI-Ac-LDL uptake.

FIGURE 3.7

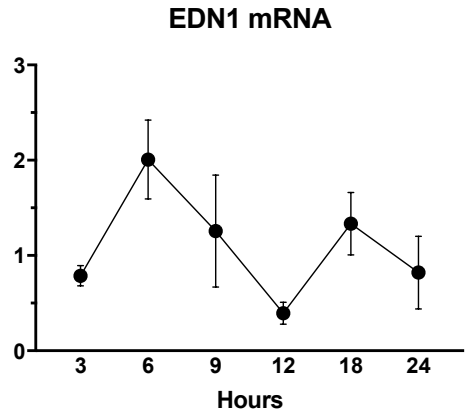

Figure 3.7 EDN1 mRNA expression in HAEC treated with FGF23

Expression of END1 mRNA is trending upward in HAEC after exposure to FGF23 for 6 hours.

Supplemental Figure 3.1

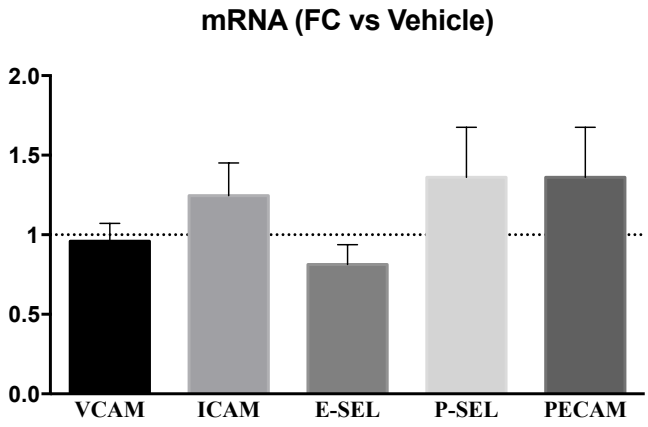

Supplemental Figure 3.1 FGF23 does not increase adhesion markers in HAEC

Expression of mRNA for endothelial cell adhesion markers as measured by RT-PCR. HAEC treated for 24 hours with FGF23 (100ng/ml) did not have a significant change in inflammatory-associated cell surface adhesion markers.

REFERENCES

1. *Chronic Kidney Disease (CKD) Surveillance Project.* [cited 2016; Available from: https://nccd.cdc.gov/ckd/.
2. (CDC), C.f.D.C.a.P. *National Chronic Kidney Disease Fact Sheet: General Information and National Estimates on Chronic Kidney Disease in the United States.* 2014; Available from: http://www.cdc.gov/diabetes/pubs/pdf/kidney_factsheet.pdf.
3. Foley, R.N., P.S. Parfrey, and M.J. Sarnak, *Clinical epidemiology of cardiovascular disease in chronic renal disease.* Am J Kidney Dis, 1998. **32**(5 Suppl 3): p. S112-9.
4. Impellizzeri, D., et al., *Targeting inflammation: new therapeutic approaches in chronic kidney disease (CKD).* Pharmacol Res, 2014. **81**: p. 91-102.
5. Kotur-Stevuljevic, J., et al., *Hyperlipidemia, oxidative stress, and intima media thickness in children with chronic kidney disease.* Pediatr Nephrol, 2013. **28**(2): p. 295-303.
6. Stenvinkel, P., et al., *Inflammation and outcome in end-stage renal failure: does female gender constitute a survival advantage?* Kidney Int, 2002. **62**(5): p. 1791-8.
7. Isakova, T., et al., *Fibroblast growth factor 23 is elevated before parathyroid hormone and phosphate in chronic kidney disease.* Kidney Int, 2011. **79**(12): p. 1370-8.

8. Portale, A.A., et al., *Disordered FGF23 and mineral metabolism in children with CKD.* Clin J Am Soc Nephrol, 2014. **9**(2): p. 344-53.

9. Feig, J.E., et al., *HDL promotes rapid atherosclerosis regression in mice and alters inflammatory properties of plaque monocyte-derived cells.* Proc Natl Acad Sci U S A, 2011. **108**(17): p. 7166-71.

10. Moore, K.J., F.J. Sheedy, and E.A. Fisher, *Macrophages in atherosclerosis: a dynamic balance.* Nat Rev Immunol, 2013. **13**(10): p. 709-21.

11. Rojas, J., et al., *Macrophage Heterogeneity and Plasticity: Impact of Macrophage Biomarkers on Atherosclerosis.* Scientifica (Cairo), 2015. **2015**: p. 851252.

12. Bellingan, G.J., et al., *In vivo fate of the inflammatory macrophage during the resolution of inflammation: inflammatory macrophages do not die locally, but emigrate to the draining lymph nodes.* J Immunol, 1996. **157**(6): p. 2577-85.

13. Linton, M.F., et al., *The Role of Lipids and Lipoproteins in Atherosclerosis*, in *Endotext*, L.J. De Groot, et al., Editors. 2000, MDText.com, Inc.: South Dartmouth MA.

14. Moore, K.J. and I. Tabas, *Macrophages in the pathogenesis of atherosclerosis.* Cell, 2011. **145**(3): p. 341-55.

15. Kashiwagi, M., et al., *Association of monocyte subsets with vulnerability characteristics of coronary plaques as assessed by 64-slice multidetector*

computed tomography in patients with stable angina pectoris. Atherosclerosis, 2010. **212**(1): p. 171-6.

16. Bouhlel, M.A., et al., *PPARgamma activation primes human monocytes into alternative M2 macrophages with anti-inflammatory properties.* Cell Metab, 2007. **6**(2): p. 137-43.
17. Feig, J.E., et al., *Reversal of hyperlipidemia with a genetic switch favorably affects the content and inflammatory state of macrophages in atherosclerotic plaques.* Circulation, 2011. **123**(9): p. 989-98.
18. Feig, J.E., et al., *Regression of atherosclerosis is characterized by broad changes in the plaque macrophage transcriptome.* PLoS One, 2012. **7**(6): p. e39790.
19. Wolfs, I.M., et al., *Reprogramming macrophages to an anti-inflammatory phenotype by helminth antigens reduces murine atherosclerosis.* FASEB J, 2014. **28**(1): p. 288-99.
20. He, H., et al., *Endothelial cells provide an instructive niche for the differentiation and functional polarization of M2-like macrophages.* Blood, 2012. **120**(15): p. 3152-62.
21. Lee, S., et al., *Distinct macrophage phenotypes contribute to kidney injury and repair.* J Am Soc Nephrol, 2011. **22**(2): p. 317-26.
22. Bacchetta, J., et al., *Fibroblast growth factor 23 inhibits extrarenal synthesis of 1,25-dihydroxyvitamin D in human monocytes.* J Bone Miner Res, 2013. **28**(1): p. 46-55.

23. Faul, C., et al., *FGF23 induces left ventricular hypertrophy.* J Clin Invest, 2011. **121**(11): p. 4393-408.

24. Grabner, A., et al., *Activation of Cardiac Fibroblast Growth Factor Receptor 4 Causes Left Ventricular Hypertrophy.* Cell Metab, 2015. **22**(6): p. 1020-32.

25. Khandelwal, P., et al., *Dyslipidemia, carotid intima-media thickness and endothelial dysfunction in children with chronic kidney disease.* Pediatr Nephrol, 2016.

26. Gracia, M., et al., *Predictors of Subclinical Atheromatosis Progression over 2 Years in Patients with Different Stages of CKD.* Clin J Am Soc Nephrol, 2016. **11**(2): p. 287-96.

27. Dai, B., et al., *A comparative transcriptome analysis identifying FGF23 regulated genes in the kidney of a mouse CKD model.* PLoS One, 2012. **7**(9): p. e44161.

28. Davenport, A.P., et al., *Endothelin.* Pharmacol Rev, 2016. **68**(2): p. 357-418.

29. Lin, C.Y., et al., *Endothelin-1 exacerbates lipid accumulation by increasing the protein degradation of the ATP-binding cassette transporter G1 in macrophages.* J Cell Physiol, 2011. **226**(8): p. 2198-205.

30. Quehenberger, P., et al., *Endothelin 1 transcription is controlled by nuclear factor-kappaB in AGE-stimulated cultured endothelial cells.* Diabetes, 2000. **49**(9): p. 1561-70.

31. Marsden, P.A. and B.M. Brenner, *Transcriptional regulation of the endothelin-1 gene by TNF-alpha.* Am J Physiol, 1992. **262**(4 Pt 1): p. C854-61.

32. Yokota, J., et al., *Retinoic acid suppresses endothelin-1 gene expression at the transcription level in endothelial cells.* Atherosclerosis, 2001. **159**(2): p. 491-6.

33. Harrison, V.J., et al., *Identification of endothelin 1 and big endothelin 1 in secretory vesicles isolated from bovine aortic endothelial cells.* Proc Natl Acad Sci U S A, 1995. **92**(14): p. 6344-8.

34. Wang, X., et al., *Intracellular redistribution of cardiac endothelin-1 receptor in rat during myocardial hypertrophy.* Chin Med Sci J, 2001. **16**(2): p. 86-92.

Chapter 4

Suppression of Iron-Regulatory Hepcidin by Vitamin D

PREFACE

Dysregulation of iron homeostasis is commonly associated with CKD often resulting in iron deficiency and anemia. Hepcidin is a small peptide that was initially characterized for its role in combating intracellular microbial infections by regulating iron toxicity within phagocytic immune cells, most commonly monocytes [Ganz paper]. Synthesized in response to infection and inflammation, Hepcidin catalyzes the degradation of the only known mammalian iron export protein, Ferroportin. This thereby traps iron within cells lacking membrane-tethered Ferroportin. Functioning as an anti-microbial agent, Hepcidin-induced iron sequestration is an effective method for fighting extracellular pathogens that are dependent upon iron for replication. However, chronic intracellular iron sequestration can lead to serious complications such as long-lasting serum iron deficiency. The chronic lack of circulating bioavailable iron due to over-production of Hepcidin inhibits proper red blood cell development leading to anemia.

Over-production of Hepcidin as well as vitamin D deficiency are closely associated with anemia of CKD, and therefore represent potential for therapeutic alternatives for targeting anemia in patients with CKD. This paper explores the relationship between vitamin D and Hepcidin in iron regulation, inflammation, and anti-microbial function in the context of CKD.

BASIC RESEARCH www.jasn.org

Suppression of Iron-Regulatory Hepcidin by Vitamin D

Justine Bacchetta,*†‡ Joshua J. Zaritsky,† Jessica L. Sea,* Rene F. Chun,* Thomas S. Lisse,* Kathryn Zavala,* Anjali Nayak,† Katherine Wesseling-Perry,† Mark Westerman,§ Bruce W. Hollis,‖ Isidro B. Salusky,† and Martin Hewison*

*Department of Orthopaedic Surgery, UCLA Orthopaedic Hospital, and †Department of Pediatrics, David Geffen School of Medicine, University of California at Los Angeles, Los Angeles, California; ‡Centre de Référence des Maladies Rénales Rares, Institut de Génomique Fonctionnelle à l'Ecole Normale Supérieure de Lyon et Université de Lyon, Lyon, France; §Intrinsic Life Sciences, La Jolla, California; and ‖Departments of Pediatrics, Biochemistry, and Molecular Biology, Medical University of South Carolina, Charleston, South Carolina

ABSTRACT

The antibacterial protein hepcidin regulates the absorption, tissue distribution, and extracellular concentration of iron by suppressing ferroportin-mediated export of cellular iron. In CKD, elevated hepcidin and vitamin D deficiency are associated with anemia. Therefore, we explored a possible role for vitamin D in iron homeostasis. Treatment of cultured hepatocytes or monocytes with prohormone 25-hydroxyvitamin D or active 1,25-dihydroxyvitamin D decreased expression of hepcidin mRNA by 0.5-fold, contrasting the stimulatory effect of 25-hydroxyvitamin D or 1,25-dihydroxyvitamin D on related antibacterial proteins such as cathelicidin. Promoter-reporter and chromatin immunoprecipitation analyses indicated that direct transcriptional suppression of hepcidin gene (*HAMP*) expression mediated by 1,25-dihydroxyvitamin D binding to the vitamin D receptor caused the decrease in hepcidin mRNA levels. Suppression of *HAMP* expression was associated with a concomitant increase in expression of the cellular target for hepcidin, ferroportin protein, and decreased expression of the intracellular iron marker ferritin. In a pilot study with healthy volunteers, supplementation with a single oral dose of vitamin D (100,000 IU vitamin D_2) increased serum levels of 25D-hydroxyvitamin D from 27 ± 2 ng/ml before supplementation to 44 ± 3 ng/ml after supplementation ($P < 0.001$). This response was associated with a 34% decrease in circulating levels of hepcidin within 24 hours of vitamin D supplementation ($P < 0.05$). These data show that vitamin D is a potent regulator of the hepcidin-ferroportin axis in humans and highlight a potential new strategy for the management of anemia in patients with low vitamin D and/or CKD.

J Am Soc Nephrol 25: 564–572, 2014. doi: 10.1681/ASN.2013040355

Patients with CKD require iron supplementation and erythropoiesis stimulating agents (ESAs) to correct disease-associated anemia.[1] However, ESA hyporesponsiveness is common, with the iron homeostasis factor hepcidin (encoded by the *HAMP* gene) emerging as a possible culprit.[2] Hepcidin post-translationally suppresses membrane expression of ferroportin, the only known exporter of intracellular iron.[3] Elevated plasma hepcidin, common to patients with CKD[4] or inflammation,[5] causes intracellular sequestration of iron and increases risk of anemia. By contrast, patients with hemochromatosis or iron deficiency exhibit decreased hepcidin.[6]

Studies of patients with CKD suggest that vitamin D status (serum concentrations of the prohormone 25-hydroxyvitamin D [25D]) correlates inversely with the prevalence of anemia[7] and ESA resistance[8] and directly with blood hemoglobin levels.[8] In hemodialysis patients with anemia, vitamin D repletion has been shown to correlate with lower ESA requirements.[9,10] Vitamin D is known to exert physiologic activities beyond its classic skeletal function, notably as a potent

Received April 8, 2013. Accepted September 13, 2013.

Published online ahead of print. Publication date available at www.jasn.org.

Correspondence: Dr. M. Hewison, Department of Orthopaedic Surgery, UCLA Orthopaedic Hospital, 615 Charles E. Young Drive South, Room 410D, Los Angeles, CA 90095-7358. Email: mhewison@mednet.ucla.edu

inducer of antimicrobial proteins such as cathelicidin antibacterial protein (encoded by the cathelicidin [*CAMP*] gene).[11,12] In this respect, it is interesting that hepcidin was initially described as an antimicrobial peptide (encoded by the gene for hepcidin antibacterial protein, *HAMP*),[13] with its role in iron homeostasis being a later observation. We therefore hypothesized that vitamin D can act to regulate expression of hepcidin, in a similar fashion to its effects on other antimicrobial proteins. To test this hypothesis, vitamin D–mediated changes in hepcidin and cathelicidin were compared using *in vitro* and *in vivo* models.

RESULTS

Vitamin D Metabolites Suppress Expression of *HAMP*

Studies *in vitro* using PBMC monocytes, THP1 cells, and HepG2 cells showed that treatment with 25D (100 nM) or 1,25-dihydroxyvitamin D (1,25D) (5 nM) for 6 hours decreased expression of mRNA for *HAMP* (Figure 1A). In PBMC monocytes and THP1 cells, this response contrasted the effect of 25D and 1,25D in stimulating expression of mRNA for antibacterial *CAMP* (Figure 1B) and the vitamin D catabolic enzyme *CYP24A1* (Figure 1C). In HepG2 cells, treatment with 25D or 1,25D appeared to have no effect on expression of *CAMP*, and 1,25D induced only a small increase in mRNA for *CYP24A1*. Additional experiments with PBMC monocytes showed that suppression of mRNA for *HAMP* was also observed after 24-hour treatments with 100 nM 25D (0.57-fold±0.21, n=3; $P<0.05$) or 1,25D (0.27-fold±0.36, n=3; $P<0.01$).

To determine whether vitamin D–mediated suppression of hepcidin also occurs in nonhuman models, further studies were carried out *in vitro* using mouse monocytes. Peripheral blood-derived monocytes from wild-type C57BL/6 mice showed no change in mouse hepcidin (*Hamp*) gene expression after 24-hour treatment with increasing doses of 1,25D (Supplemental Figure 1A). Similar results were also observed for the mouse monocyte cell line J774 after 6-hour treatment with 25D (100 nM) or 1,25D (10 nM) (Supplemental Figure 1B). To assess possible effects of vitamin D on hepatic expression of *Hamp in vivo*, 12-week-old C57BL/6 male mice were placed on a vitamin D–deficient diet for 6 weeks and then transferred to a 4 ppm iron diet for 1 week. Groups of mice (n=4 in each case) were then treated with intraperitoneal injections of either 0.2 μg/g body weight 25D, 1 μg/g 25D, or 0.2 μg/g 1,25D. A similar volume of intraperitoneal saline was used as a control. Analysis of liver mRNA from these mice 24 hours after treatment showed no effect on expression of *Hamp* (Supplemental Figure 1C).

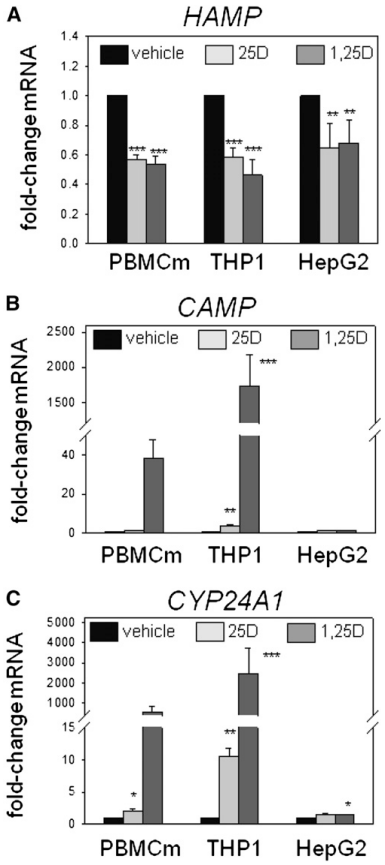

Figure 1. Vitamin D suppresses expression of hepcidin (*HAMP*) in human monocytes and hepatocytes. Effect of *in vitro* treatment of PBMC monocytes (PBMCm), monocytic THP1 cells, and HepG2 hepatocytic cells with vehicle, 25D (100 nM), or 1,25D (5 nM) for 6 hours on expression of mRNA for *HAMP* (A), *CAMP* (B), and *CYP24A1* (C). Data are shown as mean fold-change in gene expression (±SD) relative to vehicle (0.1% ethanol) controls. *$P<0.05$; **$P<0.01$; ***$P<0.001$, statistically different from vehicle-treated cells. For RT-PCR data, n=8 separate donors for PBMC monocytes, n=4 separate cultures of THP1 cells, and n=5 separate cultures of HepG2 cells.

Vitamin D Receptor–Mediated Transcriptional Repression of *HAMP*

In human cells, the suppression of *HAMP* expression by 1,25D or 25D appears to be due to direct inhibition of *HAMP* transcription. *In silico* analyses identified consensus vitamin D response elements (VDREs) within a 1071-bp *HAMP* proximal promoter DNA sequence (Supplemental Table 1). As shown in Figure 2A, chromatin immunoprecipitation (ChIP) assays using PBMC monocyte extracts demonstrated binding of vitamin D receptor (VDR) protein to DNA from a 1-kb fragment of the *HAMP* proximal promoter that includes the VDREs originally identified in Supplemental Table 1. Further ChIP analyses using extracts from the same cell type demonstrated similar VDR binding to promoter fragments for known VDR target genes such as *CAMP*

A

Treatment	Enrichment	*CYP24A1* -1Kb	*CYP24A1* - 2Kb	*CAMP* -1Kb	*HAMP* -1Kb	*IGX1A* (-VE)
Vehicle	RNA Pol II	116.6	72.0	229.9	747.9	24.4
1,25D	RNA Pol II	1418.4	407.3	636.9	660.2	23.2
Fold-change		**12.2**	**5.7**	**2.8**	**0.88**	**0.95**
Vehicle	VDR	41.4	33.9	108.4	272.5	7.62
1,25D	VDR	407.3	105.1	161.5	130.7	5.68
Fold-change		**9.8**	**3.1**	**1.5**	**0.48**	**0.75**

B

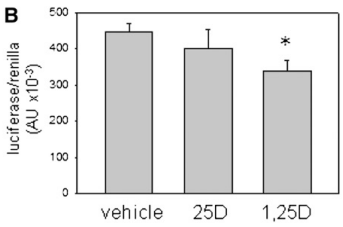

Figure 2. VDR-mediated suppression of hepcidin (*HAMP*) gene expression by 1,25D. (A) ChIP analysis of VDR and RNA Pol II interaction with the *HAMP* gene promoter. PBMC monocytes are treated with 1,25D (5 nM, 24 hours), chromatin extracts are prepared, and ChIP-grade antibodies are used to detect VDR and RNA Pol II interactions. The resulting enriched genomic DNA is qPCR amplified using primers for *CYP24A1* (−1 kb from the transcription start site and −2 kb from the transcription start site), *CAMP* (−1 kb from the transcription start site), *HAMP* (−1 kb from the transcription start site). A negative control sequence for VDR and RNA Pol II (*IGX1A)* is also used. Data are shown first as mean arbitrary units for PCR amplification of DNA associated with RNA Pol II or VDR in cells treated with vehicle or 1,25D (mean of two separate chromatin preparations). In addition, fold-change values are presented showing the change in RNA Pol II or VDR binding to DNA after treatment with 1,25D relative to vehicle-treated cells. (B) Effect of 25D (100 nM) and 1,25D (5 nM) on *HAMP* promoter-reporter activity in VDR-expressing MC3T3 mouse osteoblastic cells. Data are shown as *HAMP* target gene firefly/*Renilla* housekeeping luciferase activity ($\times 10^{-3}$). *$P<0.05$, statistically different from vehicle-treated cells.

and *CYP24A1*. Treatment of PBMCs with 1,25D enhanced VDR enrichment on the *CYP24A1* and *CAMP* promoters (Figure 2A), consistent with the transcriptional induction of these genes by 1,25D (Figure 1, B and C). By contrast, VDR enrichment decreased 0.5-fold for the *HAMP* promoter after treatment with 1,25D. A similar differential promoter response to 1,25D was also observed for ChIP analysis of RNA polymerase II (RNA Pol II), which is essential for gene transcription. Further analysis of the effects of vitamin D on *HAMP* gene expression using a luciferase promoter-reporter construct transfected into VDR-expressing MC3T3 cells showed that treatment with 1,25D produced a 24% decrease in transcription relative to vehicle-treated cells (Figure 2B). However, in the absence of *CYP27B1* expression/1α-hydroxylase activity in MC3T3 cells, treatment with 25D was without effect.

Vitamin D–Induced Suppression of HAMP Is Associated with Changes in Ferroportin and Ferritin Expression

In contrast to the suppression of *HAMP* in human monocytes or hepatocytes, 25D and 1,25D had no effect on levels of mRNA for *ferroportin* in PBMC monocytes, THP1 cells, or HepG2 cells (Figure 3A). However, Western blot and immunohistochemical analyses showed that treatment with 25D or 1,25D increased expression of ferroportin protein in hepatocytes and monocytes (Figure 3, B and C), suggesting a post-transcriptional mode of action for the effects of vitamin D metabolites on ferroportin. To assess the functional effect of vitamin D–mediated induction of ferroportin, further studies were carried out to determine expression of ferritin, an established marker of intracellular iron concentrations. Treatment with 25D or 1,25D decreased expression of mRNA for *ferritin* in PBMC monocytes, THP1 cells, and HepG2 cells (Figure 3D). Immunohistochemical analysis of ferritin protein in HepG2 cells confirmed that treatment with 25D or 1,25D also decreased expression of ferritin protein (Figure 3E).

Effect of Vitamin D Supplementation on Circulating Hepcidin in Healthy Volunteers

To assess the *in vivo* effect of vitamin D on hepcidin, a single-arm supplementation study was performed in seven healthy volunteers receiving a single oral dose of vitamin D_2 (ergocalciferol, 100,000 IU). Analysis of serum samples before and after supplementation showed that circulating levels of 25D increased from 27.0±2 ng/ml (67.5±5 nM) before supplementation to 43.5±3 ng/ml (108.8±7.5 nM, $P<0.001$) after supplementation (Figure 4A). By contrast, supplementation with vitamin D had no effect on circulating levels of active 1,25D (Figure 4B). Analysis of circulating hepcidin levels by ELISA showed no significant variation in serum hepcidin between baseline samples. However, after vitamin D supplementation, circulating hepcidin levels decreased by 34% at 24 hours after supplementation ($P<0.05$) and 33% at 72 hours after supplementation ($P<0.01$) (Figure 4C). First, analysis of serum ferritin concentrations showed that baseline (−24 hours) data for all the healthy volunteers were within normal ranges (18–160 ng/ml for female volunteers and 18–2710 ng/ml for male volunteers). Second, supplementation with vitamin D resulted in a small (10%) but significant ($P=0.04$) decrease in serum ferritin after vitamin D supplementation (138.83±25.03 ng/ml at −24 hours versus 124.50±21.70 ng/ml at 72 hours). No statistically significant changes in serum iron concentration, iron binding capacity, or transferrin saturation were observed 72 hours after vitamin D supplementation.

In parallel with analysis of hepcidin and ferritin, assays were also carried out to assess circulating concentrations of hormones classically associated with vitamin D function.

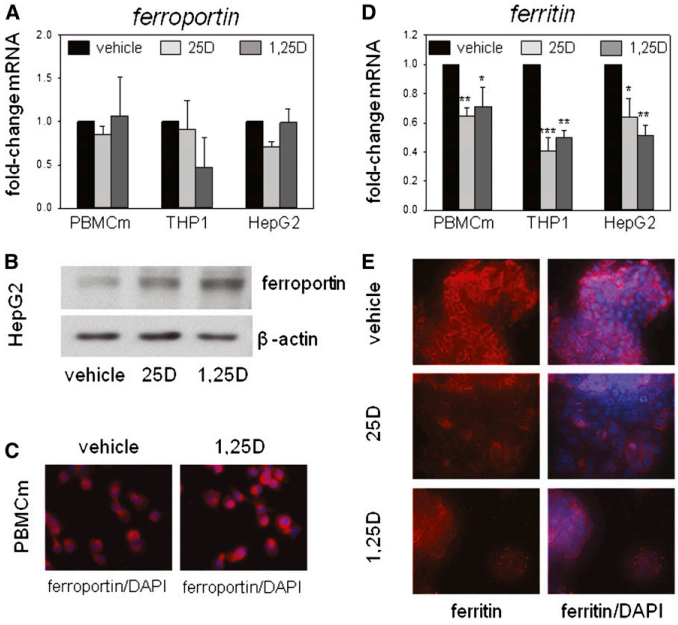

Figure 3. Effect of vitamin D metabolites on ferroportin and ferritin expression in human monocytes and hepatocytes. (A) Effect of *in vitro* treatment of PBMC monocytes (PBMCm), monocytic THP1 cells, and HepG2 hepatocytic cells with vehicle, 25D (100 nM) or 1,25D (5 nM) for 6 hours on ferroportin mRNA expression. Data are shown as mean fold-change in gene expression (±SD relative to vehicle [0.1% ethanol] controls). (B) Western blot analysis of protein for ferroportin protein in HepG2 cells treated with vehicle, 25D (100 nM), or 1,25D (5 nM) for 24 hours. Loading is normalized by analysis of the housekeeping protein β-actin. (C) Immunohistochemical analysis of ferroportin protein in PBMC monocytes after treatment with vehicle or 1,25D (5 nM) for 24 hours. Ferroportin protein is shown in red with 4′,6-diamidino-2-phenylindole (DAPI) staining of nuclei shown in blue. (D) Effect of *in vitro* treatment of PBMC monocytes, THP1 cells, and HepG2 cells with vehicle, 25D (100 nM), or 1,25D (5 nM) for 6 hours on ferritin mRNA expression. Data are shown as mean fold-change in gene expression (±SD relative to vehicle controls). (E) Immunohistochemical analysis of ferritin protein in HepG2 cells after treatment with vehicle, 25D (100 nM), or 1,25D (5 nM) for 24 hours. Ferritin protein is shown in red with DAPI staining of nuclei in blue. $*P<0.05$; $**P<0.01$; $***P<0.001$, statistically different from vehicle-treated cells. For RT-PCR data, $n=8$ separate donors for PBMC monocytes, $n=4$ separate cultures of THP1 cells, and $n=5$ separate cultures of HepG2 cells.

Fibroblast growth factor 23 (FGF23) and parathyroid hormone (PTH) concentrations were analyzed for six subjects at −24 hours and +72 hours after vitamin D supplementation. Data indicate that supplementation with vitamin D resulted in a significant increase in serum concentrations of FGF23 (62.57±6.70 RU/ml versus 74.71±9.88 RU/ml; $P=0.03$, two-tailed t test), and phosphate (3.27±0.67 mg/dl versus 3.61±0.33 mg/dl; $P<0.001$, two-tailed t test). Vitamin D supplementation resulted in a trend toward decreased serum PTH concentrations (58.86±6.43 pg/ml versus 51.29±7.47 pg/ml; $P=0.06$, two-tailed t test) but no significant change in serum calcium concentrations (9.19±0.12 mg/dl versus 9.07±0.2 mg/dl; $P=0.36$, two-tailed t test).

DISCUSSION

Data presented in this study show for the first time that vitamin D is a potent regulator of the iron-regulatory protein hepcidin in both monocytes and hepatocytes. ChIP and promoter-reporter assays indicate that this occurs as a consequence of direct transcriptional suppression of the *HAMP* gene proximal promoter by 1,25D bound to its cognate nuclear receptor, VDR. This response contrasts the 1,25D-VDR–mediated induction of related antibacterial proteins such as cathelicidin and β-defensin-2.[14] However, in a similar fashion to cathelicidin,[15] 1,25D-mediated regulation of hepcidin expression appears to occur directly, with liganded VDR binding to a specific VDRE within the *HAMP* gene promoter. Previous studies have shown that transcriptional regulation of *CAMP* by 1,25D-VDR is primate specific,[15,16] indicating that antibacterial responses to vitamin D have evolved relatively recently. It was therefore interesting to note that suppression of *HAMP* by 25D or 1,25D was not observed in murine models, suggesting that vitamin D–mediated regulation of hepcidin may be part of the same evolutionary adaptations observed for other antibacterial proteins.

In all three cell types studied, regulation of *HAMP* was observed after treatment with either active 1,25D or inactive 25D, suggesting an intracrine mode of action similar to that previously described for other antibacterial actions of vitamin D.[13] Intracrine regulation of *HAMP* is endorsed by the fact that PBMC monocytes, THP1 cells, and HepG2 cells express mRNA for the enzyme that catalyzes conversion of 25D to 1,25D, 1α-hydroxylase/CYP27B1, as well as the VDR (data not shown). A similar mode of action has been reported for antibacterial effects of vitamin D in monocytes[11,12] and antiviral responses to vitamin D in human hepatocytes.[17] Intracrine responses to vitamin D appear to be exquisitely sensitive to the availability of substrate 25D,[11,12,18] suggesting that the hepcidin-ferroportin homeostasis system may be influenced by serum vitamin D

(25D) status (Figure 5). This hypothesis is supported by supplementation data from healthy volunteers showing that elevated serum concentrations of 25D (but not 1,25D) after a single oral dose of vitamin D_2 produced a 34% decrease in serum hepcidin concentrations that persisted for 72 hours (Figure 4). Moreover, the regulation of serum hepcidin after vitamin D supplementation *in vivo* was at least as sensitive as more established markers of serum 25D status such as PTH, suggesting that hepcidin may be a useful marker of vitamin D function for future studies.

Data for ferroportin and ferritin expression in vitamin D–treated monocytes and hepatocytes are consistent with the actions of hepcidin in promoting post-transcriptional suppression of ferroportin protein.[19] On the basis of data presented in this study, we speculate that 25D and 1,25D can act to oppose this response and maintain membrane expression of ferroportin (Figure 5). Hepcidin-mediated loss of membrane ferroportin is known to be associated with intracellular retention of iron, leading in turn to iron-restrictive anemia.[5] This has immediate implications for the control of systemic iron homeostasis but will also influence host defense during acute infections. Iron is essential for the survival and growth of almost all organisms, and an important strategy for mammalian antimicrobial defense is based on depriving pathogens of this essential nutrient.[20] Thus, another facet of hepcidin physiology is its contribution to host innate immune function.[3,21] By targeting ferroportin and decreasing extracellular iron, hepcidin appears to play a pivotal role in the so-called "hypoferremia" or "anemia" of infection, in which there is restriction of systemic iron to pathogens.[5,22] Conversely, the resulting accumulation of intracellular iron will promote the growth of internalized pathogens such as *Salmonella typhimurium*,[23] *Mycobacterium tuberculosis*,[24–26] and *Chlamydia psittaci*,[27] and innate immune and viral stimuli are known to stimulate the expression of hepcidin.[25,28] In this setting, the effects of vitamin D in suppressing hepcidin and promoting ferroportin are consistent with its established intracellular antibacterial activity.[13] We therefore hypothesize that regulation of the hepcidin-ferroportin axis is another key facet of vitamin D–mediated innate immune function, complementary to its reported effects on antibacterial proteins,[11,13,29] and autophagy.[30,31] In future studies, it will be interesting to determine the extent to which regulation of monocyte/macrophage iron homeostasis contributes to the generalized antimicrobial actions of vitamin D.

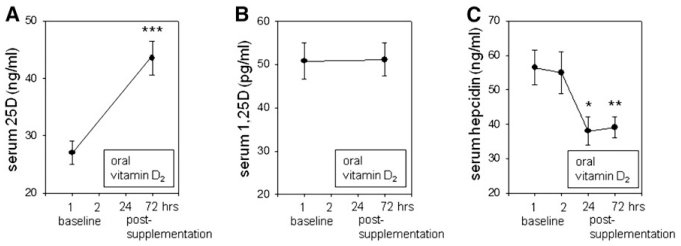

Figure 4. Effects of supplementation with vitamin D_2 on circulating hepcidin levels in healthy humans. A single-arm pharmacokinetic study is performed in seven healthy volunteers (four men; median age 42 years; range, 27–63) to assess changes in serum levels of hepcidin after a single dose of oral vitamin D_2 (100,000 IU). Two blood samples are drawn before supplementation and two are drawn after supplementation. Serum concentrations of 25D (ng/ml) (A), 1,25D (pg/ml) (B), and hepcidin (ng/ml) (C). Data are shown as the mean±SEM. Experimental means were compared statistically using a paired *t* test.*$P<0.05$; **$P<0.01$; ***$P<0.001$, statistically different from baseline values.

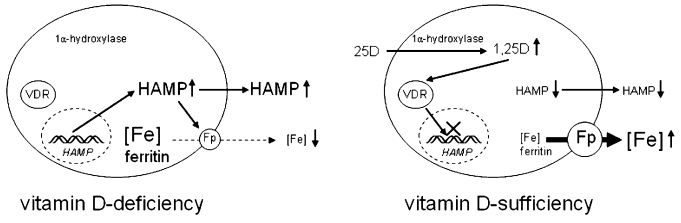

Figure 5. Vitamin D and the hepcidin-ferroportin iron-regulatory axis. Schematic representation of a proposed mechanism for vitamin D regulation of hepcidin/*HAMP* – ferroportin (Fp) interaction in hepatocytes and monocytes. Under conditions of vitamin D deficiency, elevated synthesis of hepcidin by hepatocytes or monocytes may increase intracellular and systemic concentrations of hepcidin and decrease membrane expression of Fp in these cells. The resulting suppression of iron export will, in turn, lead to intracellular accumulation, increased cellular ferritin, and decreased systemic levels of iron. Under conditions of vitamin D sufficiency, decreased transcription of *HAMP* may lead to decreased intracellular and systemic concentrations of hepcidin and concomitant increased membrane expression of Fp. The resulting enhancement of iron export may then lead to decreased intracellular iron and ferritin and increased systemic levels of iron.

Hepcidin was originally identified as an antibacterial protein, but its potential as a clinical target stems primarily from its role in the anemia of inflammation. Unlike dietary iron restriction, anemia of inflammation involves intracellular retention of iron by monocytes and macrophages,[32] and is thus intimately linked to aberrant hepcidin activity and associated dysregulation of membrane ferroportin function.[33] Although this is a problem that is common to many chronic diseases,[34] it is likely to be particularly important in patients with

CKD where elevated hepcidin levels may be a crucial factor in the development of multiple pathologic complications associated with renal impairment.[2] Consequently, targeting of hepcidin has been proposed as an alternative to supplementary iron and/or ESAs as therapy for the anemia associated with CKD.[35] Potential strategies for suppression of hepcidin include direct effects of antibodies to hepcidin,[36] hepcidin-binding oligoribonucleotides,[37] and inhibitors of hepcidin expression,[38] as well as indirect targeting *via* anti-inflammatory responses.[39] However, we believe that this is the first demonstration of rapid direct suppression of hepcidin in humans. High-dose testosterone has also been shown to suppress hepcidin, but effects were only evident after 1 week of therapy.[40] It was also interesting to note that the suppressive effect of vitamin D supplementation *in vivo* on serum hepcidin concentrations was accompanied by decreased levels of serum ferritin. The precise significance of this remains unclear but may reflect a generalized anti-inflammatory response to elevated serum levels of 25D.

The effect of vitamin D on the hepcidin-ferroportin axis also suggests that low vitamin D status may be a contributing factor to the anemia of chronic disease. CKD is characterized by impaired vitamin D status, which is closely associated with adverse CKD health outcomes.[41] In CKD patients, low serum levels of 25D correlate inversely with the prevalence of anemia[7] and ESA resistance,[8] and correlate directly with blood hemoglobin levels.[8] Data presented in this study suggest that these observations are linked by the effects of vitamin D on the hepcidin-ferroportin axis. In hemodialysis patients with anemia, vitamin D repletion has been shown to correlate with lower ESA requirements.[7,9] We therefore propose that by acting to suppress expression of hepcidin in hepatocytes and monocytes, simple vitamin D supplementation may provide a cost-effective and safe adjuvant therapy for managing the anemia associated with this disease.

CONCISE METHODS

Isolation, Treatment, and Culture of Cells

Human hepatocellular carcinoma HepG2 cells (American Type Culture Collection [ATCC], Manassas, VA) were cultured in DMEM with 10% FBS. Human THP1 monocytic cells (ATCC) were cultured in RPMI 1640 medium (Invitrogen, Carlsbad, CA) and 10% FBS. Mouse J774A macrophages (ATCC) were cultured in RPMI 1640 medium and 10% FBS. Ficoll-isolated PBMCs derived from anonymous healthy donors (screened in accordance with standard transfusion medicine protocols) were obtained from the Center for AIDS Research Virology Core/BSL3 Facility (supported by National Institutes of Health award AI-28697 and by the University of California Los Angeles [UCLA] AIDS Institute and the UCLA Council of Bioscience Resources). PBMC monocytes were isolated as previously described.[42] PBMC monocytes were seeded in RPMI 1640 (Invitrogen) with 10% human AB serum (Omega Scientific, Tarzana, CA) and GM-CSF (10 IU/ml; PeproTech, Inc., Rocky Hill, NJ). MC3T3-E1 (MC3T3) murine osteoblastic cells (ATCC) were maintained in α-MEM plus 10% FBS before transfection with promoter-reporter constructs. MC3T3 cells were cultured to 50% confluence before transfection with luciferase firefly or *Renilla* constructs. For all cell types, *in vitro* treatments at 37°C and 5% CO_2 included 25D (100 nM) and 1,25D (5 nM), with 0.1% ethanol as vehicle.

Animals

All of the animals used in these studies were subject to recommendations for animal use and welfare outlined by the UCLA Division of Laboratory Animal Medicine, as well as guidelines from the National Institutes of Health. The UCLA Animal Research Committee approved the protocol (no. 2012-024-02A) for the use of mice in our study. Twelve-week-old male C57BL/6 mice were placed on a vitamin D–deficient diet (Research Diets, Inc., New Brunswick, NJ) for 6 weeks then transferred to a 4 ppm iron diet for 1 week. Groups of mice (n=4 in each case) received the following intraperitoneal injections: 0.2 μg/g of 25D3 (Enzo Life Sciences, Farmingdale, NY), 1 μg/g 25D, 0.2 μg/g 1,25D (Enzo Life Sciences), or a similar volume of saline. In each case, mice were euthanized 24 hours after treatment and RNA were extracted from livers as previously described.[43]

Prospective Vitamin D Supplementation Pilot Study

A single-arm pharmacokinetic study was performed in seven healthy volunteers to examine the change in hepcidin serum levels, assessed by competitive ELISA (Intrinsic Life Sciences, La Jolla, CA) after a single dose of oral vitamin D_2 (100,000 IU). For serum 25D, a rapid, direct RIA developed in the laboratory of Dr. Hollis and manufactured by Diasorin Corporation (Stillwater, MN) was used.[44] An RIA manufactured by Diasorin Corporation was used to measure total circulating 1,25D concentrations.[45] Circulating levels of PTH and FGF23 were measured with an RIA kit, a first-generation immunometric assay (normal range, 10–65 pg/ml; Immutopics, San Clemente, CA), and a second-generation C-terminal kit (Immutopics), respectively. Two samples were drawn before supplementation (so that each subject acted as its own control) and two samples were drawn after supplementation (24 and 72 hours). All biologic samples were obtained at 8 AM after an overnight fast. This human study was approved by the UCLA Human Subjects Protection Committee, and consent was obtained from all subjects.

Extraction of RNA and Quantitative RT-PCR

Adherent cell cultures or centrifuged pellets of PBMC monocytes, THP1 cells, or HepG2 cells were initially lysed with 1 ml RNAzol. Each sample was then transferred to Eppendorf tubes and RNA was extracted by adding 0.2 ml chloroform in a fume cabinet, and then vortexing samples for >5 seconds followed by centrifugation at 12,000×g for 15 minutes at 4°C. The aqueous phase was collected for each sample and mixed with 1 μl glycogen and 0.5 ml isopropanol. Samples were then vortexed and centrifuged again as described above. All fluid was then discarded and the resulting RNA pellet dried in the Eppendorf tube. The resulting pellet was then washed with 1 ml 70% ethanol and vortexed and centrifuged again, followed by further air drying of the resulting pellet. Finally, RNA pellets were resuspended

in ≥14 μl of RNase free water and stored at −20°C after RNA quantification and quality assessment (260/280 ratio; Nanodrop).

Aliquots (300 ng) of resuspended RNA were reverse-transcribed using the SuperScript III RT enzyme as recommended by the manufacturer (Invitrogen) and as previously described.[12] Quantitative real-time RT-PCR was performed in a Stratagene cycler (La Jolla, CA), using TaqMan probes and primers (Applied Biosystems, Foster City, CA).[12,46] Expression of mRNA for the VDR (*VDR*) (Hs001721113_m1), the vitamin D–activating enzyme 1α-hydroxylase (*CYP27B1*) (Hs00168017_m1), the vitamin D catabolic enzyme 24-hydroxylase (*CYP24A1*) (Hs00167999_m1), *HAMP* (Hs00221783_m1), ferritin (Hs00830226_gH), ferroportin (Hs00205888_m1), *CAMP* (Hs00189038_m1), and mouse hepcidin (*Hamp*) (Mm00842044_g1) was quantified using TaqMan human gene expression assays, as previously described.[12] All reactions were amplified under the following conditions: 95°C for 10 minutes followed by 40 cycles of 95°C for 30 seconds, 55°C for 1 minute, and 72°C for 1 minute. Data were obtained as ΔCt values (the difference between Ct of the target gene and Ct of the housekeeping 18S rRNA gene). For visual representation, ΔCt data for each treatment were converted to fold-change relative to ΔCt for control vehicle-treated cells (ΔΔCt) using the equation $2^{-\Delta\Delta Ct}$.

Western Blot and Immunofluorescence Analyses

Expression of ferroportin protein was assessed by Western blot analyses using previously reported protocols,[46] involving overnight incubation with primary ferroportin antibody (1/1000; Amgen, Thousand Oaks, CA). A β-actin antibody (Sigma-Aldrich, St. Louis, MO) was used as a loading control. Immunofluorescence analysis of ferroportin and ferritin was carried out using adaptations of previously described methods.[46] Briefly, monocytes or hepatocytes were seeded on 4-well glass slides, and incubated for 1 hour with antibodies to ferroportin (1/200; Amgen) or ferritin (1/200; Abcam). Secondary antibodies labeled with Alexa 594 were applied for 1 hour, and finalized with 4′,6-diamidino-2-phenylindole (1/10,000, 5 minutes).

ChIP-qPCR Analyses of the Hepcidin Promoter

To predict potential *HAMP* promoter chromatin binding sites for the VDR protein, the NubiScan program (www.nubiscan.unibas.ch) was used. A −1071-bp *HAMP* gene promoter sequence was analyzed using the general weighted matrix for nuclear receptor half-sites (including the VDR canonical half-sites), enabling direct-repeat 3 sites characteristic of VDR to be acquisitioned. For the search parameter, an automatic scan with a raw score threshold of 0.5 was used, where the optimal match would have a raw score of 1.

To assess physical binding of the VDR and associated transcriptional machinery to the *HAMP* gene promoter, ChIP was carried out. PBMC monocytes were treated with 1,25D (5 nM, 24 hours) and chromatin extracts prepared as previously described.[47] ChIP-qPCR assays were performed using the ChIP-IT Express kit (Active Motif) and the ChampionChIP kit (SABiosciences, Inc., Valencia, CA). ChIP-grade antibodies were used to detect VDR (sc-13133) and RNA polymerase II (SABiosciences, Inc.) interactions. The resulting enriched genomic DNA was purified (QIAquick kit; Qiagen, Inc., Valencia, CA) and measured by qPCR using the EpiTect ChIP-qPCR Primer Assay for *CYP24A1* (GPH021775(−)01A (−1 kb from the transcription start site) and GPH021775(−)02A (−2 kb from the transcription start site), for *CAMP* (NM_004345.3, −1 kb: GPH1009280(−)01A), for *HAMP* (NM_021175.2, −1 kb: GPH1006776(−)01A), and for the negative control sequence *IGX1A* (all Qiagen). The qPCR program was 10 minutes at 95°C, followed by 15 seconds at 95°C and 1 minute at 60°C for 40 cycles. A dissociation curve analysis was run to monitor the specificity of amplification and lack of primer dimers. Data were shown first as arbitrary units for qPCR amplification of DNA associated with RNA Pol II or VDR in cells treated with vehicle or 1,25D. In addition, fold-change values were calculated to show the change in RNA Pol II or VDR binding to DNA after treatment with 1,25D.

Luciferase Reporter Analysis of Vitamin D–Mediated Regulation of the *HAMP* Promoter

A pGL4.17 firefly luciferase reporter vector containing the entire proximal promoter (2997 bp) DNA sequence was used for analysis of 1,25D/25D-regulated *HAMP* transcription using previously reported protocols.[48] All transient transfections were performed using Lipofectamine 2000 Reagent (Invitrogen) at a ratio of 1:1 (total DNA to lipofectamine) according to the manufacturer's recommendations. Briefly, cells were seeded into 96-well plates at a density of 2×10^4 cells per well 24 hours before transfection. Each transfection was performed using 200 ng *HAMP* construct cotransfected with 50 ng *Renilla* luciferase plasmid to normalize transfection efficiency. Transfection recipient MC3T3 cells, which express *VDR* but do not express *CYP27B1*, were treated with vehicle (<0.2% ethanol), 25D (100 nM), or 1,25D (10 nM) 24 hours before harvest with 30 μl Passive Lysis Buffer (Promega, Fitchburg, WI). Luciferase activity in cell lysates was assessed using the Dual Luciferase assay kit (Promega) according to the manufacturer's protocol and measured using a FLUOstar Omega instrument (BMG Labtech, Cary, NC). Specifically, 20 μl of each sample was transferred into a white 96-well plate. The FLUOstar was programmed to inject 90 μl Luciferase Assay Reagent II followed by 90 μl Stop & Glo. Transcriptional activity was expressed as luciferase activity relative to *Renilla* activity. Each treatment was performed in triplicate and repeated on at least three separate occasions. Results were expressed as fold-change over untreated cells by dividing the firefly/*Renilla* ratio of treated cells by the firefly/*Renilla* ratio of untreated cells.

Statistical Analyses

RT-PCR data for *in vitro* and *ex vivo* studies were compared statistically using an unpaired *t* test. Where indicated, multifactorial data involving 25D/1,25D treatments were compared using one-way ANOVA with the Holm–Sidak method used as a *post hoc* multiple comparison procedure. Statistical analyses were carried out using raw ΔCt values and fold-changes. Spearman correlation test was used for bivariate analyses.

For the vitamin D supplementation in healthy volunteers study, clinical data are presented as the mean±SD for variables with normal distributions, or median (range) for variables with skewed distribution. A paired *t* test was used to compare baseline samples, and

baseline 1 with post-treatment samples. All statistical tests were performed at the two-sided 0.05 level of significance. Analyses were performed using the SPSS software (version 19.0; SPSS, Inc., Chicago, IL) for Windows.

ACKNOWLEDGMENTS

The authors thank Drs. Thomas Ganz and Ella Nemeth (both UCLA) for kindly providing reagents and technical assistance with this manuscript. They also thank Mrs. Barbara Gales for her help in facilitating the supplementation study.

This work was supported in part by educational grants from the Académie Française/Jean Walter Zellidja, Réunion Pédiatrique de la Région Rhône Alpes, Société Française de Pédiatrie/Evian, Fondation pour la Recherche Médicale, and the Philippe Foundation (to J.B.), as well as grants from the US National Institutes of Health (DK0911672 to M.H.), US Public Health Service (DK 67563 and DK 35423 to I.B.S.), Casey Lee Ball Foundation (to I.B.S.), and National Institutes of Health/National Center for Research Resources/National Center for Advancing Translational Sciences University of California Los Angeles Center for Translational Science Institute (KL2TR000122 to J.J.Z. and UL1 RR-033176 and UL1TR000124 to I.B.S.). The content is solely the responsibility of the authors and does not necessarily represent the official views of the National Institutes of Health.

DISCLOSURES

M.W. is a stockholder and executive officer of Intrinsic LifeSciences and has received honoraria from Janssen Research and Development. In addition, M.W. is a developer of the hepcidin assay used herein and holds United States patents involving hepcidin C-ELISA compositions and methods.

REFERENCES

1. Kalantar-Zadeh K, Streja E, Miller JE, Nissenson AR: Intravenous iron versus erythropoiesis-stimulating agents: Friends or foes in treating chronic kidney disease anemia? *Adv Chronic Kidney Dis* 16: 143–151, 2009
2. Nakanishi T, Hasuike Y, Otaki Y, Kida A, Nonoguchi H, Kuragano T: Hepcidin: another culprit for complications in patients with chronic kidney disease? *Nephrol Dial Transplant* 26: 3092–3100, 2011
3. Ganz T: Hepcidin and iron regulation, 10 years later. *Blood* 117: 4425–4433, 2011
4. Young B, Zaritsky J: Hepcidin for clinicians. *Clin J Am Soc Nephrol* 4: 1384–1387, 2009
5. Ganz T: Hepcidin, a key regulator of iron metabolism and mediator of anemia of inflammation. *Blood* 102: 783–788, 2003
6. Ramos E, Kautz L, Rodriguez R, Hansen M, Gabayan V, Ginzburg Y, Roth MP, Nemeth E, Ganz T: Evidence for distinct pathways of hepcidin regulation by acute and chronic iron loading in mice. *Hepatology* 53: 1333–1341, 2011
7. Lac PT, Choi K, Liu IA, Meguerditchian S, Rasgon SA, Sim JJ: The effects of changing vitamin D levels on anemia in chronic kidney disease patients: A retrospective cohort review. *Clin Nephrol* 74: 25–32, 2010
8. Kiss Z, Ambrus C, Almasi C, Berta K, Deak G, Horonyi P, Kiss I, Lakatos P, Marton A, Molnar MZ, Nemeth Z, Szabo A, Mucsi I: Serum 25(OH)-cholecalciferol concentration is associated with hemoglobin level and erythropoietin resistance in patients on maintenance hemodialysis. *Nephron Clin Pract* 117: c373–c378, 2011
9. Kumar VA, Kujubu DA, Sim JJ, Rasgon SA, Yang PS: Vitamin D supplementation and recombinant human erythropoietin utilization in vitamin D-deficient hemodialysis patients. *J Nephrol* 24: 98–105, 2011
10. Rianthavorn P, Boonyapapong P: Ergocalciferol decreases erythropoietin resistance in children with chronic kidney disease stage 5. *Pediatr Nephrol* 28: 1261–1266, 2013
11. Liu PT, Stenger S, Li H, Wenzel L, Tan BH, Krutzik SR, Ochoa MT, Schauber J, Wu K, Meinken C, Kamen DL, Wagner M, Bals R, Steinmeyer A, Zügel U, Gallo RL, Eisenberg D, Hewison M, Hollis BW, Adams JS, Bloom BR, Modlin RL: Toll-like receptor triggering of a vitamin D-mediated human antimicrobial response. *Science* 311: 1770–1773, 2006
12. Adams JS, Ren S, Liu PT, Chun RF, Lagishetty V, Gombart AF, Borregaard N, Modlin RL, Hewison M: Vitamin D-directed rheostatic regulation of monocyte antibacterial responses. *J Immunol* 182: 4289–4295, 2009
13. Hewison M: Antibacterial effects of vitamin D. *Nat Rev Endocrinol* 7: 337–345, 2011
14. Wang TT, Nestel FP, Bourdeau V, Nagai Y, Wang Q, Liao J, Tavera-Mendoza L, Lin R, Hanrahan JW, Mader S, White JH: Cutting edge: 1,25-dihydroxyvitamin D3 is a direct inducer of antimicrobial peptide gene expression. *J Immunol* 173: 2909–2912, 2004
15. Gombart AF, Borregaard N, Koeffler HP: Human cathelicidin antimicrobial peptide (CAMP) gene is a direct target of the vitamin D receptor and is strongly up-regulated in myeloid cells by 1,25-dihydroxyvitamin D3. *FASEB J* 19: 1067–1077, 2005
16. Gombart AF, Saito T, Koeffler HP: Exaptation of an ancient Alu short interspersed element provides a highly conserved vitamin D-mediated innate immune response in humans and primates. *BMC Genomics* 10: 321, 2009
17. Gal-Tanamy M, Bachmetov L, Ravid A, Koren R, Erman A, Tur-Kaspa R, Zemel R: Vitamin D: An innate antiviral agent suppressing hepatitis C virus in human hepatocytes. *Hepatology* 54: 1570–1579, 2011
18. Hewison M: Vitamin D and the intracrinology of innate immunity. *Mol Cell Endocrinol* 321: 103–111, 2010
19. Nemeth E, Tuttle MS, Powelson J, Vaughn MB, Donovan A, Ward DM, Ganz T, Kaplan J: Hepcidin regulates cellular iron efflux by binding to ferroportin and inducing its internalization. *Science* 306: 2090–2093, 2004
20. Wang L, Cherayil BJ: Ironing out the wrinkles in host defense: Interactions between iron homeostasis and innate immunity. *J Innate Immun* 1: 455–464, 2009
21. Drakesmith H, Prentice AM: Hepcidin and the iron-infection axis. *Science* 338: 768–772, 2012
22. Nemeth E, Valore EV, Territo M, Schiller G, Lichtenstein A, Ganz T: Hepcidin, a putative mediator of anemia of inflammation, is a type II acute-phase protein. *Blood* 101: 2461–2463, 2003
23. Nairz M, Theurl I, Ludwiczek S, Theurl M, Mair SM, Fritsche G, Weiss G: The co-ordinated regulation of iron homeostasis in murine macrophages limits the availability of iron for intracellular Salmonella typhimurium. *Cell Microbiol* 9: 2126–2140, 2007
24. Schaible UE, Collins HL, Priem F, Kaufmann SH: Correction of the iron overload defect in beta-2-microglobulin knockout mice by lactoferrin abolishes their increased susceptibility to tuberculosis. *J Exp Med* 196: 1507–1513, 2002
25. Sow FB, Alvarez GR, Gross RP, Satoskar AR, Schlesinger LS, Zwilling BS, Lafuse WP: Role of STAT1, NF-kappaB, and C/EBPbeta in the macrophage transcriptional regulation of hepcidin by mycobacterial infection and IFN-gamma. *J Leukoc Biol* 86: 1247–1258, 2009
26. Sow FB, Florence WC, Satoskar AR, Schlesinger LS, Zwilling BS, Lafuse WP: Expression and localization of hepcidin in macrophages: A role in host defense against tuberculosis. *J Leukoc Biol* 82: 934–945, 2007

27. Paradkar PN, De Domenico I, Durchfort N, Zohn I, Kaplan J, Ward DM: Iron depletion limits intracellular bacterial growth in macrophages. *Blood* 112: 866–874, 2008
28. Armitage AE, Eddowes LA, Gileadi U, Cole S, Spottiswoode N, Selvakumar TA, Ho LP, Townsend AR, Drakesmith H: Hepcidin regulation by innate immune and infectious stimuli. *Blood* 118: 4129–4139, 2011
29. Adams JS, Hewison M: Unexpected actions of vitamin D: New perspectives on the regulation of innate and adaptive immunity. *Nat Clin Pract Endocrinol Metab* 4: 80–90, 2008
30. Yuk JM, Shin DM, Lee HM, Yang CS, Jin HS, Kim KK, Lee ZW, Lee SH, Kim JM, Jo EK: Vitamin D3 induces autophagy in human monocytes/macrophages via cathelicidin. *Cell Host Microbe* 6: 231–243, 2009
31. Shin DM, Yuk JM, Lee HM, Lee SH, Son JW, Harding CV, Kim JM, Modlin RL, Jo EK: Mycobacterial lipoprotein activates autophagy via TLR2/1/CD14 and a functional vitamin D receptor signalling. *Cell Microbiol* 12: 1648–1665, 2010
32. Ganz T, Nemeth E: Iron sequestration and anemia of inflammation. *Semin Hematol* 46: 387–393, 2009
33. Andrews NC: Anemia of inflammation: The cytokine-hepcidin link. *J Clin Invest* 113: 1251–1253, 2004
34. Sun CC, Vaja V, Babitt JL, Lin HY: Targeting the hepcidin-ferroportin axis to develop new treatment strategies for anemia of chronic disease and anemia of inflammation. *Am J Hematol* 87: 392–400, 2012
35. Babitt JL, Lin HY: Molecular mechanisms of hepcidin regulation: implications for the anemia of CKD. *Am J Kidney Dis* 55: 726–741, 2010
36. Sasu BJ, Cooke KS, Arvedson TL, Plewa C, Ellison AR, Sheng J, Winters A, Juan T, Li H, Begley CG, Molineux G: Antihepcidin antibody treatment modulates iron metabolism and is effective in a mouse model of inflammation-induced anemia. *Blood* 115: 3616–3624, 2010
37. Schwoebel F, van Eijk LT, Zboralski D, Sell S, Buchner K, Maasch C, Purschke WG, Humphrey M, Zöllner S, Eulberg D, Morich F, Pickkers P, Klussmann S: The effects of the anti-hepcidin Spiegelmer NOX-H94 on inflammation-induced anemia in cynomolgus monkeys. *Blood* 121: 2311–2315, 2013
38. Theurl I, Schroll A, Sonnweber T, Nairz M, Theurl M, Willenbacher W, Eller K, Wolf D, Seifert M, Sun CC, Babitt JL, Hong CC, Menhall T, Gearing P, Lin HY, Weiss G: Pharmacologic inhibition of hepcidin expression reverses anemia of chronic inflammation in rats. *Blood* 118: 4977–4984, 2011
39. Song SN, Tomosugi N, Kawabata H, Ishikawa T, Nishikawa T, Yoshizaki K: Down-regulation of hepcidin resulting from long-term treatment with an anti-IL-6 receptor antibody (tocilizumab) improves anemia of inflammation in multicentric Castleman disease. *Blood* 116: 3627–3634, 2010
40. Bachman E, Feng R, Travison T, Li M, Olbina G, Ostland V, Ulloor J, Zhang A, Basaria S, Ganz T, Westerman M, Bhasin S: Testosterone suppresses hepcidin in men: A potential mechanism for testosterone-induced erythrocytosis. *J Clin Endocrinol Metab* 95: 4743–4747, 2010
41. Pilz S, Iodice S, Zittermann A, Grant WB, Gandini S: Vitamin D status and mortality risk in CKD: a meta-analysis of prospective studies. *Am J Kidney Dis* 58: 374–382, 2011
42. Chun RF, Lauridsen AL, Suon L, Zella LA, Pike JW, Modlin RL, Martineau AR, Wilkinson RJ, Adams J, Hewison M: Vitamin D-binding protein directs monocyte responses to 25-hydroxy- and 1,25-dihydroxyvitamin D. *J Clin Endocrinol Metab* 95: 3368–3376, 2010
43. Lagishetty V, Misharin AV, Liu NQ, Lisse TS, Chun RF, Ouyang Y, McLachlan SM, Adams JS, Hewison M: Vitamin D deficiency in mice impairs colonic antibacterial activity and predisposes to colitis. *Endocrinology* 151: 2423–2432, 2010
44. Hollis BW, Kamerud JQ, Selvaag SR, Lorenz JD, Napoli JL: Determination of vitamin D status by radioimmunoassay with an ^{125}I-labeled tracer. *Clin Chem* 39: 529–533, 1993
45. Hollis BW, Kamerud JQ, Kurkowski A, Beaulieu J, Napoli JL: Quantification of circulating 1,25-dihydroxyvitamin D by radioimmunoassay with ^{125}I-labeled tracer. *Clin Chem* 42: 586–592, 1996
46. Bacchetta J, Sea JL, Chun RF, Lisse TS, Wesseling-Perry K, Gales B, Adams JS, Salusky IB, Hewison M: Fibroblast growth factor 23 inhibits extrarenal synthesis of 1,25-dihydroxyvitamin D in human monocytes. *J Bone Miner Res* 28: 46–55, 2013
47. Lisse TS, Liu T, Irmler M, Beckers J, Chen H, Adams JS, Hewison M: Gene targeting by the vitamin D response element binding protein reveals a role for vitamin D in osteoblast mTOR signaling. *FASEB J* 25: 937–947, 2011
48. Maes K, Nemeth E, Roodman GD, Huston A, Esteve F, Freytes C, Callander N, Katodritou E, Tussing-Humphreys L, Rivera S, Vanderkerken K, Lichtenstein A, Ganz T: In anemia of multiple myeloma, hepcidin is induced by increased bone morphogenetic protein 2. *Blood* 116: 3635–3644, 2010

This article contains supplemental material online at http://jasn.asnjournals.org/lookup/suppl/doi:10.1681/ASN.2013040355/-/DCSupplemental.

SUPPLEMENTAL TABLE 1

SEQUENCE LENGTH	POSITION	STRAND	RAW SCORE	P VALUE	SITE SEQUENCE
1071	72	-	0.602588	0.132854	AGTCCGatgAGTACA
1071	952	+	0.596919	0.259562	AGGGGAgggGGCTCA
1071	422	-	0.564744	0.580772	TGGCCAtaaATGACA
1071	903	-	0.564162	0.457681	AGATAAgcgGGAACA
1071	649	+	0.526702	0.868162	TGTGCAtgtAGGCGA
1071	193	-	0.525093	0.687983	AGCCCAggaGGCTGA
1071	10	+	0.507491	0.791509	GGCTGAgttGGTGCA

Supplemental Table 1. In silico nuclear receptor site prediction for vitamin D response elements in the *HAMP* gene promoter (-1071 bp) For general nuclear receptor target prediction the NubiScan program (www.nubiscan.unibas.ch) was used. A -1071bp *HAMP* gene promoter sequence was analyzed using the general weighted matrix for nuclear receptor halfsites (including the VDR canonical halfsites), whereby direct-repeat 3 sites were acquisitioned. For the search parameter, an automatic scan with a raw score threshold of 0.5 was used, where the optimal match would have a raw score of 1.

SUPPLEMENTAL FIGURE 1

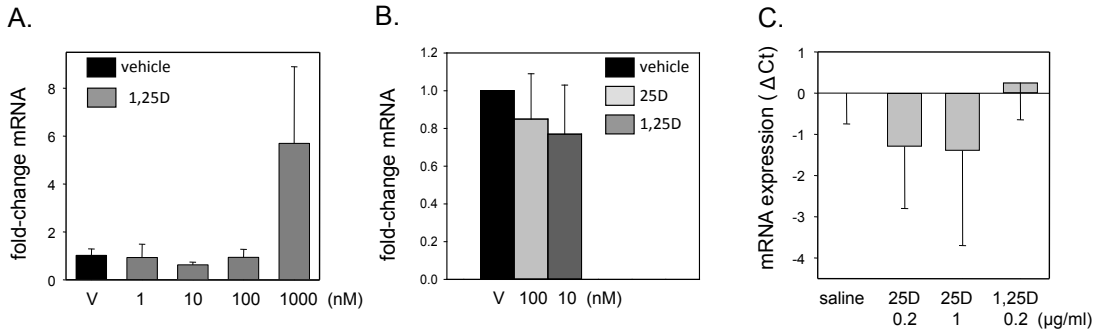

Supplemental Figure 1. **Effect of vitamin D on expression of hepcidin in mice**. S1A. Peripheral blood-derived monocytes from wild type C57BL/6 mice showed no change in mouse hepcidin (*Hamp*) gene expression following 24 hr treatment with increasing doses of 1,25D (1-100 nM). S1B. Similar results were also observed for the mouse monocyte cell line J774 following 6 hr treatment with 25D (100 nM) or 1,25D (10 nM) . S1C. To assess possible effects of vitamin D on hepatic expression of *Hamp* in vivo, 12 wk old C57BL/6 male mice were placed on a vitamin D-deficient diet for 6 weeks then transferred to a 4 parts per million (ppm) iron diet for one week. Groups of mice (n=4 in each case) were then treated with either 0.2 μg/g body weight of 25D by intraperitoneal (IP) injection, 1 μg/g 25D IP, 0.2 μg/g of 1,25D IP. A similar volume of saline IP (saline) was used as a control. Analysis of liver mRNA in these mice 24 hours after treatment showed no effect on expression of *Hamp*.

Chapter 5

1,25-dihydroxyvitamin D mitigates hypoxic responses in human aortic endothelial cells

1,25-dihydroxyvitamin D mitigates hypoxic responses in human aortic endothelial cells

Jessica L. Sea[1], Michelle Khrom[1], Bing Li[4], Michelle M. Reynoso[1], Daniel Cohn[4], Martin Hewison[3], Philip T. Liu[4]

[1]Department of Molecular, Cell and Developmental Biology, University of California at Los Angeles, Los Angeles, CA

[2]Department of Pediatrics, David Geffen School of Medicine, University of California at Los Angeles, Los Angeles, CA

[3]Centre for Endocrinology, Diabetes and Metabolism, The University of Birmingham, Birmingham, UK

[4]Department of Orthopaedic Surgery, Orthopaedic Hospital Research Center, University of California at Los Angeles, Los Angeles, CA

ABSTRACT

Cardiovascular disease (CVD) is the leading cause of morbidity and mortality in the US. Diabetes, autoimmune diseases, cancer, as well as renal diseases are associated with an increased risk in developing CVD and concomitant vascular complications. CVD is a complex, multifactorial disease with early stages hallmarked by systemic inflammation and aberrant circulating lipid profiles that lead to endothelial dysfunction and localized intravascular hypoxia. Clinical studies over the past decade have established a correlation between CVD and vitamin D deficiency; however, its function in the cardiovascular system is less understood. Given the ability of active 1α,25-dihydroxyvitamin D (1,25D) to dampen inflammation, we hypothesize that vitamin D exerts a cardioprotective effect on the endothelium; therefore, we tested whether 1,25D could mitigate inflammation- and hypoxia-driven endothelial dysfunction. Using human aortic endothelial cells (HAEC) and human umbilical vein endothelial cells (HUVEC), we demonstrate that 1,25D downregulates inflammation-induced expression of VCAM, ICAM, and E-selectin in a time-dependent manner. Our data also demonstrate that 1,25D downregulates hypoxia-driven VEGF and DDIT4 expression as well as proliferation of endothelial cells. Taken together, these results provide evidence for a cardioprotective role of 1,25D in the endothelium during inflammatory disease states through a direct effect on endothelial cells. This suggests that vitamin D may similarly play an important role in diseases with comorbid vascular complications.

INTRODUCTION

Atherosclerosis is a disease of chronic inflammation and hypoxia leading to cardiovascular disease (CVD) [1-4]. Diabetes, autoimmune diseases, cancer, and renal diseases are associated with an increased risk in developing atherosclerosis and concomitant vascular complications. Atherosclerosis, while initiated by systemic inflammation leading to endothelial dysfunction, is the process by which fatty plaques form on the blood vessel as a result of the accumulation of oxidized low-density lipoproteins (ox-LDL) in the subendothelial space [5-9]. Lipid accumulation stimulates the recruitment and retention of macrophages through monocyte extravasation to engulf excess lipids and cellular debris [3, 10]. Macrophage uptake of lipids leads to formation of lipid-laden foam cells that then undergo apoptosis, triggering the recruitment of additional macrophages to clear apoptotic cells [5, 10, 11]. As the rate of lipid and cell debris accumulation rises, macrophage efferocytosis is unable to keep abreast leading to the formation of a necrotic core of excess cellular debris [6, 12].

The necrotic core is a markedly hypoxic microenvironment characterized by high levels of reactive oxygen species, oxidized lipids, cell debris, and apoptotic cells [5, 12]. Hypoxia drives plaque growth by promoting endothelial dysfunction, stimulating the release of cytokines and chemokines by resident macrophages, inducing vasa vasorum angiogenesis, and stimulating macrophage engulfment of oxLDL [2, 13-16]. This cycle of inflammation, cell accretion, and hypoxia continues

throughout the disease until the plaque ruptures or occludes blood flow entirely, leading to the clinically emergent state of myocardial infarction [17].

Clinical studies demonstrate a correlation between vitamin D deficiency and CVD, as well as diseases with cardiovascular complications including diabetes, autoimmune diseases, and chronic kidney disease [18]. However, the function of vitamin D in the cardiovascular system, particularly cardiovascular pathology, remains unclear. The active form of vitamin D, 1α,25-dihydroxyvitamin D (1,25D), is well known for its role in bone health, regulating circulating calcium/phosphorus, and modulating innate and adaptive immune functions [19-22]. 1,25D stimulates macrophage engulfment of bacterial pathogens and can also function in anti-inflammatory and antioxidant capacities [21, 22]. We hypothesized that 1,25D could potentially mitigate the inflammatory conditions contributing to atherogenesis or its resulting increase of reactive oxygen species (ROS) due to the hypoxic local environment in the necrotic lesions. In this study, we explore potential cardioprotective roles for 1,25D in human aortic endothelial cells (HAEC) exposed to either inflammatory stimulus or hypoxic conditions.

MATERIALS AND METHODS

Endothelial Cell Culture

HAEC (cat no. 2535), HUVEC (cat. no 2517), and EGM-2 BulletKit (cat. no. 3162) were purchased from Lonza (Walkersville, MD). Cells used were between passages four to eight for all experiments. Endothelial cells were grown in EBM-2 growth media to 75- 100% confluence prior to experimentation. M199 media, purchased from Corning CellGro (10-060-CV), with either 1% fetal bovine serum (FBS) or 10% FBS was used during experiments.

Inflammatory Stimulation

Recombinant human TNFα, purchased from R&D Systems in Minneapolis, MN (cat. no. 210-TA) was reconstituted in sterile PBS with 0.1% BSA in accordance with manufacturer's instructions and used at a concentration of 100ng/ml. 1α,25-dihydroxyvitamin D (1,25D), purchased from Enzo was reconstituted in ethanol in accordance with manufacturer's instructions. EBM-2 growth media was replaced by M199 media containing either 1% or 10% FBS just prior to treatments. HAEC were supplemented with either 1,25D (100nM) or vehicle control (0.1% ethanol) one hour prior to stimulation with TNFα (100ng/ml). TNFα or vehicle control (0.1% PBS with BSA) were added to culture media and cells incubated at 32°C in 5% CO_2 for 18 hours before lysing cells to collect RNA or protein.

Hypoxia Stimulation

EC were grown to confluence in EBM-2 media. Media was changed to M199 culture media with 1% FBS and cells incubated in 32°C with 5% CO_2 for 6-8hrs. 1,25D (100nM) or vehicle control (0.1% ethanol) was added to the cell cultures one hour prior to either treatment with $CoCl_2$ (200mM) or transfer into SANYO MCO-5M multi-gas incubator set to 5% O_2, 5% CO_2, and 32°C. Cells were incubated in $CoCl_2$ or 5% O_2 for 18 hours.

RNA extraction and cDNA synthesis by reverse transcription

Qiagen mini RNase kits were used in accordance with the manufacture's instructions to extract RNA from cells. Aliquots of 1μg RNA were reverse-transcribed using SuperScript III Reverse Transcriptase as recommended by the manufacturer (Invitrogen, Carlsbad, CA).

Quantitative real-time RT-PCR amplification of cDNA

Taqman human gene expression assays were used for PCR amplification of target gene cDNA per the manufacture's instructions and as previously described (Justine and Jess et al). Stratagene MX3005P machine was used to quantify mRNA expression of VDR, VCAM, ICAM, and E-selectin. Reactions were amplified using the following conditions: 10 minutes at 95°C, 40 cycles of 95°C for 30 seconds, followed by 1 minute at 55°C and 1 minute at 72°C. Data were expressed as mean ± SD ΔCt values. Individual reactions were normalized by multiplex analysis with

18S rRNA housekeeping gene (Applied Biosystems, Foster City, CA, USA). Fold-change values were calculated using the equation $2^{-\Delta Ct}$ as previously described (Bacchetta and Sea et al). The probes and primer kits from Applied Biosystems used include: VDR (Hs00172113_m1), VEGFA (HS0090055_m1), VCAM1 (Hs01003372_m1), ICAM1 (Hs00164932_m1), E-selectin (Hs_00950401_m1), DDIT-1 (Hs0111686_g1).

RNA sequencing and bioinformatics analysis

Libraries were created using TruSeq RNA v2 library prep by UCLA Neurosciences Genomics Core. Libraries were sequenced at PE 2x69 on Illumina HiSeq 2500 next generation sequencing instrument.

Protein isolation and western blots

Cells were lysed with RIPA buffer (R0278, Sigma Aldrich, St Louis, MO, USA) containing 1% protease inhibitor cocktail (P8340, Sigma Aldrich, St Louis, MO, USA), and centrifuged at 5,000*g* for 20 minutes at 4°C. Protein lysates were separated by molecular weight using 10% SDS-PAGE followed by western blot transfer and immunoblotting. Biotinylated protein ladder (7727, Cell Signaling Technology, Danvers, MA, USA) was used to validate molecular weights. After blocking with 5% BSA, blots were incubated overnight at 4°C with primary antibody against human VDR (sc-1008 rabbit polyclonal, Santa Cruz Biotechnology). Horse-radish peroxidase (HRP)-conjugated secondary anti-rabbit antibody was incubated

for 1 hour at room temperature. Enhanced Chemiluminescence Western Blotting Substrate (Pierce Thermo Fisher Cat No. 32106) was used to detect HRP. Densitometery of band intensities were quantified using ImageJ software (National Institutes of Health, Bethesda, MD).

Analysis of 25D metabolism in HAEC

HAEC assessed for synthesis of 1,25D by quantifying the metabolism of radiolabeled 25OHD as described previously [23]. Briefly, HAEC were incubated with radiolabeled ^{3}H-25D substrate (300,000 cpm, 155Ci/mmol; Perkin Elmer, Waltham, Massachusetts) for 6 hrs in serum-free culture medium. The resulting mix of ^{3}H-vitamin D metabolites was then extracted from the total cell lipids using initial C18 Sep-pak purification (Waters, Milford, Massachusetts) and subsequent HPLC (ZorbaxSil column; Agilent, Santa Clara, California) separation of 1α-hydroxylated vitamin D metabolites. Biological replicates n=4.

Proliferation assay

The colorimetric WST proliferation assay, obtained from Abcam (ab155902), was used in accordance with manufacture's guidelines to quantify proliferation rates in HAEC. Briefly, after treatment periods in 98-well plates, WST reagent was added to HAEC cell cultures and incubated at 32°C in 5% CO_2 for 30 minutes. Absorbance was measured at 450nm using a plate reader. Data was normalized against a standard curve of cell densities and corresponding absorbency readings.

RESULTS

Vitamin D system in HAEC

Cytochrome P450, Family 27, Subfamily B, Polypeptide 1 (CYP27B1) mRNA, the enzyme required to convert 25D to 1,25D, was expressed in HAEC (Figure 5.1A). Previous studies in monocytes demonstrated a robust increase in CYP27B1 in response to inflammatory stimulation by TNFα. To test whether this effect was present in HAEC, we treated with TNFα (30ng/ml) for 6, 12, and 24 hours and measured mRNA by RT-PCR (Figure 5.1A). Results show a slightly increasing trend; however, the increases were not statistically significant. To assess protein expression, we treated with 30ng/ml of TNFα for 24 hours and assessed changes in CYP27B1 protein expression by western blot. Results showed low baseline CYP27B1 expression, and a modest increase upon TNFα treatment with a fold change of 1.96 after normalization to β-actin loading control (Figure 5.1B).

However, we were unable to detect activity of CYP27B1 in HAEC (Figure 5.2). HAEC were treated with either vehicle or TNFα (30ng/ml) for 24 hours and incubated with radio-labeled ^{3}H-25D for 6 hours. No ^{3}H-1,25D was detected by HPLC in either HAEC sample (repeated with 4 biological replicates).

This is contrary to human umbilical vein endothelial cells (HUVEC), in which a functional vitamin D system was previously established [24]. However, this is possibly due to the differences in CYP27B1 protein expression, which is much higher in untreated HUVEC compared to HAEC (Supplemental Figure 5.1).

Given that 1,25D functions largely as an endocrine and paracrine factor, we explored whether HAEC are be able to respond to 1,25D. We demonstrated HAEC express the vitamin D receptor (VDR) at similar levels to those observed in HUVEC. The monocytic cell line THP-1, which has established robust responses to 1,25D, was used for comparison in addition to HUVEC, and showed significant amount of VDR protein (Figure 5.3).

To assess whether HAEC could respond to 1,25D via changes in gene expression, we sequenced mRNA isolated from HAEC after a 6-hour incubation with either 1,25D (100nM) or vehicle control (0.01% ethanol). Sequencing results showed few changes in mRNA expression in both treatments suggesting vitamin D may not play role in maintaining normal function in HAEC (data not shown), particularly in comparison to cell types with more robust responses [21].

HAEC vs. HUVEC: 1,25D responses to inflammatory-stimulation

To explore potential differences between HAEC and HUVEC, we stimulated each with TNFα(100ng/ml) for 24 hours in the presence of 1,25D (100nM) or vehicle. TNFα induced expression of several markers for endothelial activation to comparable levels in both cell types. Vascular cell adhesion molecule (VCAM), intracellular cell adhesion molecule (ICAM), and endothelial selectin (E-sel) mRNA was significantly elevated following exposure to TNFα. However, supplementation with 1,25D 1 hour prior to TNFα treatment did not significantly reduce inflammatory-driven increases in VCAM or ICAM in either HAEC or HUVEC

(Figure 5.4A-D). To test whether this was the result of serum starvation conditions (1% FBS) that were used, experiments were carried out using 10% FBS. Results showed differences in serum concentration between 1% and 10% did not change cellular responses to 1,25D upon TNFα stimulation. However, 1,25D did have an effect on E-sel expression by in HAEC, but not HUVEC, by down regulating TNFα-induced E-sel expression in both 1% and 10% FBS (Figure 5.4E-F).

1,25D lowers hypoxia-induced VEGF and DDIT4 expression in HAEC

Given that hypoxia is a potent inducer of VEGF expression and endothelial dysfunction, we explored whether 1,25D could mitigate endothelial responses to hypoxia. To test whether 1,25D displayed anti-oxidant properties in endothelial cells, we exposed HAEC to hypoxic environments in the presence of either 1,25D or vehicle. Supplementation of 1,25D (100nM), but not 25D (data not shown) significantly lowered hypoxia-induced VEGF mRNA expression in HAEC (Figure 5.5A). We next sough to determine whether a downstream target of VEGF, DDIT4 was affected by 1,25D supplementation in hypoxia. DDIT4 mRNA expression patterned that of VEGF: demonstrating a trend in dramatically increasing levels of DDIT4 with hypoxia that were reduced by 1,25D supplementation in HAEC (Figure 5.5B).

DISCUSSION

Vitamin D has demonstrated anti-oxidant effects in previous studies, and given that many cell types respond differently to stimulus when cultured under stressed conditions, we tested the ability of HAEC to respond to 1,25D in hypoxic environment [25]. Hypoxia is well established to affect the endothelium in several diseases including, atherosclerosis and cancer. The lipid core of atherosclerotic plaques is highly hypoxic, driving endothelial activation, proliferation, and eventual dysfunction. Vascular endothelial growth factor (VEGF) expression is dramatically increased by hypoxia in endothelial cells, acting as a potent inducer of proliferation, which in a disease state can lead to endothelial dysfunction [26]. In atherosclerosis, hypoxia-driven VEGF expression can be both beneficial and detrimental to fighting plaque growth. VEGF overexpression is involved in several pathological functions contributing to atherosclerosis initiation and progression. In addition to driving endothelial dysfunction, VEGF also facilitates endothelial-dependent formation of vasa vasorum, which are neovascularizations within the vessel wall that supply the hypoxia core with oxygen and nutrients. This is thought to aid in vessel stability during certain points in the disease, however, the vasa vassorum have been implicated in the initiation of fatty plaques via LDL transportation leading to lipid accumulation [27, 28]. Although VEGF over expression appears to be beneficial at certain points in atherosclerosis, its role as a pathological agent is overwhelmingly dominant in plaque development [28].

Future directions to include characterizing proliferative effects of 1,25D in HAEC

VEGF and DDIT4 each play key roles in endothelial proliferation, which in a pathological setting can be detrimental. To assess the effects of 1,25D on endothelial proliferation, future directions will aim to address the question of whether 1,25D can regulate HAEC proliferation under physiological as well as hypoxic conditions. We plan to explore this using *in vitro* systems consisting of both monolayers and 3D culture matrices to mimic the *in vivo* environment. Future studies will also focus on characterizing the signaling pathways and mechanism by which 1,25D down regulates VEGF and DDIT4. We will do this by performing *in vitro* experiments to knock down expression of VDR to assess hypoxia responses for potential changes. Our hypothesis is that 1,25D is acting through VEGF and DDIT4 to down regulate mammalian target of rapamycin complex 1 (mTORC1) that is largely responsible for regulating cellular responses for proliferation.

FIGURE 5.1

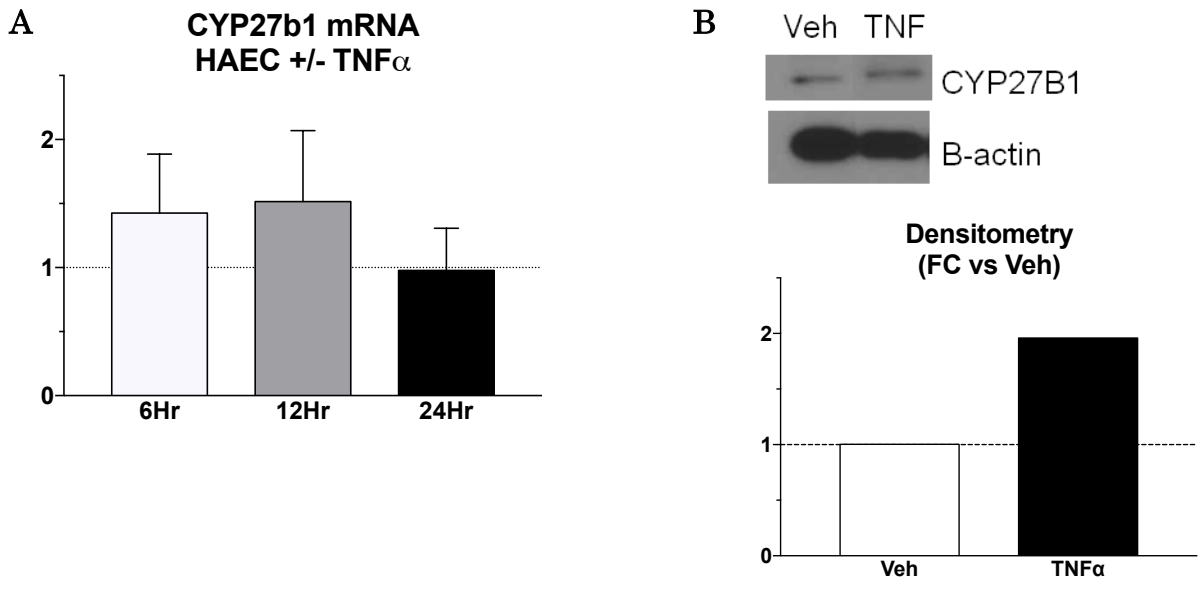

Figure 5.1 CYP27B1 expression in HAEC treated with TNFα

CYP27B1 mRNA as measured by RT-PCR and protein as measured by western blot in HAEC treated with TNFα (30ng/ml). **(A)** RT-PCR results indicate no significant difference in HAEC CYP27B1 expression in response to TNFα (30ng/ml) after 6, 12, or 24 hours. **(B)** CYP27B1 protein showed only a modest increase after 24 hours of TNFα (30ng/ml).

FIGURE 5.2

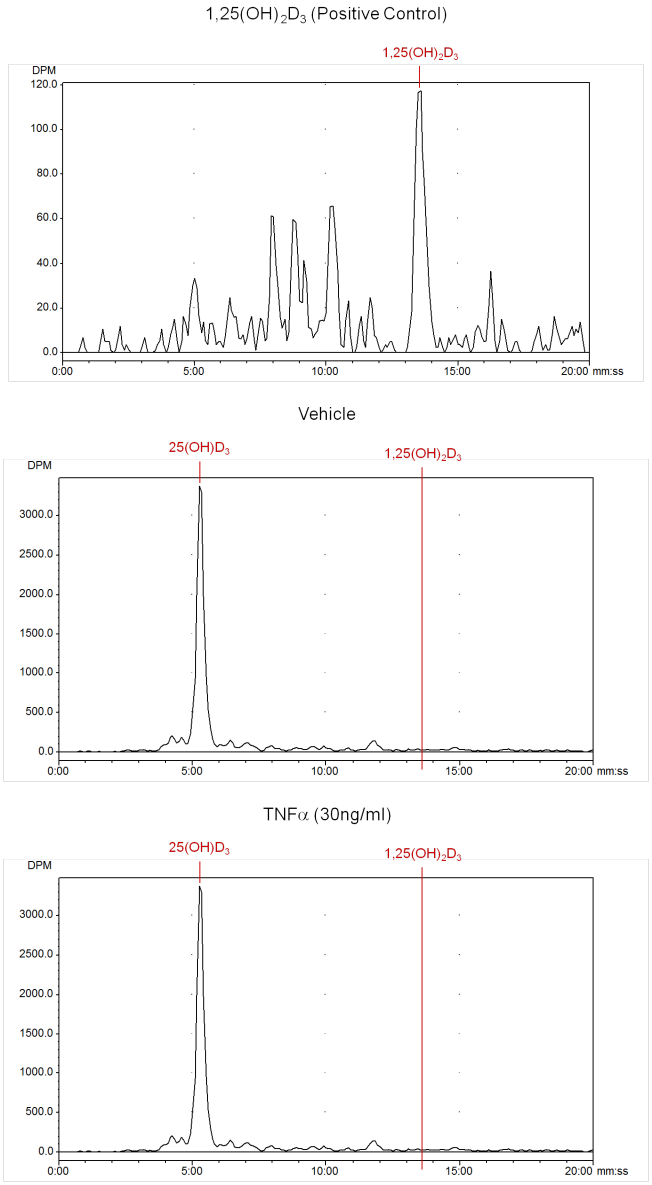

Figure 5.2 HAEC do not convert 25D to 1,25D at baseline or when stimulated with TNFα

HPLC results showed no activity of CYP27B1 in HAEC as measured by conversion of radio-labeled of ^{3}H-25D to ^{3}H-1,25D. Top plot showing positive control for ^{3}H-

1,25D. Middle plot showing HAEC treated with vehicle control. Bottom plot showing HAEC treated with TNFα (30ng/ml) for 24 hours. Plots are representative of 4 biological replicates.

FIGURE 5.3

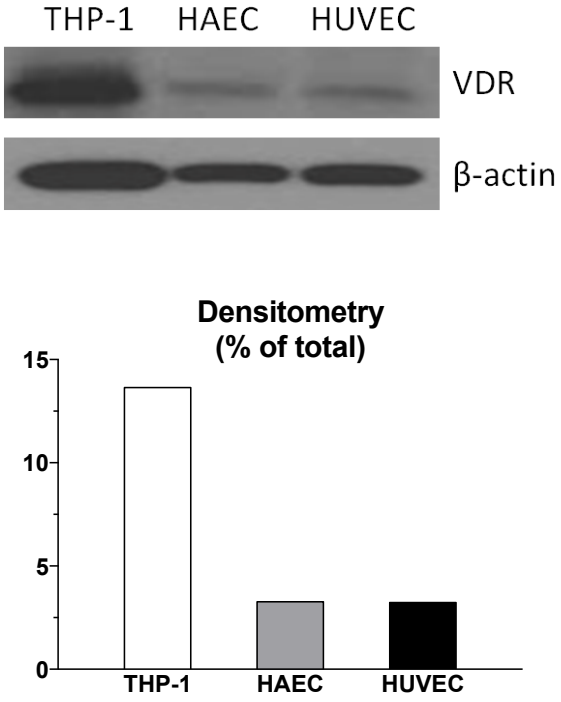

Figure 5.3 Expression of the VDR in HAEC

Untreated THP-1, HAEC, and HUVEC were assessed for VDR protein expression observed by western blot. Data indicate HAEC and HUVEC express similar amounts of VDR, albeit lower than the THP-1 monocytic cell line.

FIGURE 5.4

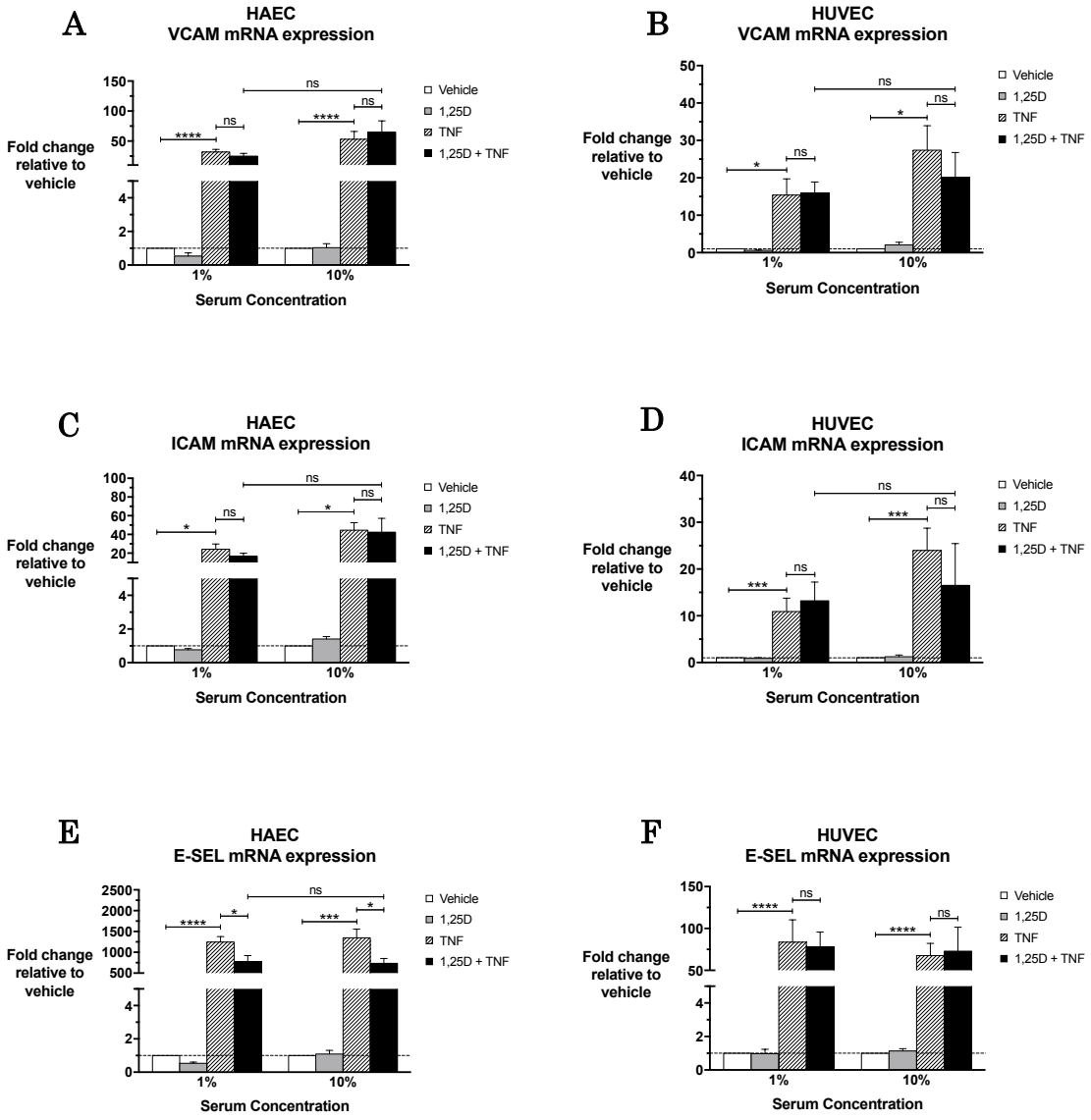

Figure 5.4 HAEC and HUVEC responses to inflammatory-stimulation in vitamin D supplemented conditions

HAEC and HUVEC were pre-treated with 1.25D, followed by TNFα stimulation for 24 hours in two different FBS concentrations and assessed for changes in mRNA of

adhesion markers: VCAM, ICAM, and E-sel. **(A-D)** TNFα induced significant increases in VCAM and ICAM in both serum concentrations across both cell types. 1,25D supplementation did not significantly inhibit TNFα-driven increases in VCAM or ICAM mRNA in either cell type and serum concentration. **(E-F)** TNFα stimulation resulted in significant induction of E-sel in both HAEC and HUVEC; however, inhibition of this increase by 1,25D only occurred in HAEC.

*p< 0.05; *** p< 0.001; ****p< 0.0001.

FIGURE 5.5

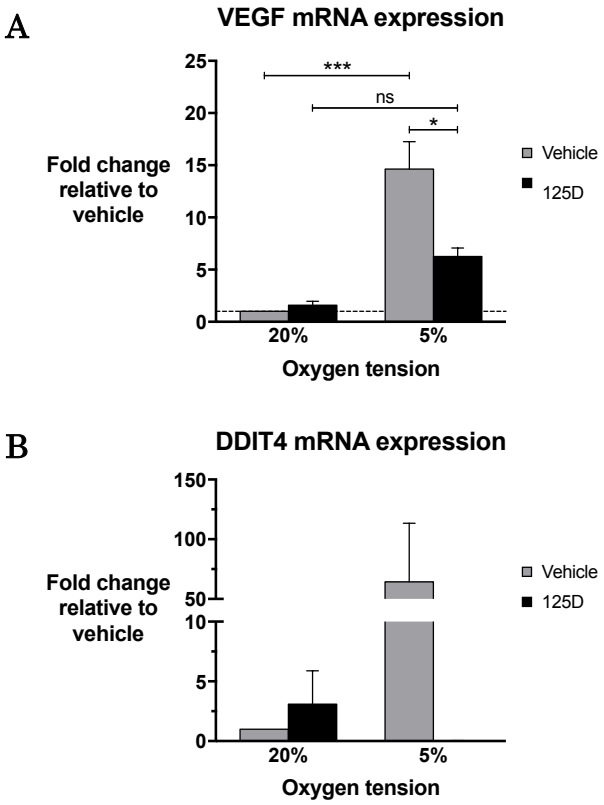

Figure 5.5 Effects of 1,25D on VEGF and DDIT4 expression in HAEC

Expression of VEGF and DDIT4 mRNA in HAEC supplemented with 1,25D (100nM) and cultured in hypoxic conditions. (A) HAEC cultured under 5% oxygen tension had a significant increase in VEGF mRNA that was significantly lowered by pre-treatment with 1.25D. (B) HAEC cultured under 5% oxygen tension demonstrated a trending increase in DDIT4 mRNA that was lowered by pre-treatment with 1.25D. *$p < 0.05$.

SUPPLEMENTAL FIGURE 5.1

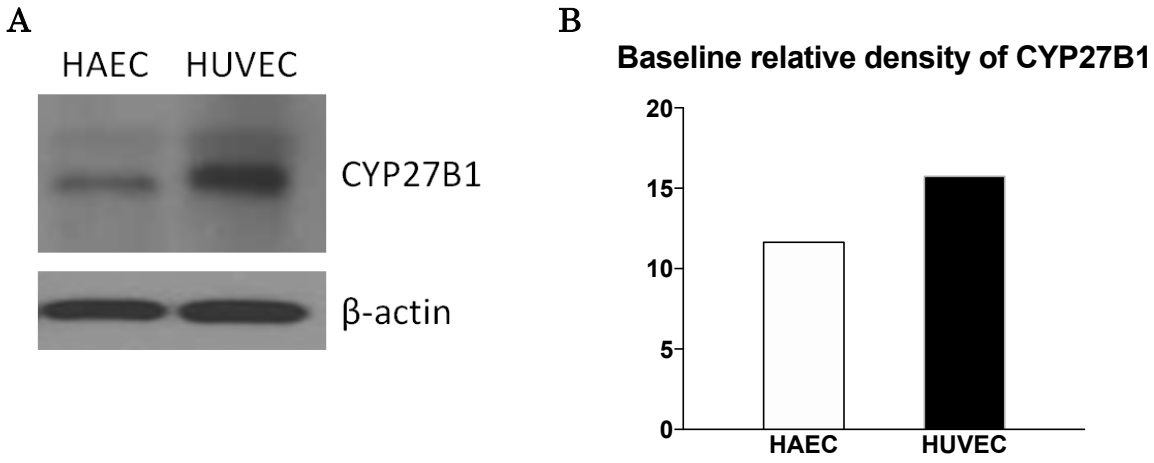

Supplemental Figure 5.1 Expression of CYP27B1 in HAEC and HUVEC

HAEC and HUVEC baseline expression of CYP27B1. **(A)** Western blot shows higher expression of CYP27B1 protein in HUVEc as compared to HAEC. **(B)** Densitometery of band intensities was quantified using ImageJ software.

REFERENCES

1. Bellingan, G.J., et al., *In vivo fate of the inflammatory macrophage during the resolution of inflammation: inflammatory macrophages do not die locally, but emigrate to the draining lymph nodes.* J Immunol, 1996. **157**(6): p. 2577-85.
2. Bonomini, F., et al., *Atherosclerosis and oxidative stress.* Histol Histopathol, 2008. **23**(3): p. 381-90.
3. Feig, J.E., et al., *Reversal of hyperlipidemia with a genetic switch favorably affects the content and inflammatory state of macrophages in atherosclerotic plaques.* Circulation, 2011. **123**(9): p. 989-98.
4. Heitzer, T., et al., *Endothelial dysfunction, oxidative stress, and risk of cardiovascular events in patients with coronary artery disease.* Circulation, 2001. **104**(22): p. 2673-8.
5. Linton, M.F., et al., *The Role of Lipids and Lipoproteins in Atherosclerosis*, in *Endotext*, L.J. De Groot, et al., Editors. 2000, MDText.com, Inc.: South Dartmouth MA.
6. Moore, K.J., F.J. Sheedy, and E.A. Fisher, *Macrophages in atherosclerosis: a dynamic balance.* Nat Rev Immunol, 2013. **13**(10): p. 709-21.
7. Pober, J.S. and R.S. Cotran, *The role of endothelial cells in inflammation.* Transplantation, 1990. **50**(4): p. 537-44.

8. Khandelwal, P., et al., *Dyslipidemia, carotid intima-media thickness and endothelial dysfunction in children with chronic kidney disease.* Pediatr Nephrol, 2016.

9. Gimbrone, M.A., Jr., *Vascular endothelium, hemodynamic forces, and atherogenesis.* Am J Pathol, 1999. **155**(1): p. 1-5.

10. Feig, J.E., et al., *HDL promotes rapid atherosclerosis regression in mice and alters inflammatory properties of plaque monocyte-derived cells.* Proc Natl Acad Sci U S A, 2011. **108**(17): p. 7166-71.

11. Bouhlel, M.A., et al., *PPARgamma activation primes human monocytes into alternative M2 macrophages with anti-inflammatory properties.* Cell Metab, 2007. **6**(2): p. 137-43.

12. Moore, K.J. and I. Tabas, *Macrophages in the pathogenesis of atherosclerosis.* Cell, 2011. **145**(3): p. 341-55.

13. Carmeliet, P., *Angiogenesis in health and disease.* Nat Med, 2003. **9**(6): p. 653-60.

14. Risau, W., *Mechanisms of angiogenesis.* Nature, 1997. **386**(6626): p. 671-4.

15. Van der Veken, B., G.R. De Meyer, and W. Martinet, *Intraplaque neovascularization as a novel therapeutic target in advanced atherosclerosis.* Expert Opin Ther Targets, 2016.

16. Xu, R., et al., *Assessment of carotid plaque neovascularization by contrast-enhanced ultrasound and high sensitivity C-reactive protein test in patients with acute cerebral infarction: a comparative study.* Neurol Sci, 2016.

17. Lusis, A.J., *Atherosclerosis.* Nature, 2000. **407**(6801): p. 233-41.

18. Liu, M., et al., *Vitamin D nutritional status and the risk for cardiovascular disease.* Exp Ther Med, 2016. **11**(4): p. 1189-1193.

19. Shimada, T., et al., *Targeted ablation of Fgf23 demonstrates an essential physiological role of FGF23 in phosphate and vitamin D metabolism.* J Clin Invest, 2004. **113**(4): p. 561-8.

20. Sterling, K.A., et al., *The immunoregulatory function of vitamin D: implications in chronic kidney disease.* Nat Rev Nephrol, 2012. **8**(7): p. 403-12.

21. Liu, P.T., et al., *Toll-like receptor triggering of a vitamin D-mediated human antimicrobial response.* Science, 2006. **311**(5768): p. 1770-3.

22. Fabri, M., et al., *Vitamin D is required for IFN-gamma-mediated antimicrobial activity of human macrophages.* Sci Transl Med, 2011. **3**(104): p. 104ra102.

23. Bacchetta, J., et al., *Fibroblast growth factor 23 inhibits extrarenal synthesis of 1,25-dihydroxyvitamin D in human monocytes.* J Bone Miner Res, 2013. **28**(1): p. 46-55.

24. Zehnder, D., et al., *Synthesis of 1,25-dihydroxyvitamin D(3) by human endothelial cells is regulated by inflammatory cytokines: a novel autocrine determinant of vascular cell adhesion.* J Am Soc Nephrol, 2002. **13**(3): p. 621-9.

25. Peery, S.L. and I. Nemere, *Contributions of pro-oxidant and anti-oxidant conditions to the actions of 24,25-dihydroxyvitamin D3 and 1,25-dihydroxyvitamin D3 on phosphate uptake in intestinal cells.* J Cell Biochem, 2007. **101**(5): p. 1176-84.

26. Kliche, S. and J. Waltenberger, *VEGF receptor signaling and endothelial function.* IUBMB Life, 2001. **52**(1-2): p. 61-6.

27. Herrmann, J., et al., *Coronary vasa vasorum neovascularization precedes epicardial endothelial dysfunction in experimental hypercholesterolemia.* Cardiovasc Res, 2001. **51**(4): p. 762-6.

28. Kwon, T.G., L.O. Lerman, and A. Lerman, *The Vasa Vasorum in Atherosclerosis: The Vessel Within the Vascular Wall.* J Am Coll Cardiol, 2015. **65**(23): p. 2478-80.

Chapter 6

Conclusions

Chronic kidney disease (CKD) is a serious worldwide health issue in which patients most often die of cardiovascular diseases (CKD) [1-3]. Elevated FGF23 is among the first clinically detectable signs of renal dysfunction and is independently associated with all –cause mortality in these patients [4-6]. Even children, who lack the traditional risk factors of CVD, suffer from cardiovascular co-morbidities that result in death [7-10]. Given the early onset of increased FGF23, CVD development associated with CKD, we hypothesized FGF23 may contribute to CVD pathology in patients with renal disease. We specifically focus on monocytes and endothelial cells as they are key initiating factors in CVD, and are dysregulated in CKD. In this study, we aim to understand the effects of FGF23 on several aspects of both monocytes and endothelial cells, as well as the interrelationship between the two cell types.

Starting with the effects of FGF23 on the monocyte vitamin D system, we demonstrated a unique role for FGF23 in mitigating innate immune function through down regulation of vitamin D synthesis. Active vitamin D (1,25D), synthesized in monocytes, is key to stimulating bacterial killing during pathogenic infections [11]. Patients with CKD, who have high levels of circulating FGF23, are at an increased risk of infections due to a compromised immune system [12-14]. The data presented in the second chapter of this dissertation suggests a link between FGF23 and weakened innate immune function in fighting bacterial infections.

Cardiovascular pathologies, particularly atherosclerosis, are initiated by chronic inflammation, increased oxidized low-density lipoprotein (ox-LDL), and

endothelial dysfunction [15, 16]. The purpose of the study described in chapter 3 was to investigate the effects of FGF23 on the relationship between endothelial cells and monocytes. Phagocytic monocytes taking up ox-LDL eventually develop into foam cells and when coupled with systemic inflammation and endothelial dysfunction, lead to the formation of a fatty plaque on the vessel wall [17-20]. As the plaque develops, cells, ox-LDL, and cellular debris accumulate leading to the development of an atherosclerotic lipid core [16]. In this study, we demonstrated that FGF23 acts on endothelial cells and monocytes in co-culture to facilitate the acquisition of modified LDL particles by monocytes; thereby demonstrating a connection between FGF23 and foam cell formation contributing to CVD. Future studies will aim to further characterize the mechanism by which FGF23 facilitates aberrant lipid responses in the endothelial/monocyte microenvironment.

In addition to CVD, patients in renal failure often develop anemia and have a weakened immune system. The iron-regulatory protein, Hepcidin catalyzes the degradation of the only mammalian iron-export protein, Ferroportin [21, 22]. In facilitating this process, Hepcidin overexpression causes iron sequestration important for fighting extra-cellular pathogens that require iron for replication [23-25]. In a pathological setting such as renal disease, Hepcidin overexpression can lead to iron-deficiency and anemia [26-29]. Patients with CKD are also often vitamin D deficient, also contributing to weakened immune responses [30]. This study explored the connection between Hepcidin over-expression and vitamin D deficiency associated with CKD in monocytes. Our results demonstrate a direct

regulation of Hepcidin by the vitamin D system while also proposing a mechanism for Hepcidin over production in vitamin D deficient patients. Future studies will explore potential contributions of elevated FGF23 in Hepcidin over production in monocytes.

The final study of this dissertation aimed to characterize the vitamin D system in human aortic endothelial cells (HAEC). Our data show HAEC do not possess the ability to synthesize 1,25D. However, expression of the vitamin D receptor (VDR) led us to hypothesize that 1,25D might act on HAEC by way of endocrine/paracrine effects. This study demonstrates a potential role for 1,25D in mitigating hypoxia-driven VEGF mRNA expression. Preliminary data show 1,25D may also mitigate VEGF-induced DNA-damage-inducible transcript 4 (DDIT4) upregulation in HAEC. Given that VEGF and DDIT4 are potent regulators of proliferation, and are up regulated in hypoxic conditions and CVD, future studies will involve assessing whether 1,25D elicits an effect on proliferation in a pathological setting.

Taken together, this body of work demonstrates an important role for FGF23 and vitamin D in CKD-mediated cardiovascular pathologies. Future work will aim to further explore the mechanisms by which FGF23 and 1,25D function within the cardiovascular system, with the goal of developing alternative therapeutics and immunotherapies to treat CVD/CKD.

REFERENCES

1. Ene-Iordache, B., et al., *Chronic kidney disease and cardiovascular risk in six regions of the world (ISN-KDDC): a cross-sectional study.* Lancet Glob Health, 2016. 4(5): p. e307-19.
2. Foley, R.N., P.S. Parfrey, and M.J. Sarnak, *Clinical epidemiology of cardiovascular disease in chronic renal disease.* Am J Kidney Dis, 1998. 32(5 Suppl 3): p. S112-9.
3. Jha, V., et al., *Chronic kidney disease: global dimension and perspectives.* Lancet, 2013. 382(9888): p. 260-72.
4. Dai, B., et al., *A comparative transcriptome analysis identifying FGF23 regulated genes in the kidney of a mouse CKD model.* PLoS One, 2012. 7(9): p. e44161.
5. Isakova, T., et al., *Fibroblast growth factor 23 is elevated before parathyroid hormone and phosphate in chronic kidney disease.* Kidney Int, 2011. 79(12): p. 1370-8.
6. Portale, A.A., et al., *Disordered FGF23 and mineral metabolism in children with CKD.* Clin J Am Soc Nephrol, 2014. 9(2): p. 344-53.
7. Chavers, B.M., et al., *Cardiovascular disease in pediatric chronic dialysis patients.* Kidney Int, 2002. 62(2): p. 648-53.
8. Flynn, J.T., *Cardiovascular disease in children with chronic renal failure.* Growth Horm IGF Res, 2006. 16 Suppl A: p. S84-90.
9. Lin, I.C., et al., *Low urinary citrulline/arginine ratio associated with blood pressure abnormalities and arterial stiffness in childhood chronic kidney disease.* J Am Soc Hypertens, 2016. 10(2): p. 115-23.
10. Parekh, R.S., et al., *Cardiovascular mortality in children and young adults with end-stage kidney disease.* J Pediatr, 2002. 141(2): p. 191-7.

11. Liu, P.T., et al., *Toll-like receptor triggering of a vitamin D-mediated human antimicrobial response.* Science, 2006. 311(5768): p. 1770-3.

12. Naqvi, S.B. and A.J. Collins, *Infectious complications in chronic kidney disease.* Adv Chronic Kidney Dis, 2006. 13(3): p. 199-204.

13. Sarnak, M.J. and B.L. Jaber, *Mortality caused by sepsis in patients with end-stage renal disease compared with the general population.* Kidney Int, 2000. 58(4): p. 1758-64.

14. Wu, H.S., et al., *Comparison between patients under hemodialysis with community-onset bacteremia caused by community-associated and healthcare-associated methicillin-resistant Staphylococcus aureus strains.* J Microbiol Immunol Infect, 2013. 46(2): p. 96-103.

15. Bonomini, F., et al., *Atherosclerosis and oxidative stress.* Histol Histopathol, 2008. 23(3): p. 381-90.

16. Lusis, A.J., *Atherosclerosis.* Nature, 2000. 407(6801): p. 233-41.

17. Feig, J.E., et al., *HDL promotes rapid atherosclerosis regression in mice and alters inflammatory properties of plaque monocyte-derived cells.* Proc Natl Acad Sci U S A, 2011. 108(17): p. 7166-71.

18. Feig, J.E., et al., *Regression of atherosclerosis is characterized by broad changes in the plaque macrophage transcriptome.* PLoS One, 2012. 7(6): p. e39790.

19. Moore, K.J., F.J. Sheedy, and E.A. Fisher, *Macrophages in atherosclerosis: a dynamic balance.* Nat Rev Immunol, 2013. 13(10): p. 709-21.

20. Moore, K.J. and I. Tabas, *Macrophages in the pathogenesis of atherosclerosis.* Cell, 2011. 145(3): p. 341-55.

21. Drakesmith, H., E. Nemeth, and T. Ganz, *Ironing out Ferroportin.* Cell Metab, 2015. 22(5): p. 777-87.

22. Park, C.H., et al., *Hepcidin, a urinary antimicrobial peptide synthesized in the liver.* J Biol Chem, 2001. 276(11): p. 7806-10.

23. Maccio, A., et al., *The role of inflammation, iron, and nutritional status in cancer-related anemia: results of a large, prospective, observational study.* Haematologica, 2015. 100(1): p. 124-32.

24. Michels, K., et al., *Hepcidin and Host Defense against Infectious Diseases.* PLoS Pathog, 2015. 11(8): p. e1004998.

25. Rodriguez, R., et al., *Hepcidin induction by pathogens and pathogen-derived molecules is strongly dependent on interleukin-6.* Infect Immun, 2014. 82(2): p. 745-52.

26. Nakanishi, T., et al., *Iron Localization and Infectious Disease in Chronic Kidney Disease Patients.* Am J Nephrol, 2016. 43(4): p. 237-244.

27. Girelli, D., E. Nemeth, and D.W. Swinkels, *Hepcidin in the diagnosis of iron disorders.* Blood, 2016.

28. Noguchi-Sasaki, M., et al., *Treatment with anti-IL-6 receptor antibody prevented increase in serum hepcidin levels and improved anemia in mice inoculated with IL-6-producing lung carcinoma cells.* BMC Cancer, 2016. 16(1): p. 270.

29. Pan, X., et al., *Hepcidin and ferroportin expression in breast cancer tissue and serum and their relationship with anemia.* Curr Oncol, 2016. 23(1): p. e24-6.

30. Sterling, K.A., et al., *The immunoregulatory function of vitamin D: implications in chronic kidney disease.* Nat Rev Nephrol, 2012. 8(7): p. 403-12.